



National Library
of Canada

Acquisitions and
Bibliographic Services Branch

395 Wellington Street
Ottawa, Ontario
K1A 0N4

Bibliothèque nationale
du Canada

Direction des acquisitions et
des services bibliographiques

395, rue Wellington
Ottawa (Ontario)
K1A 0N4

Vous le *Vous référence*

Vous le *Vous référence*

NOTICE

The quality of this microform is heavily dependent upon the quality of the original thesis submitted for microfilming. Every effort has been made to ensure the highest quality of reproduction possible.

If pages are missing, contact the university which granted the degree.

Some pages may have indistinct print especially if the original pages were typed with a poor typewriter ribbon or if the university sent us an inferior photocopy.

Reproduction in full or in part of this microform is governed by the Canadian Copyright Act, R.S.C. 1970, c. C-30, and subsequent amendments.

AVIS

La qualité de cette microforme dépend grandement de la qualité de la thèse soumise au microfilmage. Nous avons tout fait pour assurer une qualité supérieure de reproduction.

S'il manque des pages, veuillez communiquer avec l'université qui a conféré le grade.

La qualité d'impression de certaines pages peut laisser à désirer, surtout si les pages originales ont été dactylographiées à l'aide d'un ruban usé ou si l'université nous a fait parvenir une photocopie de qualité inférieure.

La reproduction, même partielle, de cette microforme est soumise à la Loi canadienne sur le droit d'auteur, SRC 1970, c. C-30, et ses amendements subséquents.

Canada

UNIVERSITY OF ALBERTA

The Effect of Core Length on the Instability of Miscible Displacement

by

XILING ZHANG



A THESIS

SUBMITTED TO THE FACULTY OF GRADUATE STUDIES AND RESEARCH

IN PARTIAL FULFILLMENT OF THE REQUIREMENTS FOR THE DEGREE OF

Master of Science

in

Petroleum Engineering

Department of Mining, Metallurgical and Petroleum Engineering

Edmonton, Alberta

Fall 1993



National Library
of Canada

Acquisitions and
Bibliographic Services Branch

395 Wellington Street
Ottawa, Ontario
K1A 0N4

Bibliothèque nationale
du Canada

Direction des acquisitions et
des services bibliographiques

395, rue Wellington
Ottawa (Ontario)
K1A 0N4

Your file / Votre référence

Our file / Notre référence

The author has granted an irrevocable non-exclusive licence allowing the National Library of Canada to reproduce, loan, distribute or sell copies of his/her thesis by any means and in any form or format, making this thesis available to interested persons.

L'auteur a accordé une licence irrévocable et non exclusive permettant à la Bibliothèque nationale du Canada de reproduire, prêter, distribuer ou vendre des copies de sa thèse de quelque manière et sous quelque forme que ce soit pour mettre des exemplaires de cette thèse à la disposition des personnes intéressées.

The author retains ownership of the copyright in his/her thesis. Neither the thesis nor substantial extracts from it may be printed or otherwise reproduced without his/her permission.

L'auteur conserve la propriété du droit d'auteur qui protège sa thèse. Ni la thèse ni des extraits substantiels de celle-ci ne doivent être imprimés ou autrement reproduits sans son autorisation.

ISBN 0-315-88214-X

Canada

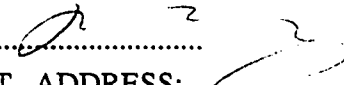
UNIVERSITY OF ALBERTA

RELEASE FORM

NAME OF AUTHOR: XILING ZHANG
TITLE OF THESIS: The Effect of Core Length on the
Instability of Miscible Displacement
DEGREE FOR WHICH THESIS WAS PRESENTED: MASTER OF SCIENCE
YEAR THIS DEGREE WAS GRANTED: FALL, 1993

Permission is hereby granted to THE UNIVERSITY OF ALBERTA LIBRARY to reproduce single copies of this thesis and to lend or sell such copies for private, scholarly or scientific research purposes only.

The author reserves other publication rights, and neither the thesis nor extensive extracts from it may be printed or otherwise reproduced without the author's written permission.

(SIGNED).....

PERMANENT ADDRESS:

Dept. of Mining, Metallurgical
and Petroleum Engineering
University of Alberta
Edmonton, Alberta

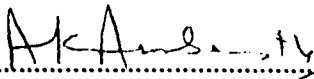
DATED.....*May 18 1993*.....

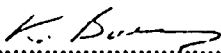
UNIVERSITY OF ALBERTA

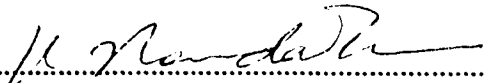
FACULTY OF GRADUATE STUDIES AND RESEARCH

The undersigned certify that they have read, and recommend to the Faculty of Graduate Studies and Research, for acceptance, a thesis entitled "**The Effect of Core Length on the Instability of Miscible Displacement**" submitted by **Xiling Zhang** in partial fulfillment of the requirements for the degree of **Master of Science** in petroleum Engineering.


.....
Professor R. G. Bentsen (Supervisor)


.....
Professor A. K. Ambastha


.....
Professor K. Barron (Chairman)


.....
Professor K. Nandakumar (External Examiner)

DATED: *May 17* *1993*

ABSTRACT

Miscible displacement has long been recognized as being one of the more efficient schemes for oil recovery. However, application of such a technique is limited partially because high expenditure is involved, and partially because the theoretical description of miscible displacement is incomplete. As previous researchers have demonstrated, there are many factors influencing the outcome of a miscible displacement employed either in the laboratory or in the field. In general, the efficiency of a miscible displacement process is related to the stability of the displacement. The most influential factors known to affect the stability of miscible displacements are the displacement rate, the viscosity and density differences of the fluids, the properties of the porous medium and the geometric dimensions of the core used for the miscible displacement.

The study presented here was essentially experimental. Miscible displacements using fluids of unequal density and unequal viscosity were conducted in glass-bead columns of varying length. Using a new theoretical interpretation of the critical stable-zone length, together with a dimensionless scaling group developed previously, the effect of core length on the instability of the displacements was studied. The experimental data were interpreted and examined by applying different empirical relationships for the evaluation of the dispersion coefficients.

It is shown that, under the same experimental conditions, the breakthrough recovery of a miscible displacement remained relatively unchanged when the displacement was predicted to be stable, but the breakthrough recovery decreased significantly with an increase in pack length when the displacement was predicted to be unstable. This observation may suggest that the instability of a displacement is related to core length

because a difference in core length may cause differences in magnitude of the dispersion coefficients and differences in the pattern of the finger development.

ACKNOWLEDGEMENTS

There are several people who were instrumental in the completion of this investigation. I especially would like to thank Dr. Ramon G. Bentsen for his guidance, encouragement, long-term support and his careful reading of the manuscript. Dr. Gokhan Coskuner's helpful discussions and supervision also were essential to this project.

Mr. R. W. Smith deserves special thanks for designing the physical apparatus used in the experiments. Thanks also to Dr. S. M. Farouq Ali and Mrs. Sara Thomas for offering some needed instruments to carry out the experiments; to the Natural Sciences and Engineering Research Council of Canada for the financial assistance which made this study possible, and to Imperial Oil for supply of the oil.

CONTENTS

1.	INTRODUCTION.....	1
2.	LITERATURE REVIEW.....	3
	2.1 Viscous-Finger Free and Gravity-Stable Displacement.	4
	2.1.1 Diffusion and Dispersion Phenomena of Miscible Fluids.....	4
	2.1.1.1 Molecular Diffusion Coefficient.....	5
	2.1.1.2 Longitudinal and Transverse Dispersion.....	6
	2.1.2 Microscopic Dispersion Coefficient.....	8
	2.1.3 Factors Affecting Displacement Behavior.....	14
	2.1.3.1 Effect of Viscosity ratio.....	14
	2.1.3.2 Effect of Density Differences.....	15
	2.1.3.3 Effect of Velocity.....	15
	2.1.3.4 Effect of Model Dimensions.....	16
	2.1.4 Mathematical Models and Solutions.....	17
	2.1.4.1 Convection-Dispersion Model.....	17
	2.1.4.2 Coats-Smith Model.....	19
	2.1.4.3 Porous Sphere Model.....	21

2.1.4.4	Transverse-Matrix-Diffusion Model.....	22
2.2	Theory of Unstable Displacement.....	23
2.2.1	Viscous Fingering.....	24
2.2.2	Mathematical Models and Solutions.....	25
2.2.2.1	K-Factor Method.....	25
2.2.2.2	Dougherty's Method.....	26
2.2.2.3	Jankovic's Method.....	27
2.2.2.4	Peaceman's Method.....	27
2.2.2.5	Vossoughi's Method.....	29
2.2.3	Criteria of Instability in Miscible Displacement.....	30
2.2.3.1	Dumore's Method.....	30
2.2.3.2	Coskuner and Bentsen's Method.....	32
3.	STATEMENT OF THE PROBLEM.....	35
4.	THEORY.....	37
4.1	A Generalized Convection-Dispersion Equation.....	37
4.2	The Stable Mixing-Zone Length.....	49
5.	EXPERIMENTAL.....	61
5.1	Experimental Apparatus.....	61

5.2	Properties of the Porous Medium.....	63
5.3	Experimental Procedure.....	64
5.3.1	Packing.....	64
5.3.2	Determination of Pore Properties.....	66
5.3.3	Displacement.....	68
5.3.4	Cleaning.....	70
5.3.5	Measurement of Refractive Index Number.....	70
6.	RESULTS AND DISCUSSION.....	74
6.1	Properties of the Miscible Fluids.....	74
6.2	Evaluation of the Relevant Parameters and Variables.....	80
6.2.1	The Viscosity and Density Gradients.....	80
6.2.2	Molecular Diffusion Coefficient.....	81
6.2.3	Transverse Dispersion Coefficient.....	82
6.2.4	Longitudinal Dispersion Coefficient.....	82
6.2.5	The Average Concentration Gradient.....	87
6.3	Effect of Bead-Pack Length on Breakthrough Recovery.....	88
6.4	The Stable Mixing-Zone Length.....	89
6.5	Evaluation of the Instability Number.....	92

6.6 Comparison of Concentration Curves.....	69
6.6 Discussion of Errors.....	109
7. SUMMARY AND CONCLUSIONS.....	111
8. SUGGESTIONS FOR FUTURE STUDY.....	113
9. REFERENCES.....	114
10. BIBLIOGRAPHY.....	120
11. APPENDIX A.....	123
12. APPENDIX B.....	126
13. APPENDIX C.....	131
14. APPENDIX D.....	133

LIST OF TABLES

1.	Properties of the Porous Media.....	65
2.	The Stable and Critical Velocities.....	69
3.	Properties of the Miscible Fluids.....	75
4.	Comparison of Evaluation of Longitudinal Dispersion Coefficient.....	84
5.	Displacement Result Summary.....	90
6.	Comparison of Stable Mixing-Zone Length.....	93
7.	Comparison of the Instability Numbers.....	95
8.	Comparison of Breakthrough Recovery with Theoretical Predictions.....	101
9.	Theoretical Concentration Profile Calculations.....	108

LIST OF FIGURES

1.	Schematic Drawing of Experimental Apparatus.....	62
2.	Effluent Concentration Profile Comparison Between Two Runs at Identical Flow Conditions.....	72
3.	Refractive Index of Varsol-Marcol Mixtures as a Function of Volume Per Cent Varsol.....	73
4.	Density of Varsol-Marcol Mixtures as a Function of Volume Per Cent Varsol.....	76
5.	Viscosity of Varsol-Marcol Mixtures as a Function of Volume Per Cent Varsol.....	77
6.	Effect of Bead Pack Length on the Breakthrough Recovery at Varied Velocities.....	91
7.	Comparison of Breakthrough Recovery with Instability Number.....	98
8.	Comparison of Experimental Concentration Curve with Theoretical Predictions for Run 13.....	102
9.	Comparison of Experimental Concentration Curve with Theoretical Predictions for Run 14.....	103

10.	Comparison of Experimental Concentration Curve with Theoretical Predictions for Run 15.....	104
11.	Comparison of Brigham's Experimental Data with the Modified Theoretical Prediction.....	106
12.	Comparison of Experimental Concentration Curve with Theoretical Predictions for Run 1.....	134
13.	Comparison of Experimental Concentration Curve with Theoretical Predictions for Run 2.....	135
14.	Comparison of Experimental Concentration Curve with Theoretical Predictions for Run 3.....	136
15.	Comparison of Experimental Concentration Curve with Theoretical Predictions for Run 4.....	137
16.	Comparison of Experimental Concentration Curve with Theoretical Predictions for Run 5.....	138
17.	Comparison of Experimental Concentration Curve with Theoretical Predictions for Run 6.....	139
18.	Comparison of Experimental Concentration Curve with Theoretical Predictions for Run 7.....	140

19.	Comparison of Experimental Concentration Curve with Theoretical Predictions for Run 8.....	141
20.	Comparison of Experimental Concentration Curve with Theoretical Predictions for Run 9.....	142
21.	Comparison of Experimental Concentration Curve with Theoretical Predictions for Run 10.....	143
22.	Comparison of Experimental Concentration Curve with Theoretical Predictions for Run 11.....	144
23.	Comparison of Experimental Concentration Curve with Theoretical Predictions for Run 12.....	145

NOMENCLATURE

A	Cross-sectional area, m^2 [cm^2]
a	Empirical parameter
C	Solvent concentration of the mixture, dimensionless
C_f	Solvent flowing concentration, dimensionless
C_i	Solvent in-situ concentration, dimensionless
\bar{C}_i	Average in-situ solvent concentration, dimensionless
\bar{C}	Unperturbed solvent concentration, dimensionless
C^*	Solvent concentration perturbation, dimensionless
\bar{C}_x	Amplitude of solvent concentration perturbation, dimensionless
D'	Molecular diffusion coefficient, m^2/s [cm^2/s]
D_L	Longitudinal dispersion coefficient, m^2/s [cm^2/s]
D_T	Transverse dispersion coefficient, m^2/s [cm^2/s]
D_p	Pseudo-dispersion coefficient, m^2/s [cm^2/s]
d_p	Diameter of the particle, m [cm]
E	Effective viscosity ratio, dimensionless
F	Formation electrical resistivity factor, dimensionless
f_s	Solvent fractional flow, dimensionless
	Correction factor, dimensionless
g	Gravitational acceleration, m/s^2
I_e	Experimental instability number, m^{-2}
I_m	Marginal instability number, m^{-2}
k	Absolute permeability, m^2 [darcy]
K_d	Ratio of transverse to longitudinal dispersion coefficient, dimensionless
L	Length of the porous medium, m [cm]

L_m	Length of the mixing zone, m [cm]
L_x	Width of the porous medium, m [cm]
L_y	Height of the porous medium, m [cm]
M	Viscosity ratio, dimensionless
N_{Pe}	Peclet number, $\bar{U}L/D_L$, dimensionless
P	Pressure, Pa [kg/cm ²]
\bar{P}	Unperturbed pressure, Pa [kg/cm ²]
P^*	Perturbed pressure, Pa [kg/cm ²]
\tilde{P}_x	Amplitude of pressure perturbation, Pa [kg/cm ²]
q	Total volumetric flow rate, m ³ /s [cm ³ /hr.]
q_s	Volumetric flow rate of displacing fluid, m ³ /s [cm ³ /hr.]
R	Dimensionless parameter
R_i	Ratio of average interstitial velocity to isoconcentration velocity, dimensionless
S	Pseudosaturation of solvent, dimensionless
t	Real time, s [min]
U	Interstitial velocity in the flowing direction, m/s [cm/min]
U_L	Error function parameter
\bar{U}	Unperturbed velocity in the flowing direction, m/s [cm/min]
U^*	Perturbed velocity in the flowing direction, m/s [cm/min]
\bar{U}_x	Amplitude of perturbation velocity in the flowing direction, m/s [cm/min]
V	Displacement velocity, m/s [cm/min]
V_c	Critical velocity, m/s [cm/min]
V_{CS}	Critical stable velocity, m/s [cm/min]
V_i	Injected volume, m ³ [cc]
V_p	Pore volume, m ³ [cc]

V_{pi}	Pore volumes injected, dimensionless
V_{st}	Stable velocity, m/s [cm/min]
W	Velocity in the z-direction, m/s [cm/min]
z	Vertical distance, m [cm]
α	Eigenvalue, m^{-1}
α_{md}	Macroscopic dispersivity, dimensionless
β	Empirical constant
δ	Ratio of bead-pack length to the length of the longest bead pack
γ	Dimensionless dispersion
γ_m	Modified dimensionless dispersion
ξ	Any perturbed dependent variable
$\bar{\xi}$	Any unperturbed dependent variable
ξ^*	Perturbation to any of the dependent variables
$\tilde{\xi}$	Amplitude of perturbation to any of the dependent variables
μ_m	Viscosity of the mixture, Pa.s [cp]
$\bar{\mu}$	Unperturbed viscosity, Pa.s [cp]
μ^*	Viscosity perturbation, Pa.s [cp]
μ_o	Oil viscosity, Pa.s [cp]
μ_s	Solvent viscosity, Pa.s [cp]
ρ_m	Density of the mixture, kg/m^3 [g/cm^3]
$\bar{\rho}$	Unperturbed density, kg/m^3 [g/cm^3]
ρ^*	Density perturbation, kg/m^3 [g/cm^3]
ρ_o	Oil density, kg/m^3 [g/cm^3]
ρ_s	Solvent density, kg/m^3 [g/cm^3]

ω	Empirical constant
τ	Einsteinian constant
ϕ	Porosity, dimensionless
Ω	Dimensionless length
σ	Inhomogeneity factor, dimensionless

1. INTRODUCTION

The search for an effective and economical miscible-flooding process has continued since the early 1950s. It is known that two fluids are miscible when they can be mixed together in all proportions, and when the mixture of the miscible fluids remains single phase. The objective of miscible displacement, therefore, is to reduce residual oil saturation to its lowest possible value by eliminating the interfacial tension between the oil and the displacing fluid. Such a process, however, has not been as widely applicable as waterflooding because of the higher expenditure involved in using chemicals, such as micellar/polymer or light crudes, as displacing fluids, and because of the lack of certainty in displacement efficiency due to an incomplete understanding of the fingering process.

Numerous theoretical and supporting laboratory studies lead to the conclusion that the low efficiency of miscible displacement in enhanced oil recovery processes is mainly because of mixing effects. Three mechanisms contribute to the mixing of miscible fluids: diffusion, microscopic convective dispersion, and macroscopic convective dispersion. Molecular diffusion is a result of the random thermal motion of molecules. When fluids flow through a porous medium, more mixing takes place in the direction of flow than would be expected from molecular diffusion alone. This additional mixing appears to be explained by microscopic and macroscopic inhomogeneities. The microscopic process, or longitudinal dispersion, depends fundamentally on flow conditions as well as on fluid and medium properties; the macroscopic process, or channeling, which results in by-passing of the resident fluid in large regions of the medium, can result from permeability stratification, segregation of the fluids by gravity, and viscous fingering.

Longitudinal and transverse microscopic dispersion coefficients are commonly used to describe mixing of fluids by dispersion. There are many factors influencing the process of mixing and the evaluation of dispersion coefficients from laboratory displacements. Variables such as displacement rate, mobility ratio, density ratio, model dimensions, particle-size distribution and particle shape all affect the magnitude of the dispersion coefficients to some degree.

Several experimental investigations have suggested that the length of a porous system may also be one of the important factors which affects the efficiency of miscible displacement. More recently, some authors have noted, that in a one-dimensional system, the measured dispersion coefficients increase with the length scale of a miscible displacement, and that, in a two-dimensional system, fingering development becomes length dependent because the ratio of viscous force to gravity force increases with the length of the system.

Few theoretical models seem able to include length dependence as a variable because of the need to simplify the problem by assuming an infinitely long system. A newly developed analytical model, which was proposed by Coskuner and Bentsen, enables one to examine the effect of length on the onset of instability in a porous medium with a finite length.

This investigation focuses mainly on the experimental research needed to verify the effect of core length on the instability of miscible displacements which is predicted in Coskuner's mathematical model. Moreover, there is a great need to establish both a theoretical and a physical basis to explain why and how core length affects the instability of miscible displacements.

2. LITERATURE REVIEW

Being aware of the importance of applying miscible displacement techniques to improve oil recovery, various investigators have reported theoretical studies as well as experimental analyses. The displacement of oil by first-contact miscible solvent in homogeneous porous media is mechanistically simple when the process is free of fingering. Under such conditions the oil is displaced efficiently ahead of the solvent, and the solvent does not penetrate into the oil except as dictated by dispersion. When the displacement front is stable, laboratory miscible displacement experiments may be interpreted in terms of the one-parameter convection-dispersion equation. The dispersion equation has been solved numerically as well as analytically to obtain concentration profiles and to determine the dispersion coefficients.

However, when the mobility ratio of the miscible fluids is greater than one, the displacement has a quite different character: the solvent front becomes unstable, and numerous fingers of solvent develop and penetrate into the oil in an irregular fashion. With unstable displacements, the validity of many mathematical models and their solutions becomes limited. Viscous fingering occurs when a more viscous fluid is displaced by a less viscous fluid. Finger-shaped intrusions of displacing fluid into the displaced fluid have been observed and reported in the literature for immiscible as well as miscible displacement processes. These viscous fingers result in earlier solvent breakthrough and poorer oil recovery after breakthrough, for a given volume of solvent injected, than would be the case if the displacing front were to remain stable. The mechanisms and factors which contribute to the development of fingers and to the dispersion process are also far from being well understood.

2.1 VISCOUS-FINGER-FREE AND GRAVITY-STABLE DISPLACEMENT

The displacement of oil by first-contact miscible solvents in homogeneous porous media is mechanistically simple when the solvent/oil mobility ratio is less than or equal to one and when gravity does not influence the displacement by segregating the two fluids. Under these conditions, oil is displaced efficiently ahead of the solvent, and no solvent fingers penetrate into the oil except as dictated by dispersion. Gravity-stable displacements are those in which gravity prevents solvent overriding or gravity tonguing. In order to apply this technique, the density difference between solvent and oil is exploited by injecting the less dense solvent at the top of the core and conducting the displacement downward at a rate low enough for the density difference between the solvent and the oil to overcome the tendency for solvent fingers to protrude into the oil.

2.1.1 Diffusion and Dispersion Phenomena of Miscible Fluids

Molecular diffusion and convective dispersion phenomena are known to have a strong influence, not only on the mixing of solvent with oil in miscible displacements, but also on the efficiency of the displacements. Molecular diffusion is a result of random thermal motion of the molecules. It is known also that molecular diffusion is the dominant mixing process at reservoir conditions of rate, length and pore size. When a miscible displacement is conducted in a porous medium, the mixing of the two fluids is caused by microscopic convective dispersion and macroscopic convective dispersion, which are associated with inhomogeneities in the shape and size of the particles, the pore structure, the permeability heterogeneities and the dimensions of the porous medium. Because of this mixing, a transition zone, composed of a mixture of solvent and oil, separates 100% solvent from

100% oil. Mixing in the direction of flow is called "longitudinal dispersion", and mixing orthogonal to the direction of flow is called "transverse dispersion".

2.1.1.1 Molecular Diffusion Coefficient

If two miscible fluids are in contact with an initially sharp interface, mixing by diffusion will take place subsequently. As time passes, the sharp interface between the two fluids will become a mixed zone with a concentration gradient from one pure fluid to the other. The mixing caused by molecular diffusion is represented by the well-known Fick's [1] diffusion equation.

Typically, the molecular diffusion coefficient defined in Fick's equation is a function of concentration. However, to simplify the problem, it is often possible to represent diffusive behavior approximately by selecting an average diffusion coefficient which is constant and independent of concentration.

The molecular diffusion coefficient is usually determined experimentally. Taylor [2] has shown that the diffusion coefficient can be calculated by plotting per cent of initial tracer concentration versus traveling distances from the original interface at each particular time on arithmetic-probability co-ordinate paper, which yields a straight line for equal-viscosity and equal-density miscible fluids.

With little information available on the molecular diffusion coefficients of reservoir fluids, Van der Poel [3] reviewed Reamer and Sage's [4] and Trevoy and Drickamer's [5] reports. He suggested that the molecular diffusion coefficients have the same order of magnitude ($10^{-5} \text{ cm}^2/\text{sec.}$) in both water-glycerine systems and reservoir fluid mixtures. The measurement of diffusion in multi-compositional and unequal-density liquids, to the best of author's knowledge, is not as advanced; nor are experimental data as plentiful as for

single-composition fluids. An empirical expression developed by Warren and Skiba [6] may be used to calculate the diffusion coefficients approximately.

In the oil industry, the apparent diffusion coefficient in a porous medium must be adjusted to account for the tortuous path for diffusion in the pores of the rock. Many investigators [3,7,8] have recognized that there is an analogy between apparent diffusion and electrical conductivity in porous media.

2.1.1.2 Longitudinal and Transverse Dispersion

In porous media there are flow channels of varying sizes with frequent junctures between the channels. More mixing between oil and solvent tends to occur in this complex geometry than in a straight capillary. The increased mixing caused by rock inhomogeneities, permeability heterogeneities, or concentration gradients resulting from fluid flow is designated dispersion. The degree of mixing depends on the interplay between the mechanisms of molecular diffusion and convective dispersion. Molecular diffusion perpendicular to the direction of flow tends to decrease the convective dispersion produced either by velocity variations in a single channel or by velocity variations arising from geometrical complexities of the porous medium.

There are two types of dispersion to be considered: longitudinal dispersion and transverse dispersion. Each type of dispersion has two components: one due to diffusion and another due to mechanical mixing. Considerable effort has been directed to the study of dispersion phenomena in flow through porous media. In 1954, Morse [9] observed that the length of the mixing zone is dependent on variables such as rate of displacement, distance traveled, and viscosity ratio of the fluids. He also found that the mixing zone grows rapidly at the beginning, and the rate of growth then gradually falls off to where it becomes nearly stabilized. Brigham et al. [7] observed that mixing zone length increases at

very low and at very high flow rates; and that the mixing-zone length achieves a minimum value at a particular growth rate. At this velocity, diffusion contributes only a small fraction of the total dispersion coefficient.

In 1965, Kyle and Perrine [10] conducted a series of experiments to measure the growth rate of the mixing zone as a function of the viscosity ratio and average fluid velocity. The experimental results show that, in the range of flow rates used, mixing zone expansion depends on the amount of solvent injected, and not on the displacing rate, for a given viscosity ratio of fluids used.

After reviewing published data on diffusion and dispersion in porous media, Perkins and Johnston [11] suggested that if one flows fluid through a pack at a very low rate, then there may be enough time for diffusion to equalize concentration variation within each pore space. However, if one increases the velocity in the interstices to a high enough value, one will eventually reach a velocity at which there is insufficient time for diffusion to equalize concentration within each pore space. The ratio of the time needed to smooth away concentration variations to the time available is proportional to a dimensionless parameter, or Peclet number, Ud_p/D' . Hence, the dimensionless group should be a measure of how effectively diffusion can equalize concentration within pore spaces. Perkins and Johnston's data also show that transverse dispersion is dominant compared to transverse diffusion if Ud_p/D' is greater than about 100; therefore, under such a displacement condition, there is not enough time to equalize the concentration variation within the pore space by diffusion. Slobod and Thomas [12] also observed that, at low flow rates of the order of *1 ft/day*, which provides a long residence time for the fluid to remain in contact, transverse diffusion is sufficiently rapid to modify the finger geometry. Blackwell [13] suggested that the dimensionless parameter Ud_p/D' characterizes the relative importance of convective dispersion and molecular diffusion in the microscopic mixing process in a porous

medium. Moreover, Blackwell observed that the transverse dispersion becomes more influential as the particle radius d_p decreases.

In most miscible displacements, which are not stabilized by gravity, transverse dispersion plays a much more important role than does longitudinal dispersion. This is because, in such displacements, solvent fingers penetrate into the oil for a variety of reasons, exposing a large surface area along the sides of the fingers over which transverse dispersion can occur. Thus, transverse dispersion can affect the growth of viscous fingers (especially in laboratory models) and have an influence on the sweepout of the oil.

2.1.2 Microscopic Dispersion Coefficients

The diffusion-convection equation, given below as Eq. 2.1.1, describes the overall transport and mixing of fluids flowing through a porous medium [2]. Terms here show the relation " convective flow " plus " dispersive flow " equals " accumulation "; that is,

$$-(\mathbf{U} \cdot \nabla C) + \nabla \cdot (\mathbf{D} \cdot \nabla C) = \frac{\partial C}{\partial t} \quad (2.1.1)$$

where D is the tensor formulation of dispersion coefficients, which represents both the longitudinal and the transverse dispersion coefficients. Furthermore, both of the dispersion coefficients include a molecular diffusion contribution and a convective dispersion contribution. However, convective dispersion is nonisotropic because the longitudinal and transverse convective dispersion coefficients are not equal.

For a constant velocity in the x direction only, Eq. 2.1.1 becomes

$$D_L \frac{\partial^2 C}{\partial x^2} + D_T \left(\frac{\partial^2 C}{\partial y^2} + \frac{\partial^2 C}{\partial z^2} \right) - U \frac{\partial C}{\partial x} = \frac{\partial C}{\partial t} \quad (2.1.2)$$

The first term in Eq. 2.1.2 accounts for longitudinal dispersion in the x direction, and the second and third terms account for transverse dispersion in the y and z directions. The parameters D_L and D_T stand for longitudinal and transverse dispersion coefficients, respectively.

One of the goals of laboratory miscible displacement is to obtain longitudinal and transverse dispersion coefficients. Typically, the experiments are conducted by using equal-viscosity and equal-density fluids, and by assuming that no fingering exists during the miscible displacement; consequently, the flow is described well by convection-diffusion theory. Methods for determining longitudinal and transverse dispersion coefficients from laboratory displacements are discussed by various authors. These methods generally involve fitting the solvent effluent concentration profile from a laboratory displacement with an appropriate solution of the diffusion-convection equation, and determining the value of the dispersion coefficient that results in the best agreement of experimental and calculated concentration profiles.

The classic work of Sir G. Taylor [2] and its extension by Aris [14] have shown that it is possible to describe, theoretically, the amount of mixing in single straight capillaries when solvent displaces a fluid of equal viscosity and equal density. Aris showed that the lengths of the mixing zones, L_m , corresponding to 10% and 90% concentration levels of the solvent, is related to either D_L or D_T by Eq. 2.1.3; that is,

$$L_m = 3.62\sqrt{Dt} \quad (2.1.3)$$

If one prefers to use other concentration values, such as 20% and 80% , or 16% and 84%, a different constant would be necessary (e. g., 2.380 for 20 and 80 per cent concentrations). These constants can be obtained from any standard table of error integrals [7].

Blackwell [13] presented the results of an experimental investigation concerning the mixing of miscible fluids in sand-packed tubes. By plotting D/D' versus Ud_p/D' , he demonstrated that for values of Ud_p/D' less than 0.04, which correspond to small particle sizes and/or low rates typical of reservoir conditions, the dispersion coefficient is equal to the molecular diffusivity divided by a tortuosity factor of 1.5. This tortuosity factor is typical of values obtained for unconsolidated sand packs. For values of Ud_p/D' greater than 0.04, convective mixing causes the dispersion coefficients to increase above the molecular diffusivities. For values of Ud_p/D' greater than 0.5, all the results can be represented by Eq. 2.1.4

$$\frac{D}{D'} = 8.8 \left(\frac{Ud_p}{D'} \right)^{1.17} \quad (2.1.4)$$

Furthermore, convective dispersion becomes important for values of Ud_p/D' greater than 6 in capillary tubes, and for values of Ud_p/D' greater than 0.04 in porous media. The fact that convective dispersion in porous media becomes dominant for smaller values of Ud_p/D' is interpreted as being a result of unequal flow velocities in adjacent channels. Blackwell also suggested that a correlation of dispersion coefficients with Ud_p/D' may give adequate approximations of dispersion coefficients for most practical calculations.

In 1961, Brigham et al. [7] showed a convenient method for determining the longitudinal dispersion coefficient for fluids using a favorable viscosity ratio. For the purposes of simplifying the measurement, they defined an error function parameter, U_E , which is expressed as $(V_p - V_i)/V_i^{1/2}$, and related the parameter to the longitudinal dispersion coefficient. By plotting the per cent of displacing fluid versus the error function parameter on probability co-ordinates, a best straight line can be drawn through the data

points. Values of U_E are read from this line at the 10 per cent U_{10} and 90 per cent U_{90} concentration values. The dispersion coefficient is then defined as follows

$$D_L = \frac{1}{V_p T} \left[\frac{L(U_{90} - U_{10})}{3.625} \right]^2 \quad (2.1.5)$$

For fluids having an unfavorable viscosity ratio, as they have shown, the data exhibit obvious curvature, instead of a straight line, on probability co-ordinates, which indicates both a greater amount of mixing and the effect of instability.

In 1962, after reviewing the published data on longitudinal and transverse dispersion coefficients, Perkins and Johnston [11] recommended the following equations for calculating the longitudinal dispersion coefficient, D_L , and the transverse dispersion coefficient, D_T , for fluids of equal-viscosity and equal-density:

$$\frac{D_L}{D'} = \frac{1}{F\phi} + 0.5 \frac{U\sigma d_p}{D'}, \quad \left(\frac{U\sigma d_p}{D'} < 50 \right) \quad (2.1.6)$$

and

$$\frac{D_T}{D'} = \frac{1}{F\phi} + 0.0157 \frac{U\sigma d_p}{D'}, \quad \left(\frac{U\sigma d_p}{D'} < 10^4 \right) \quad (2.1.7)$$

where σ is defined as the inhomogeneity parameter; for unconsolidated uniform beads, σ is equal to one. The formation factor, F , was shown by Slawinski [15] to be a function of porosity of the porous media; that is,

$$F = \frac{[1.3219 - 0.3219 \cdot \phi]^2}{\phi} \quad (2.1.8)$$

In 1988, Arya et al. [16] examined the length dependence of the macroscopic dispersivity, α_{md} , and defined it as follows

$$\alpha_{md} = \frac{\phi D_L}{U} \quad (2.1.9)$$

As they pointed out, measured dispersion coefficients increase with the length scale of the displacement, which is considered a reflection of the fact that larger-scale local variations in permeability can be present as the length of the system increases. In an examination of the data of Lelleman-Barres and Peaudecerf, as well as Pickens and Grisak [17], they made log-log data fits to present an empirical relationship which may be applied for a single type of porous medium; that is,

$$\alpha_{md} = 0.044L^{1.13} \quad (2.1.10)$$

However, as they noted, Eq. 2.1.10 should not be considered conclusive because of a wide scatter in the data used.

In 1990, by assuming that the flow is described well by convection-diffusion theory, Udey and Spanos [18] suggested that the longitudinal dispersion coefficient, which varies linearly with both velocity and length of the porous medium, could be estimated from effluent concentration measurements using Eq. 2.1.11 as follows

$$D_L = D_L^0 L U \quad (2.1.11)$$

where the D_L^0 is given by

$$D_L^0 = \frac{1}{8} \left[\left(\sqrt{U_i|_{c=0.16}} - \frac{1}{\sqrt{U_i|_{c=0.16}}} \right) - \left(\sqrt{U_i|_{c=0.84}} - \frac{1}{\sqrt{U_i|_{c=0.84}}} \right) \right]^2 \quad (2.1.12)$$

In Eq. 2.1.12, $U_i|_{c=0.16}$ and $U_i|_{c=0.84}$ are time-independent isoconcentration velocities at solvent concentration values of 0.16 and 0.84, respectively.

Theoretical and experimental investigations of transverse dispersion have been few, and data are in scant supply, especially when the viscosity and density of fluids are not equal. Pozzi and Blackwell [19] presented the results of an investigation which tested the effects of viscosity and density differences on the transverse dispersion coefficient. They observed that there is a close similarity between the correlation of D_T/D' versus $d_p U/D'$ for equal-density, equal-viscosity fluid systems and the correlation of D_T/D' versus $d_p U/D' N_p$ for unequal-density, unequal-viscosity fluid systems, where N_p is oil recovery (fraction of a pore volume). Therefore, they suggested that the transverse dispersion coefficient for fluid systems of equal-density and equal-viscosity may be adapted for use in unequal-density and unequal-viscosity fluid systems.

However, several experimental observations [7, 19] have shown that a small increase in the density difference of the fluids used resulted in a significant decrease in the transverse dispersion coefficient. Van der Poel [3] used a simple approach, which was referred to as "technique of steady-state experiments", to determine the transverse dispersion coefficient under steady-state conditions. The technique enables one to calculate

the coefficient by measuring the width of the transition zone due to molecular diffusion. The experiments, performed in horizontally laid glass-bead packs ranging in permeability from 805 darcies to 0.43 darcies, showed that a transition zone is formed whose width, once steady-state is reached, varies with distance traveled, but not with time. In particular, these experiments demonstrated that the width of the transition zone increases in direct proportion to the square root of the distance traveled.

2.1.3 Factors Affecting Miscible Displacement Behavior

There are many factors that control the efficiency of miscible displacements. In general, these factors influence the mixing process at both the microscopic level and the macroscopic level.

2.1.3.1 Effect of Viscosity Ratio

Various investigators have noted that the dispersion coefficient decreases as the mobility ratio of the miscible fluids becomes more favorable. In particular, Lacey et al. [20] found that the length of the mixing zone increases as the oil viscosity increases. Blackwell et al. [21] presented an investigation on the effects of adverse mobility ratios in which they observed that both breakthrough and cumulative recoveries decrease because of the increased instability in the displacements. Brigham et al. [7] reported that the value of the dispersion coefficient and the rate of dispersion increase with an increase in mobility ratio, and that with an unfavorable mobility ratio, viscous fingering usually occurs and the theoretical error function curve is no longer valid. Perkins and Johnston [11] suggested that a favorable mobility ratio will tend to suppress the effects of packing or permeability heterogeneities.

2.1.3.2 Effect of Density Differences

It has been well recognized that unequal density of fluids may, as a result of gravitational forces, influence dispersion. Favorable gravity forces tend to suppress dispersion while unfavorable gravity forces tend to increase the length of the mixing zone. However, in some reservoirs with dip, gravity can be used to advantage to improve sweepout and oil recovery. This is achieved by injecting the solvent updip and producing the reservoir at a rate low enough for gravity to keep the less dense solvent segregated from the oil, suppressing fingers of solvent as they try to form.

2.1.3.3 Effect of Velocity

It was first shown by Lacey et al. [20] that the mixing-zone length increases as the flow rate increases. Brigham et al. [7] have suggested that the dispersion coefficient is a measure of the rate of dispersion, and thus would be proportional to velocity. Blackwell et al. [21] noted that at low flow rates no fingers were observed and a piston-like displacement of the oil was achieved, but fingers were observed at high flow rates, and poor displacement efficiencies resulted. They also found that the dispersion coefficient at low flow rates for spherical glass bead packs is 70 per cent of the molecular diffusion coefficient.

At high flow rates, Keulemans' theory [22] predicts that the dispersion coefficient is proportional to the first power of flow rate. Other theories predict a second power dependence. Brigham et al. [7] showed that the magnitude of the exponent should lie somewhere between the values of 1 and 2, which agrees with the 1.17 power reported by Blackwell et al. [21], and a 1.20 power suggested by Aronofsky and Heller [23].

2.1.3.4 Effect of Model Dimensions

Control of displacement efficiency is also found to depend on the geometry of the model. In 1954, Offeringa and Van der Poel [24] first noted the deviations in the results of miscible displacements using short cores as compared to those using long cores. In the tests reported, results with tubes of *1.60* and *3.0 m* in length are in good agreement, whereas those with a *1.03 m* tube show appreciable deviations. The reason for the difference, as they suggested, may possibly be that the diameter of the short tube (*6.4 cm*) is too small as compared to the grain size of the sand (*0.07 cm*).

Lacey et al. [20] reported that an increase in core diameter causes a drastic increase in the length of the mixing zone, which they explained by postulating an increased variation in permeability for larger diameter cores. As a consequence, they concluded that the transverse dispersion process may stabilize laboratory displacements because disturbances are limited to short 'wave lengths', but that it may not stabilize field floods because of the larger cross section of reservoirs. Blackwell et al. [21] presented similar observations as those of Lacey et al., in which they found that breakthrough recovery decreases with decreasing length-to-width ratio of the model.

However, Brigham et al. [7] showed an opposite observation from those of Lacey et al.; that is, they observed a longer mixing zone in a smaller diameter pack. Their explanation of this fact is that boundary effects arise when smaller models are considered, or that it is more difficult to achieve uniform packing in a small tubing.

Coskuner and Bentsen extended the small perturbation theory of Chuoke [25,26], which enables one to describe the effect of length theoretically. The variational analysis from the theory indicates that fingers are more readily formed in a longer system than in a shorter one under similar flow conditions, provided that the transverse dimensions are the

same in both systems. They suggested that it is due to the fact that perturbations in the flow direction have wavelengths longer than the length of the porous medium and, therefore, the instability can not manifest itself. As a consequence, the system behaves as if it were stable. However, in a longer porous medium, these perturbation will be felt causing the displacement to be unstable.

2.1.4 Mathematical Models and Solutions

It has been shown [7,22,27,28] that, for fluids having favorable viscosity ratios, the diffusion equation with convection satisfactorily describes the behavior of a miscible displacement in a porous medium. Moreover, Taylor's [2] theory of displacement in capillary tubes, Keulemans' [22] "eddy diffusion" theory, Scheidegger's [27] statistical theory of porous media and Frankel's [28] "stagnant pockets" theory all predict that longitudinal dispersion is governed by the diffusion-convection equation, and that a plot of the concentration profile shows a straight line on arithmetic probability co-ordinate paper because the solution of the diffusion-convection equation is an error function.

2.1.4.1 Convection-Dispersion Model

For viscous-finger free and gravity-stable miscible displacement in a linear uniform porous medium, the convection-dispersion equation is often used to describe the displacement process; that is,

$$D_L \frac{\partial^2 C}{\partial x^2} - U \frac{\partial C}{\partial x} = \frac{\partial C}{\partial t} \quad (2.1.13)$$

Brigham [29] presented several solutions of Eq. 2.1.13 which differ in form according to the different boundary conditions imposed. These solutions generally include an error function term and some other terms from the asymptotic expansion. However, the results calculated from different solutions, as Brigham has shown, become identical when the porous medium is long compared with the length of the mixed zone. The well-known solution of Eq. 2.1.13 for predicting effluent flowing (instead of in-situ) concentration is

$$C_f = \frac{1}{2} \operatorname{erfc}\left(\frac{1-V_{pi}}{2\sqrt{V_{pi}/\gamma}}\right) + \frac{1}{2\sqrt{\pi\gamma V_{pi}}} e^{-\left(\frac{1-V_{pi}}{2\sqrt{V_{pi}/\gamma}}\right)^2} \quad (2.1.14)$$

where C_f is related to the in-situ concentration C by Eq. 2.1.15

$$C_f = C - \frac{D_L}{U} \left(\frac{\partial C}{\partial x}\right) \quad (2.1.15)$$

Correa et al. [30] presented the dimensionless form of Eq. 2.1.13; that is

$$\frac{\partial^2 C_D}{\partial x_D^2} - \frac{\partial C_D}{\partial x_D} = \frac{\partial C_D}{\partial t_D} \quad (2.1.16)$$

where $x_D = (U/D_L)x$, $t_D = (U^2/D_L)t$, and $C_D(x_D, t_D) = (C(x, t) - C_0)/(C_I - C_0)$. Here, C_0 equals the initial solvent concentration in the core and C_I equals the solvent concentration at the injection face.

The analytical solution for the flowing concentration from Eq. 2.1.16 is

$$C_{fD}(x_D, t_D) = \frac{1}{2} \left[\operatorname{erfc} \left(\frac{x_D - t_D}{2\sqrt{t_D}} \right) + e^{x_D} \operatorname{erfc} \left(\frac{x_D + t_D}{2\sqrt{t_D}} \right) \right] \quad (2.1.17)$$

where the flowing concentration is related to the in-situ concentration by Eq. 2.1.18

$$C_{fD}(x_D, t_D) = C_D(x_D, t_D) - \frac{\partial C_D(x_D, t_D)}{\partial x_D} \quad (2.1.18)$$

Often, in the laboratory, one measures the effluent concentration at the outlet of the core. Therefore, it has been practical to set x equal to L , and to set x_D equal to $(U/D_L)L$. The dimensionless flowing concentration can be calculated for various values of injected pore volume. By taking the same approach as Brigham's [29], and noting that x_D/t_D results in Ut/L , or V_{pi} , which is pore volumes injected, the resulting equation is given by Eq. 2.1.19.

$$C_{fD}(V_{pi}, x_D) = \frac{1}{2} \left[\operatorname{erfc} \left(\frac{1 - V_{pi}}{2\sqrt{V_{pi}/x_D}} \right) + e^{x_D} \operatorname{erfc} \left(\frac{1 + V_{pi}}{2\sqrt{V_{pi}/x_D}} \right) \right] \quad (2.1.19)$$

2.1.4.2 Coats-Smith Model

When the porous medium is not uniform, the effluent concentration may not be described by Eq. 2.1.13, and an early breakthrough should be expected. To represent the

effect of rock heterogeneity or non-uniform flow, Deans [31] proposed a finite-stage model consisting of the mixing cell model augmented by terms accounting for mass transfer from the flowing stream into the stagnant volume. This "capacitance" model has three parameters: number of stages, amount of stagnant volume, and a rate constant for the mass transfer to the amount of stagnant volume. The capacitance model allows determination of the amount of the dead-end pore space in a porous matrix and the effect of velocity on the rate of diffusion into this space. Coats and Smith [32] extended Deans' model to include the effects of dispersion in the flowing fraction. The Coats-Smith (C-S) model is

$$\frac{\partial^2 C_D}{\partial x_D^2} - \frac{\partial C_D}{\partial x_D} = f \frac{\partial C_D}{\partial t_D} + (1 - f) \frac{\partial C_D^*}{\partial t_D} \quad (2.1.20)$$

and

$$(1 - f) \frac{N_{Pe}}{N_{Da}} \frac{\partial C_D^*}{\partial t_D} = (C_D - C_D^*) \quad (2.1.21)$$

where C_D equals the in-situ concentration in the flowing fraction, and C_D^* equals the in-situ concentration in the stagnant fraction. The three parameters are the flowing fraction, f , the macroscopic Peclet number, N_{Pe} , and the Damkohler number, N_{Da} . The C-S model can be solved either by a fully explicit finite-difference method, or by Laplace transform to obtain analytical approximations for short and long times [30]. The C-S model has been

used extensively to interpret miscible displacements in the reported investigations. However, as Coats and Smith pointed out, if macroscopic heterogeneity is present, in the sense that regions of the porous medium are significantly different in permeability or pore structure, none of the currently available convection-dispersion models which allow an analytical solution take heterogeneity into account. Furthermore, the C-S model does not take into consideration displacements with fluids of unfavorable viscosity ratio.

2.1.4.3 Porous-Sphere Model

A more complex model, the Porous-Sphere (P-S) model, was presented by Bretz and Orr [33]. In addition to taking convection and longitudinal dispersion in the flowing fraction into consideration, diffusive interchange of material in the pore spheres with fluid flowing past them is included as well. In the P-S model, flow occurs between spheres, which are themselves porous. The model is quite similar to the C-S model except that there is an explicit representation of the length scale of the low-permeability (stagnant) regions. Moreover, the P-S model also depends on three parameters which are the fractional flow, the Peclet number associated with convection and dispersion in the flowing stream, and a second Peclet number which is defined as a ratio of characteristic times for diffusion in the spheres to that for the flow through the core.

However, the P-S model has the same limitations for miscible fluids, as it requires matched viscosities and densities. Furthermore, as Bretz and Orr observed, the theoretical prediction using the P-S model for slower displacements agrees well with experimental data; at higher velocities, however, it is not as good. Neither the prediction of the P-S model nor the best fit of the C-S model fits the experimental observations at higher velocities, which may be explained as effects of instability.

2.1.4.4 Transverse-Matrix-Diffusion Model

A similar approach to that of the P-S model was taken by Grisak and Pickens [34]; that is, convection and longitudinal dispersion are considered in the flowing fraction, and transverse diffusion is taken into account between the flowing and stagnant fractions. The equations are as follows,

$$\frac{\partial^2 C_D}{\partial x_D^2} - \frac{\partial C_D}{\partial x_D} = f \frac{\partial C_D}{\partial t_D} + (1-f) \frac{1}{\lambda} \left(\frac{\partial C_D^*}{\partial z_D} \right)_{z_D=0} \quad (2.1.22)$$

and

$$\lambda \frac{\partial C_D^*}{\partial t_D} = \frac{\partial^2 C_D^*}{\partial z_D^2} \quad (2.1.23)$$

where $z_D = z/h_t$, z = the vertical thickness of the core, h_t = the thickness of the stagnant zone, and

$$\lambda = \frac{h_t^2 U^2}{D_T D_L} = N_{Pe} N_{Pe_t} \quad (2.1.24)$$

Correa et al. [30] presented the solution of Eq. 2.1.22 and 2.1.23 in Laplace space, and used an efficient numerical inverter to invert the model solutions from Laplace space to

real-time space. They suggested that the transverse-matrix-diffusion model is suitable for describing reservoir miscible performance, provided the parameters may be determined from laboratory displacements.

2.2 THEORY OF UNSTABLE DISPLACEMENT

It has long been recognized that miscible displacement with a low viscosity fluid displacing a more viscous oil will be an unstable process leading to the development of viscous fingers. Although laboratory experiments [35-42] and perturbation theory [28,39] have indicated the manner in which fingers will be initiated and grow, there is little direct evidence that fully developed finger growth will necessarily depend on the geometrical features of the porous medium. It has been shown that, for favorable viscosity ratios, the convection-dispersion equation and its extended models may describe satisfactorily the behavior of miscible displacements in porous media; however, the prediction fails whenever viscous fingering occurs. Numerous attempts [35-41] to develop a satisfactory mathematical description for the case of an unfavorable viscosity ratio have been reported, but they have met with only partial success. These attempts, which are reviewed by Koval [40], have taken two approaches: 1) development of a flow model analogous to the Buckley-Leverett method by neglecting the effects of mixing, and 2) simultaneous application of the diffusion equation with a convection term for mass transfer. The former method is simpler from a mathematical point of view, but is limited to displacements with negligible mixing effects. The latter method has to be solved numerically even though it represents a more precise description of the process.

2.2.1 Viscous Fingering

The exact process of finger initiation is still obscure although it generally is attributed to the small microscopic variations in a porous medium. Finger initiation takes place in any porous medium whose pore structure is microscopically random. Viscous fingers are observed even in laboratory Hele-Shaw models, which are physical models constructed of two parallel plates with a gap between the plates for the flow of the liquids. Apparently, even slight variations on the plate surface and/or of the gap width are sufficient to initiate fingers.

By applying Darcy's equation for linear flow and assuming that longitudinal dispersion is negligible, it is found that a small perturbation of the undisturbed front grows exponentially with time when the mobility ratio is larger than one, but decays exponentially with time if the mobility ratio is less than unity.

Frontal perturbation theory [39,41,42] has been used commonly to describe finger initiation. In this method, a spectrum of wavelengths of perturbations of the front is assumed. The resulting analysis shows that for any given set of displacement conditions, perturbations below a critical wavelength will be eliminated by dispersion which acts to oppose finger growth by moderating the viscosity contrast; that is, only perturbations above the critical wavelength will grow continuously at an unfavorable mobility ratio. The theory also suggests that transverse dispersion is insufficient to damp out all the flow perturbations in most laboratory cores.

Gardner and Ypma [42] published the following equation to calculate the critical wavelength for the case of an initially sharp solvent/oil interface

$$\lambda_c = 5.6569\pi \frac{\mu_o + \mu_s}{\mu_o - \mu_s} \frac{D_T}{U} \quad (2.2.1)$$

Once fingers above the critical wavelength are initiated, they begin to grow in length, and the fingering mechanism rapidly becomes dominant. They found that longitudinal dispersion is a relatively unimportant factor in the growth of fingers. A large degree of transverse dispersion, on the other hand, can stabilize the displacement by eliminating fingers, or at least suppressing them to one or two large ones.

2.2.2 Mathematical Models and Solutions

Miscible displacement at an unfavorable mobility ratio is known to be subject to viscous fingering of solvent into the oil. There have been many attempts to characterize this phenomenon through laboratory experiments, empirical methods, and direct simulations. These studies focused mainly on the factors determining fingering behavior in miscible displacement, such as adverse mobility ratio, system size and heterogeneity.

2.2.2.1 K-Factor Method

In 1963, Koval [40] introduced the K-factor method for the mathematical treatment of viscous fingering in miscible displacement. Koval's K-factor method allows for taking into account the effects of viscosity ratio and heterogeneity of porous media. He suggested that fingering is caused by viscosity differences, and is aggravated by inhomogeneities in the porous medium. Effects of mixing, as considered by Koval, could be represented by a single parameter, H , called the heterogeneity parameter. To take into account the decrease in the actual viscosity ratio, which happens when solvent dissolves in the oil, he defined the following expression for the effective viscosity ratio

$$E = \left[0.78 + 0.22 \left(\frac{\mu_o}{\mu_s} \right)^{1/4} \right]^4 \quad (2.2.2)$$

The product of H and E was termed the K-factor. Application of the K-factor is limited because it neglects the most important miscible phenomena, namely, diffusion and dispersion. The method produces good matches with some experimental data in which diffusion and dispersion have little influence on the formation of viscous fingers. However, when the effect of dispersion is not negligible, good matches are not easy to produce, as some investigators [38] have found. Furthermore, it is at least questionable to assume a linear dependence of relative permeability on saturation. Koval's justification for the linear dependency was the assumption that no interaction occurred between solvent and oil, which may not hold true in the mixing zone where the individual identities of the fluids are no longer retained.

In Koval's investigation, although length, length to diameter, and length to cross sectional area of the cores used varied over a considerable range, no systematic study was made to evaluate the specific effects of these variables. In general, it was observed that the shorter the core, the higher the heterogeneity factor. This observation could be the result of the greater significance of longitudinal dispersion in short cores.

2.2.2.2 Dougherty's Method

In 1963, Dougherty [38] presented a pair of non-linear hyperbolic partial differential equations for a one-dimensional unstable miscible displacement, which are based upon a flow model similar to the Buckley-Leverett model for immiscible displacement. The effect of mixing is included and three parameters, in addition to the heterogeneity factor, are used to characterize the mixing process. Numerical integration of the nonlinear hyperbolic

partial differential equations gives volumes of dissolved and undissolved solvent as functions of space and time. By using a trial-and-error approach, the values of the parameters can be obtained to make theoretical predictions in agreement with experimental results.

Dougherty suggested that the heterogeneity factor H proposed by Koval may be a satisfactory concept only for horizontal systems. Moreover, he observed that mixing varies in a highly nonlinear manner with the degree of fingering and the concentration of solvent in the oil phase.

2.2.2.3 Jankovic's Method

Jankovic [41] introduced an analytical model to represent miscible relative permeability curves which enables one to predict the saturation distribution and recovery efficiency at breakthrough for both stable and unstable miscible displacements. However, there are at least three concerns which need further examination. These are 1) the problem of an unclearly defined solvent fractional flow equation; 2) the assumption that the dispersion coefficient is a linear function of velocity, which may not be valid at high flow rates as some investigators have shown; and 3) the fact that the solution is only exact where the solvent fractional flow is equal to the solvent concentration.

2.2.2.4 Peaceman And Rachford's Method

In 1962, Peaceman and Rachford [43] presented a finite-difference method for calculating miscible displacement of fluids in porous media. The approach takes into account the influence of gravity, permeability variations, two-dimensional dispersion, and fluid viscosity and density differences. The set of partial differential equations are

$$\nabla \cdot \frac{k}{\mu} (\nabla P + \rho g \nabla h) = 0 \quad (2.2.3)$$

and

$$D_L \frac{\partial^2 C}{\partial x^2} + D_T \frac{\partial^2 C}{\partial y^2} + \nabla \cdot \frac{C \cdot k}{\mu} (\nabla P + \rho g \nabla h) = \phi \frac{\partial C}{\partial t} \quad (2.2.4)$$

They introduced an average density and viscosity to represent the mixed fluids, which are expressed as the following functions of the solvent concentration

$$\rho_m = \rho_s C + \rho_o (1 - C) \quad (2.2.5)$$

and

$$\ln \mu_m = X \ln \mu_s + (1 - X) \ln \mu_o \quad (2.2.6)$$

where

$$X = \frac{C}{C + \beta(1 - C)} \quad (2.2.7)$$

Peaceman and Rachford's numerical procedure permits one to calculate viscous fingers formed spontaneously in the presence of small, random variations of permeability with position. However, whenever a numerical approach is taken, problems such as grid orientation, numerical instability and numerical dispersion may affect adversely the results of numerical solutions, which limits the application in many cases.

2.2.2.5 Vossoughi's Method

Based on material-balance concepts, Vossoughi et al. [44] developed a generalized form of the convection-dispersion equation for one-dimensional miscible flow where the viscosity ratio may be unfavorable, and consequently viscous fingers may exist. The mathematical model incorporates a fractional flow function in the convection term, and the fractional flow is derived from Darcy's law by using a concentration-dependent average viscosity. The partial differential equation in dimensionless form is given by

$$\frac{\partial^2 C_D}{\partial x_D^2} - N_{Pe} \frac{\partial f_s}{\partial S} \frac{\partial C_D}{\partial x_D} = \frac{\partial C_D}{\partial t_D} \quad (2.2.8)$$

The fractional flow function, f_s , as defined by Vossoughi et al., is different in form for stable and unstable displacement processes. If the displacing and displaced fluids have equal viscosities, and the displacement is stable, then

$$f_s = S \quad (2.2.9)$$

Hence,

$$\frac{\partial f_s}{\partial S} = 1 \quad (2.2.10)$$

But, if the viscosity ratio becomes unfavorable, the relationship is given by

$$f_s = \frac{M - [S + (1-S)M^{1/a}]^a}{M-1} \quad (2.2.11)$$

The complexity of Eq. 2.2.8 makes it impossible to achieve an analytical solution. Vossoughi et al. suggested that a variational Galerkin [45] method, which makes the highly non-linear original partial differential equations linear, should be used to integrate Eq. 2.2.8.

2.2.3 Criterion of Instability in Miscible Displacement

The stability of a miscible displacement is of particular importance, as it determines the success of the miscible drive and the recovery efficiency of the process. When the displacement is stable, a piston-like mixing zone tends to reduce finger development and, eventually, to suppress the growing fingers. Otherwise, the viscous fingers will develop increasingly and lead to an early breakthrough of displacing solvent. A few investigations have been conducted to study the conditions under which the displacement becomes unstable, or under which a gravity tongue and/or viscous fingers begin to develop. In particular, Dumore [46] derived a stability criterion by investigating how the pressure gradient, determined using Darcy's law, changed with depth in the direction of flow, while Coskuner and Bentsen [47] employed small-perturbation theory to obtain a stability criterion.

2.2.3.1 Dumore's Method

In 1964, Dumore [46] presented a criterion for predicting the instability of vertical flow in a homogeneous permeable medium saturated with oil which is displaced downwards by a less viscous solvent. In the development of such a criterion, Dumore assumed that a horizontal interface divided the oil and solvent initially, and that the pressures at the interface were distributed evenly; but that the pressure at the interface becomes unevenly distributed even with a small protrusion of solvent into the oil phase.

The interface is neutrally stable or unstable depending on whether the pressure gradient in the solvent is less than, equal to, or greater than that in the oil. By applying Darcy's law, a critical velocity was given as follows

$$V_c = \frac{\rho_o - \rho_s}{\mu_o - \mu_s} K_g \quad (2.2.12)$$

Practically, the horizontal interface will be stable if the velocity has a lower value than the critical velocity. A similar determination of instability applies to the case of immiscible flow.

Taking the effect of mixing into account, Dumore suggested that the displacement would be completely stable when the pressure gradient in the mixing zone increases continuously with depth, which implies that the second derivative of pressure with respect to vertical distance must have a positive value for each layer in the mixing zone. The stable velocity, which differs from the critical velocity, is defined by

$$V_{st} = \frac{\beta (\rho_o - \rho_s)}{\mu_o (\ln \mu_o - \ln \mu_s)} K_g \quad (2.2.13)$$

The ratio of the stable and the critical velocity is given by

$$\frac{V_{st}}{V_c} = \beta \left(1 - \frac{1}{M} \right) / \ln M \quad (2.2.14)$$

where β is the empirical constant shown in Eq. 2.2.7. Dumore noted that if the actual average displacement velocity, V , is greater than V_C , that is, if $V > V_C$, the displacement is unstable and solvent fingers into the oil. If $V < V_{st}$, the displacement is completely stable. However, if $V_{st} < V < V_C$, a portion of the transition zone is unstable and fingers into the oil. When this latter condition is met, as observed by Dumore, there is no instability causing the pure solvent to finger into the oil because the displacement rate is below the critical rate. However, fingering within a portion of the solvent/oil transition zone causes more rapid dilution of a solvent slug by mixing than would be the case with a completely stable displacement. The experimental results showed fair agreement with the behavior predicted using the instability criterion. For velocities above the critical rate, pronounced viscous fingers were observed, which led to a further decrease in recovery at breakthrough. Moreover, the breakthrough recovery is low if $V > V_{st}$, and continuously decreases as the displacement rate increases. Nevertheless, as Dumore observed, oil recovery at one pore volume injected is not as much affected by velocity as that at breakthrough; that is, the breakthrough recovery may decline from 90% to 40% as soon as the displacing rate exceeds the critical rate, but oil recovery at one pore volume injected varies less than 10% at such a displacing rate. The amount of solvent needed for 100% recovery of oil increases when $V > V_C$, whereas it remains the same when $V < V_C$.

2.2.3.2 Coskuner and Bentsen's Method

Coskuner and Bentsen [47] derived a dimensionless scaling group and a theoretical marginal instability boundary for miscible displacement in a three-dimensional porous medium, which was extended for application in a Hele-Shaw system as well. The theory is based on small perturbation concepts, and a variational technique is utilized to solve the

resulting equations with appropriate boundary conditions. The resulting analytical expression for determining the marginal instability boundary is shown to be

$$-R^2 = \frac{1}{\alpha^2} \left(\frac{\pi^2}{L^2} + \alpha^2 \right) \left(\frac{\pi^2}{L^2} + K_d \alpha^2 \right) \quad (2.2.15)$$

where K_d is the ratio of the transverse to the longitudinal dispersion coefficient, and $-R^2$ is a function of fluid and porous medium properties. For a three-dimensional system, $-R^2$ is defined by

$$-R^2 = - \frac{K \left[g \frac{\partial \rho}{\partial C} \Big|_{C=\bar{C}} - \frac{v \partial \mu}{K \partial C} \Big|_{C=\bar{C}} \right] \frac{\partial C}{\partial z} \Big|_{C=\bar{C}}}{\mu \phi D_L} \quad (2.2.16)$$

and α^2 is defined by

$$\alpha^2 = \pi^2 \left(\frac{1}{L_x^2} + \frac{1}{L_y^2} \right) \quad (2.2.17)$$

For an infinitely long porous medium, Eq. 2.1.15 becomes

$$-R^2 = K_d \alpha^2 \quad (2.2.17)$$

The experimental results of Coskuner and Bentsen demonstrated the validity of the criterion for miscible flows in a Hele-Shaw system. A distorted zero concentration line at the displacing front was observed whenever the instability number was greater than the marginal instability boundary; and an almost unperturbed zero concentration line was observed when the instability number was less than the marginal instability boundary. However, as noted by Coskuner and Bentsen, the magnitude of any instability criterion which is derived by using any small-perturbations theory may not be used to describe the degree of the instability in the displacement. In other words, the instability number may be used only to determine whether a displacement is stable or not by comparing the number with the marginal boundary; a large instability number may not indicate that a more distorted zero concentration line at the displacing front would occur. Furthermore, Coskuner and Bentsen's model, like all the existing analytical analyses of unstable miscible displacement, does not take into account the effect of heterogeneity in a porous medium, and is limited to fluids with small density and viscosity differences.

3. STATEMENT OF THE PROBLEM

From the review of the previous research on miscible displacement in porous media, it becomes clear that several factors have been identified as being influential in the stability, dispersion and oil recovery of miscible displacements. These factors are the heterogeneity of the porous medium, the viscosity ratio, the density difference, the displacement rate and the geometry of the porous medium. The length of the porous medium, however, has been studied little, even though it has been theoretically identified as being influential [47]. Thus, there is a need for obtaining more theoretical and experimental information concerning the effect of the core length on the instability of miscible displacements.

The main objectives of this investigation were two-fold. The first objective was to derive a scaling group which removes the limitation, underlying Coskuner and Bentsen's instability criterion, of having fluids with the same (or a small difference in) viscosity and density. The second was to study linear miscible displacement in glass-bead packs which varied in length, and thus to verify experimentally the effect of system length on the instability of the displacements as predicted by Coskuner and Bentsen's instability theory.

In order to realize the first objective, it is proposed to use a material balance technique to derive a generalized concentration-dispersion equation which takes into account the difference of density and viscosity between the displacing fluid and the displaced fluid. Then, by using this equation, together with the small perturbation and instability theory of Coskuner and Bentsen, it is proposed to derive a new scaling group, which allows one to estimate the distance from the inlet face of a linear porous medium at which the displacement becomes unstable. Moreover, an attempt will be made to establish a theoretical basis for the dependence of instability on core length.

In order to apply Coskuner and Bentsen's instability criterion, which was given as a scaling group, one has to evaluate parameters such as the transverse and longitudinal dispersion coefficients of the miscible fluids. Previous theoretical and experimental investigations of miscible displacement have shown that a stable miscible displacement may be described adequately by the convection-dispersion equation, and that the dispersion coefficients may be determined experimentally, provided that the densities and viscosities of the fluids are matchable. However, there is a lack of adequate models and the means of determining dispersion coefficients for displacements where viscous fingers occur and appear to dominate the process. In the present study, as the fluids had an unfavorable viscosity ratio and different densities, the available theoretical and/or empirical correlations for estimating these coefficients were no longer valid. Thus, a problem arises in finding a method to estimate the dispersion coefficients approximately. Consequently, an attempt will be made to develop an approach for approximating the longitudinal dispersion coefficient under the conditions employed in this study.

4. THEORY

This chapter consists of two main sections. In the first section, a new approach is presented to show the development of a generalized convection-dispersion equation and its simplified form which incorporates a fractional flow term in the convection term. This fractional flow term is derived from Darcy's law and is related to solvent concentration. This new approach is based on a differential material balance technique, which leads to a generalized convection-dispersion equation by taking into account miscible fluids with unequal density and unequal viscosity. In comparison with other generalized convection-dispersion equations [see Appendix A], this model gives clearer insight into the mathematical description of the miscible displacement process.

In the second section, using the generalized convection-dispersion equation, together with the small perturbation and instability theory of Coskuner and Bentsen, a new scaling group is derived, which defines the distance from the inlet face at which a miscible displacement in a one-dimensional porous system becomes unstable. This new criterion allows fluids to have large differences in density and viscosity. Moreover, a correlation between the core length of porous media and the amplitude of perturbations in solvent concentration is presented to show a theoretical basis for the dependence of instability of a miscible displacement on core length.

4.1 A GENERALIZED CONVECTION-DISPERSION EQUATION

It is assumed that the flow system is comprised of two miscible fluids: oil with density ρ_o and viscosity μ_o , which is the displaced fluid; and solvent with density ρ_s and viscosity μ_s , which is the displacing fluid. The viscosity ratio of the two fluids may be

unfavorable, and consequently viscous fingers may exist. The two fluids are incompressible and miscible in all proportions. It is also assumed that displacements take place in a one-dimensional homogeneous and isotropic porous medium. The linear displacement is in the x direction, and there is a net dispersion of material only in the direction of flow.

Consider now a resident oil being displaced by a solvent. The solvent, which is called a free solvent, has the properties of pure solvent. A free solvent phase exists when a solvent of lower density displaces a heavier oil. The fraction of pore volume occupied by this phase is defined to be the solvent saturation, which is designated S . The fraction of pore volume occupied by the oil phase is designated S_o . The solvent-oil mixing phase consists of oil containing dissolved solvent; hence, it has properties of the mixture such as density ρ_m and viscosity μ_m which vary with the composition of the mixture. The fractional volume of the solvent in the oil phase is designated by the symbol C , which is also called the solvent volume concentration. Solvent is transferred from the free solvent phase to the solvent-oil phase at a rate which depends on the composition of the mixing phase, the solvent saturation as well as the solvent-oil saturation, or $I-S-S_o$.

A material balance on the displacing fluid across the inlet plane of an element gives

$$\text{ACCUMULATION} = \text{INPUT} - \text{OUTPUT} \quad (4.1.1)$$

If two miscible fluids are brought into contact with an initially sharp interface, the subsequent transport and mixing of the fluids occurring at the inlet face of the element, which is located at x , is the amount of solvent entering the element by convection and dispersion in a time interval Δt . The convection term is represented by a fractional flow

function, f_s , and the dispersion term is represented by two kinds of dispersive contribution in the direction of flow; that is, the longitudinal dispersion of the free solvent phase with the solvent-oil mixing phase, and of the mixing phase with the oil phase. The resulting expression is given by

$$\left[V f_s \rho_s - D_L \left(\frac{\partial}{\partial x} (S \rho_s) + \frac{\partial}{\partial x} [(1 - S - S_o) C \rho_m] \right) \right]_x \Delta t \quad (4.1.2)$$

where V is the volumetric velocity, D_L is the longitudinal dispersion coefficient, which is a function of velocity, core-length and the effective viscosity ratio defined by Koval [40]. The subscripts s , o , and m denote free solvent, oil and the mixture of the two, respectively. The displacing fluid fractional flow, f_s , is defined as

$$f_s = \frac{q_s}{q} \quad (4.1.3)$$

where q_s is the solvent, or the displacing fluid flow rate, and q is the total volumetric flow rate. Similarly, at the outlet plane of the element, or $x + \Delta x$, the amount of solvent leaving the element by convection and dispersion over the time interval Δt is given by

$$\left[V f_s \rho_s - D_L \left(\frac{\partial}{\partial x} (S \rho_s) + \frac{\partial}{\partial x} [(1 - S - S_o) C \rho_m] \right) \right]_{x+\Delta x} \Delta t \quad (4.1.4)$$

Finally, the accumulation of solvent in the length increment Δx over the time interval Δt is

$$\phi \left[(S|_{t+\Delta t} - S|_t) \rho_s \Delta x + (1-S-S_o) C|_{t+\Delta t} - (1-S-S_o) C|_t \right] \rho_m \Delta x \quad (4.1.5)$$

If Eqs. 4.1.2, 4.1.4 and 4.1.5 are substituted into Eq. 4.1.1, both sides of Eq. 4.1.1 are divided by $\Delta x \Delta t$, and $\Delta x \rightarrow 0$, $\Delta t \rightarrow 0$ are allowed, Eq. 4.1.1 becomes

$$\begin{aligned} & D_L \left[\frac{\partial^2 S}{\partial x^2} \rho_s + \frac{\partial^2}{\partial x^2} [(1-S-S_o) C \rho_m] \right] - v \frac{\partial f_s}{\partial x} \rho_s \\ & = \phi \left[\frac{\partial S}{\partial t} \rho_s + \frac{\partial}{\partial t} [(1-S-S_o) C \rho_m] \right] \end{aligned} \quad (4.1.6)$$

If a pseudoconcentration, or an average in-situ mass concentration across the planar slice at which the material balance is made, \bar{C}_i , is defined as

$$\bar{C}_i = S \rho_s + (1-S-S_o) C \rho_m \quad (4.1.7)$$

where the density of the solvent-oil mixture is defined as

$$\rho_m = \rho_s C + \rho_o (1-C) \quad (4.1.8)$$

then Eq. 4.1.6 becomes

$$D_L \frac{\partial^2 \bar{C}_i}{\partial x^2} - v \rho_s \frac{\partial f_s}{\partial x} = \phi \frac{\partial \bar{C}_i}{\partial t} \quad (4.1.9)$$

Assuming that the displacing fluid must leave the core at a rate equal to the rate at which it crosses a plane lying at a distance x along the core, the rate, q_s , at which the displacing fluid crosses any plane, is defined by

$$q_s = UA\phi C - D_L A\phi \frac{\partial C}{\partial x} \quad (4.1.10)$$

where U is the interstitial velocity which is related to the average volumetric velocity V by $V = U\phi$, and A is the cross-sectional area of the core. As the total volumetric flow rate is $q = UA\phi$, the fractional flow of displacing fluid defined in Eq. 4.1.3 may be written as

$$f_s = C - \frac{D_L}{U} \frac{\partial C}{\partial x} \quad (4.1.11)$$

Differentiating f_s with respect to x leads to

$$\frac{\partial f_s}{\partial x} = \frac{\partial C}{\partial x} - \frac{D_L}{U} \frac{\partial^2 C}{\partial x^2} \quad (4.1.12)$$

and substituting Eq. 4.1.12 into Eq. 4.1.9 and rearranging yields

$$D_L \frac{\partial^2 C}{\partial x^2} + \frac{D_L}{\rho_s \phi} \frac{\partial^2 \bar{C}_i}{\partial x^2} - U \frac{\partial C}{\partial x} = \frac{1}{\rho_s} \frac{\partial \bar{C}_i}{\partial t} \quad (4.1.13)$$

It is interesting to note that Eq. 4.1.13 is similar in form to the convection-dispersion equation except that in two of the partial derivative terms the solvent concentration, C , is replaced by the pseudoconcentration, \bar{C}_i , and that an extra function of porosity and solvent density appears in front of the second-order partial derivative term, and that the solvent density appears on the right-hand side of the equation. However, it is essential for application purposes to define the pseudoconcentration term, \bar{C}_i , properly.

After solvent breakthrough, as shown in the experiments of the present study, the concentration variation for stable displacements reveals different features from that for unstable displacements. In stable displacements, the solvent concentration profile follows the typical error function curve after solvent breakthrough, whereas in unstable displacements, it shows two distinguishable periods of increase in solvent concentration: in the first period, the concentration value fluctuates with an increase in pore volume injected, which suggests that a finger-shaped solvent front passes through the outlet together with the displaced oil during this period; in the second period, the concentration profile follows the error function curve, which seems to indicate a solvent-oil mixture arriving at the outlet. Consequently, it is assumed that the free-solvent saturation S and the oil saturation S_o become negligible, once the major solvent-oil mixture arrives at the outlet, and that the pseudoconcentration is given by

$$\bar{C}_i = C\rho_m \quad (4.1.14)$$

where C is the average volumetric concentration of the solvent-oil mixture. Noting that the density of the solvent-oil mixture is also a function of the concentration C , as shown in Eq. 4.1.8, Eq. 4.1.14 can be rewritten as

$$\bar{C}_i = C[\rho_s C + \rho_o (1 - C)] \quad (4.1.15)$$

Taking the first- and the second-order derivatives of \bar{C}_i with respect to the distance x , and taking the first-order derivative of \bar{C}_i with respect to the time t , and substituting the resulting derivative terms into Eq. 4.1.13, one obtains

$$D_L \left[\frac{F(C) + \rho_s \phi}{\rho_s \phi} \right] \frac{\partial^2 C}{\partial x^2} + \frac{2 D_L (\rho_s - \rho_o)}{\rho_s \phi} \left(\frac{\partial C}{\partial x} \right)^2 - U \frac{\partial C}{\partial x} = \frac{1}{\rho_s} F(C) \frac{\partial C}{\partial t} \quad (4.1.16)$$

where

$$F(C) = \rho_o + 2C(\rho_s - \rho_o) \quad (4.1.17)$$

The above partial differential equation (Eq. 4.1.16) is a generalized convection-dispersion equation which takes into account the effects of unequal density and unequal viscosity. In Eq. 4.1.16, the difference in viscosities of the fluids does not appear explicitly. However, it is known [7,11,20,21,50] that the longitudinal dispersion coefficient, D_L , is dependent on viscosity ratio. Consequently, when the viscosities are not equal, value of D_L which reflects this fact must be used.

In general, such a complex non-linear partial differential equation can be solved only by using a numerical approach. The numerical solution of Eq. 4.1.16 is not the object of the present study, and will not be discussed further here. To obtain an analytical solution of

Eq. 4.1.16, a simplification has to be made. If the displacing and displaced fluids have equal densities ($\rho_o = \rho_s$), and noting that $F(C) = \rho_o$, Eq. 4.1.16 becomes

$$D_L \left[1 + \frac{1}{\phi} \right] \frac{\partial^2 C}{\partial x^2} - U \frac{\partial C}{\partial x} = \frac{\partial C}{\partial t} \quad (4.1.18)$$

Eq. 4.1.18 is identical in form to the convection-dispersion equation for stable displacement, except that there is a function of porosity in front of the second-order partial derivative term. This function appears because the effect of dispersion (see Eq. 4.1.11) is taken into account in defining solvent fractional flow. By neglecting the effect of the dispersive term in the solvent flow rate, one obtains

$$q_s = UA\phi C \quad (4.1.19)$$

and the fractional flow is given as

$$f_s = C \quad (4.1.20)$$

Hence, Eq. 4.1.9 becomes

$$D_L \frac{\partial^2 \bar{C}_i}{\partial x^2} - v\rho_s \frac{\partial C}{\partial x} = \phi \frac{\partial \bar{C}_i}{\partial t} \quad (4.1.21)$$

Similarly, for the case where dispersion is neglected in the fractional flow term, another generalized convection-dispersion equation for miscible fluids of unequal density and unequal viscosity can be derived. The resulting equation is given by

$$D_L \left[\frac{F(C)}{\rho_s \phi} \right] \frac{\partial^2 C}{\partial x^2} + \frac{2 D_L (\rho_s - \rho_o)}{\rho_s \phi} \left(\frac{\partial C}{\partial x} \right)^2 - U \frac{\partial C}{\partial x} = \frac{1}{\rho_s} F(C) \frac{\partial C}{\partial t} \quad (4.1.22)$$

If the fluids have equal densities, $\rho_o = \rho_s$, $F(C) = \rho_o$, and Eq. 4.1.22 becomes the familiar classical convection-dispersion equation shown below:

$$\frac{D_L}{\phi} \frac{\partial^2 C}{\partial x^2} - U \frac{\partial C}{\partial x} = \frac{\partial C}{\partial t} \quad (4.1.23)$$

In comparison with Eq. 4.1.18, Eq. 4.1.23 seems to represent less impact of dispersion on the solvent concentration profile which is a function of space and time. Moreover, Eq. 4.1.23 is limited because it holds true only when the displacing fluid and the displaced fluid have equal densities, and only when the solvent fractional flow, f_s , is equal to the solvent-oil mixture concentration, C .

By assuming that the porous medium extends infinitely in both the $+x$ and $-x$ directions, the boundary conditions are given as

$$\text{as } x \rightarrow +\infty \quad C(x,t) \rightarrow 0$$

and

$$\text{at } x = Ut \quad C(x,t) = 0.5 \quad (4.1.24)$$

The resulting solution of Eqs. 4.1.18 and 4.1.23 is well known [48]. It is

$$C = \frac{1}{2} \operatorname{erfc} \left[\frac{x - Ut}{2\sqrt{D_L t}} \right] \quad (4.1.25)$$

For the solution of Eq. 4.1.18 D_L' is

$$D_L' = D_L \left[\frac{1+\phi}{\phi} \right] \quad (4.1.26)$$

and for the solution of Eq. 4.1.23 D_L' is

$$D_L' = \frac{D_L}{\phi} \quad (4.1.27)$$

Often, in the laboratory, one measures the effluent concentration at the outlet end of the core. Therefore, it is more practical to set x equal to L in Eq. 4.1.25 and express the concentration in terms of injected pore volumes of the displacing fluid. If this is done, Eq. 4.1.25 may be written as

$$C = \frac{1}{2} \operatorname{erfc} \left[\frac{1 - V_{pi}}{2\sqrt{V_{pi}' \gamma}} \right] \quad (4.1.28)$$

where $V_{pi} = V_i / V_p$, or Ut/L ; and where γ , which is equal to UL/D_L' , is called dimensionless dispersion by Brigham [29]. Note that γ is defined in terms of D_L' instead of D_L , as defined by Brigham. To emphasize this difference, γ is written as γ_m in the next chapter.

Noticing the error in the theoretically predicted material balance, Brigham defined an effluent flowing concentration of the displacing fluid to make the convection-dispersion equation consistent with the boundary conditions. By Brigham's definition, the flowing concentration, C_f , is equal to the rate of displacing fluid divided by the total rate; that is,

$$C_f = \frac{q_s}{UA\phi} = C - \frac{D_L}{U} \frac{\partial C}{\partial x} \quad (4.1.29)$$

By taking the same approach as Brigham, one may evaluate the flowing concentration, C_f , by differentiating Eq. 4.1.25 as follows

$$\frac{\partial C}{\partial x} = -\frac{1}{2} \frac{\partial}{\partial x} \left[\operatorname{erf} \left(\frac{x - Ut}{2\sqrt{D_L' t}} \right) \right] = -\frac{1}{2\sqrt{D_L' t} \pi} e^{-\left(\frac{x - Ut}{2\sqrt{D_L' t}} \right)^2} \quad (4.1.30)$$

Substituting Eqs. 4.1.25, and 4.1.30 into Eq. 4.1.29, and evaluating the resulting expression at $x = L$, one obtains

$$C_f = \frac{1}{2} \operatorname{erfc} \left[\frac{1 - V_{pi}}{2\sqrt{V_{pi}/\gamma}} \right] + \frac{1}{2\sqrt{V_{pi} \pi \gamma}} e^{-\left[\frac{1 - V_{pi}}{2\sqrt{V_{pi}/\gamma}} \right]^2} \quad (4.1.31)$$

Notice that the effluent flowing concentration at one pore volume injected can be evaluated from Eq. 4.1.31 by setting V_{pi} equal to unity; that is,

$$C_f|_{V_{pi}=1} = \frac{1}{2} \left[1 + \frac{1}{\sqrt{\pi \gamma}} \right] \quad (4.1.32)$$

Eq. 4.1.32 shows that one can expect the effluent concentration at one pore volume injected to be greater than 50%. Moreover, Eq. 4.1.32 shows the possibility of a new approach to determine the longitudinal dispersion coefficient. As shown in Eq. 4.1.32, γ is equal to UL / D_L' . By determining the effluent concentration value at one pore volume injected, one may estimate the longitudinal dispersion coefficient using Eq. 4.1.32. It can be shown that, when the fluids used have a favorable viscosity ratio, the longitudinal dispersion coefficient determined using both the straight-line method [7] and the method suggested above yield comparable values. For example, in one of Brigham et al.'s displacements [7], the fluids had a viscosity ratio of 0.175, the core length was 83.3 cm (bead pack 131-1) and the velocity varied from 5.2 to 6.3×10^{-3} cm/sec. The dispersion coefficients obtained from the straight line on probability co-ordinate paper (Fig. 1) varied from 6.9736 to 8.4479×10^{-5} cm²/sec. The dispersion coefficients obtained using the effluent concentration curve of the displacement conducted in this bead pack (Fig. 2A) varied from 6.3015×10^{-5} cm²/sec. to 1.3107×10^{-4} cm²/sec. Because the straight-line method depends on many points on the plot, whereas the second method depends on one

point on the concentration profile, it is suggested that when fluids have a favorable viscosity ratio, to be more precise, one should use the straight-line method to estimate the longitudinal dispersion coefficient.

4.2 THE STABLE MIXING-ZONE LENGTH

Linear perturbation theory has been utilized by Coskuner and Bentsen [47] to develop a dimensionless scaling group to predict the instability of miscible displacements in three-dimensional porous media. However, the convection-dispersion equation used in their derivation is limited to fluids having identical density and viscosity. It is desirable to obtain a new scaling group defining the marginal instability boundary for a one-dimensional flow system when fluids of unequal density and unequal viscosity are considered.

Consider a vertical column of a homogeneous permeable medium saturated with oil. A solvent less dense and less viscous than the oil is used to displace the in-situ fluid downwards in the z direction at a constant rate. It is assumed that the two fluids are miscible in all proportions and the velocities of the oil and the solvent in the column are uniform. Generally, as a result of molecular diffusion and convective dispersion effects, a transition zone between the displacing fluid and the displaced fluid develops when the two miscible fluids are in contact. It is assumed that in the transition zone the solvent concentration C , which is a function of space and time, monotonically decreases from the solvent region to the oil region. Moreover, following Peaceman and Rachford's approach [43], it is assumed that the viscosity and density of the mixture, μ_m and ρ_m , are monotonic functions of solvent concentration, as shown in Eqs. 2.2.5 and 2.2.6.

The mathematical models describing the displacement are as follows:

$$\frac{\rho_m}{\phi} \frac{\partial W}{\partial t} + \frac{\partial P}{\partial z} + \frac{\mu_m}{K} W - \rho_m g = 0 \quad (4.2.1)$$

and

$$D_L \left[\frac{F(C) + \rho_s \phi}{\rho_s} \right] \frac{\partial^2 C}{\partial z^2} + \frac{2 D_L (\rho_s - \rho_0)}{\rho_s} \left(\frac{\partial C}{\partial z} \right)^2 - W \frac{\partial C}{\partial z} = \frac{\phi}{\rho_s} F(C) \frac{\partial C}{\partial t} \quad (4.2.2)$$

where W is the volumetric velocity of the mixture in the z direction.

According to small perturbation theory, each variable can be expressed as a sum of unperturbed values (constant) of the variable and its arbitrarily small perturbed value (function of space and time); that is,

$$\xi = \bar{\xi} + \xi^* \quad (4.2.3)$$

where

$$\xi = C, W, P, \rho_m, \mu_m \quad (4.2.4)$$

In Eq. 4.2.3, the variables superimposed with a bar represent values at stable or unperturbed conditions, whereas the asterisk variables represent small arbitrary perturbations. Small perturbation theory provides a method to predict the stability of the flow system by examining whether the perturbed values grow or decay with time. The equations describing stable displacements are defined as follows:

$$\bar{W} = V = \text{CONSTANT} \quad (4.2.5)$$

$$\frac{\partial \bar{P}}{\partial z} + \frac{\bar{\mu}_m}{K} V - \bar{\rho}_m g = 0 \quad (4.2.6)$$

and

$$D_L \left[\frac{F(\bar{C}) + \rho_s \phi}{\rho_s} \right] \frac{\partial^2 \bar{C}}{\partial z^2} + \frac{2 D_L (\rho_s - \rho_0)}{\rho_s} \left(\frac{\partial \bar{C}}{\partial z} \right)^2 - V \frac{\partial \bar{C}}{\partial z} = \frac{\phi}{\rho_s} F(\bar{C}) \frac{\partial \bar{C}}{\partial t} \quad (4.2.7)$$

Substituting Eqs. 4.2.3 through 4.2.7 into Eqs. 4.2.1 and 4.2.2, respectively, and eliminating the products of small perturbations because the values are negligible, the resulting equations are

$$\frac{\bar{\rho}_m}{\phi} \frac{\partial W^*}{\partial t} + \frac{\partial P^*}{\partial z} + \frac{\bar{\mu}_m}{K} W^* + \frac{V}{K} \bar{\mu}_m^* - \rho_m^* g = 0 \quad (4.2.8)$$

and

$$\begin{aligned} & D_L \left[\frac{F(\bar{C}) + \rho_s \phi}{\rho_s} \right] \frac{\partial^2 C^*}{\partial z^2} + \frac{2 D_L (\rho_s - \rho_0)}{\rho_s} \left(\frac{\partial C^*}{\partial z} \right)^2 - W^* \frac{\partial \bar{C}}{\partial z} - V \frac{\partial C^*}{\partial z} \\ & = \frac{\phi}{\rho_s} F(\bar{C}) \frac{\partial C^*}{\partial t} \end{aligned} \quad (4.2.9)$$

For perturbations in linear systems, a general disturbance can be represented by a Fourier series. Thus, the perturbed variables are given by

$$\xi^* = \bar{\xi}(z) e^{\alpha t} \quad (4.2.10)$$

where $\bar{\xi}(z)$ represents the amplitude of the disturbance, and α is called the time coefficient [47]. Coskuner and Bentsen suggest that the stability coefficient may be used to determine the instability of displacements; that is, the displacement is stable when the value of the stability coefficient is negative as the perturbation decays with time; and the displacement is unstable when the value of the stability coefficient is positive, as the perturbation grows with time.

If the viscosity and the density of the mixture are expanded in a Taylor series about the mean solvent concentration, \bar{C} , it follows that

$$\mu_m = \bar{\mu}_m + \mu_m^* = \mu_m(\bar{C}) + \frac{\partial \mu_m}{\partial C} C^* + \dots \quad (4.2.11)$$

and that

$$\rho_m = \bar{\rho}_m + \rho_m^* = \rho_m(\bar{C}) + \frac{\partial \rho_m}{\partial C} C^* + \dots \quad (4.2.12)$$

If the second and higher order terms in the Taylor series expansion can be neglected, Eqs. 4.2.11 and 4.2.12 lead to

$$\mu_m^* = \frac{\partial \mu_m}{\partial C} C^* \quad (4.2.13)$$

and

$$\rho_m^* = \frac{\partial \rho_m}{\partial C} C^* \quad (4.2.14)$$

Substituting Eqs. 4.2.10, 4.2.13 and 4.2.14 into Eqs. 4.2.8 and 4.2.9, and assuming that $\partial P^*/\partial z$ is negligible, the following two ordinary differential equations are obtained:

$$\bar{W}(z) = \frac{\left. \frac{\partial \rho_m}{\partial C} \right|_{C=\bar{C}} - \frac{V}{K} \left. \frac{\partial \mu_m}{\partial C} \right|_{C=\bar{C}}}{\frac{\alpha \rho_m}{\phi} + \frac{\mu_m}{K}} \bar{C}(z) \quad (4.2.15)$$

and

$$\begin{aligned} & D_L \left[\frac{F(\bar{C}) + \rho_s \phi}{\rho_s} \right] \frac{\partial^2 \bar{C}}{\partial z^2} + \frac{2 D_L (\rho_s - \rho_0)}{\rho_s} \left(\frac{\partial \bar{C}}{\partial z} \right)^2 e^{\alpha t} \\ & = \bar{W} \frac{\partial \bar{C}}{\partial z} + V \frac{\partial \bar{C}}{\partial z} + \frac{\phi}{\rho_s} F(\bar{C}) (\alpha e^{\alpha t}) \bar{C} \end{aligned} \quad (4.2.16)$$

Substituting Eq. 4.2.15 into Eq. 4.2.16 and rearranging

$$\begin{aligned}
& D_L \left[\frac{F(\bar{C}) + \rho_s \phi}{\rho_s} \right] \frac{\partial^2 \bar{C}}{\partial z^2} + \frac{2 D_L (\rho_s - \rho_0)}{\rho_s} \left(\frac{\partial \bar{C}}{\partial z} \right)^2 e^{\alpha t} \\
& = V \frac{\partial \bar{C}}{\partial z} + \left(N_c \frac{\partial \bar{C}}{\partial z} + \frac{\phi}{\rho_s} F(\bar{C}) (\alpha e^{\alpha t}) \right) \bar{C}
\end{aligned} \tag{4.2.17}$$

where

$$N_c = \frac{\left. \frac{g \partial \rho_m}{\partial C} \right|_{C=\bar{C}} - \frac{V \partial \mu_m}{K \partial C} \Big|_{C=\bar{C}}}{\frac{\alpha \bar{\rho}_m}{\phi} + \frac{\bar{\mu}_m}{K}} \tag{4.2.18}$$

Eq. 4.2.17 is a non-linear, second-order differential equation. In order to obtain the solutions of $\bar{C}(z)$ and $\bar{W}(z)$, two other definitions of solvent concentration have to be introduced. Brigham has shown [29] that the average concentration flowing *across* a plane is always greater than the concentration *in* the plane, and that the flowing concentration is the concentration one obtains from the effluent concentration measurement. This flowing concentration at each plane is given as

$$C_f = C - \frac{\phi D_L}{V} \frac{\partial C}{\partial z} \tag{4.2.19}$$

where C_f is the flowing concentration, and C is the in-situ concentration. According to small-perturbation theory, one may define the flowing concentration at each plane as a combination of the unperturbed concentration, \bar{C} , and the perturbed concentration, C^* .

Considering that solvent concentration decreases with core length (or depth) at each particular displacing moment, the expression is given as

$$C_f = \bar{C} - C^* = \bar{C} - \bar{C}(z) e^{\alpha t} \quad (4.2.20)$$

Defining the average in-situ concentration, C , as the unperturbed concentration, \bar{C} , and equating Eq. 4.2.19 with Eq. 4.2.20 gives

$$\bar{C}(z) e^{\alpha t} = \frac{\phi D_L}{V} \frac{\partial \bar{C}}{\partial z} \quad (4.2.21)$$

Coskuner and Bentsen have suggested that the condition of marginal instability is characterized by $\alpha = 0$, provided that the principle of exchange of stabilities is valid. If α equals zero, Eq. 4.2.21 becomes

$$\bar{C}(z) = \frac{\phi D_L}{V} \frac{\partial \bar{C}}{\partial z} \quad (4.2.22)$$

Eq. 4.2.22 is a linear, first-order differential equation which can be solved by applying inner or outer boundary conditions. At the inlet boundary ($z=0$), one has

$$\bar{C} = 1$$

and

(4.2.23)

$$\bar{C}(z) = 0$$

Then, the solution of Eq. 4.2.22 is given as

$$\bar{C}(z) = e^{(V/\phi D_L)z} \quad (4.2.24)$$

Substituting Eqs. 4.2.18 and 4.2.24 into Eq. 4.2.15, one has

$$\bar{W}(z) = N_c e^{(V/\phi D_L)z} \quad (4.2.25)$$

It can be seen from Eqs. 4.2.24 and 4.2.25 that the amplitudes of the perturbed concentration and the perturbed velocity are exponential functions of the distance traveled by the displacing front, z . That is, the further the plane is displaced from the inlet, the greater the perturbation of the solvent concentration and the velocity at the displacing front. This length dependency of the perturbation provides a theoretical basis for explaining the length dependency of the instability of the miscible displacement.

Substituting Eq. 4.2.24 into Eq. 4.2.17, one obtains

$$\begin{aligned}
& D_L \left[\frac{F(\bar{C}) + \rho_s \phi}{\rho_s} \right] \left(\frac{V}{\phi D_L} \right)^2 + \frac{2D_L (\rho_s - \rho_o)}{\rho_s} \left(\frac{V}{\phi D_L} \right)^2 e^{\frac{V}{\phi D_L} z} \\
& = N_c \frac{\partial \bar{C}}{\partial z} + \frac{V^2}{\phi D_L} + \frac{\phi}{\rho_s} F(\bar{C}) (\alpha e^{\alpha t})
\end{aligned} \tag{4.2.26}$$

Letting α equal zero to obtain a marginal instability condition, Eq. 4.2.26 becomes

$$\begin{aligned}
& D_L \left[\frac{F(\bar{C}) + \rho_s \phi}{\rho_s} \right] + \frac{2(\rho_s - \rho_o)}{\rho_s} e^{\frac{V}{\phi D_L} z} \\
& = \left(\frac{\phi D_L}{V} \right)^2 \left[N_c \frac{\partial \bar{C}}{\partial z} + \frac{V^2}{\phi D_L} \right]
\end{aligned} \tag{4.2.27}$$

By rearranging Eq. 4.2.27, it may be shown that

$$e^{\frac{V}{\phi D_L} z} = M_c \tag{4.2.28}$$

from which it follows that

$$z = \frac{\phi D_L}{V} \ln M_c \tag{4.2.29}$$

where

$$M_c = \frac{\rho_s}{2(\rho_s - \rho_o)} \left(\frac{N_c D_L}{U^2} \frac{\partial \bar{C}}{\partial z} - \frac{F(\bar{C})}{\rho_s} \right) \quad (4.2.30)$$

In Eq. 4.2.29, z is the distance from the inlet face of the core to the displacing front where the miscible displacement becomes unstable. It can be seen that this distance is proportional to the longitudinal dispersion coefficient, and that it is inversely proportional to the velocity. In other words, the greater the longitudinal dispersion is, the more quickly unevenly distributed fingers will be smeared out; and the higher the velocity is, the shorter the length of the stabilized mixing zone [21].

Coskuner and Bentsen [25] suggested that a displacement process is considered to be stable if

$$\frac{d\bar{W}(z)}{dz} = 0 \quad (4.2.31)$$

Taking the derivative of Eq. 4.2.25 with respect to z , and setting it equal to zero, one can see that the two possible solutions for Eq. 4.2.31 are either that the velocity, V , equals zero, or that Nc equals zero. If the latter condition applies, the critical stable velocity can be defined as

$$V_{cs} = K g \left[\frac{d\rho_m}{dC} / \frac{d\mu_m}{dC} \right]_{c=\bar{c}} \quad (4.2.32)$$

where V_{cs} is the critical stable velocity. When fluids have unequal density and unequal viscosity, the derivative terms such as $d\rho_m / dC$ and $d\mu_m / dC$ are given as follows [43]:

$$\frac{d\rho_m}{dC} = \rho_s - \rho_o \quad (4.2.33)$$

and

$$\frac{d\mu_m}{dC} = \mu_m (\ln \mu_s - \ln \mu_o) \frac{\beta}{[C + \beta(1 - C)]^2} \quad (4.2.34)$$

When fluids have equal density and equal viscosity, from Eqs. 4.2.33 and 4.2.34 one has

$$d\rho_m / dC = 0$$

and

$$d\mu_m / dC = 0 \quad (4.2.35)$$

As a consequence, when fluids have unit viscosity and density ratios, Eq. 4.2.32 becomes undefined.

In comparison with Dumore's criteria (Eqs. 2.1.13 and 2.1.14), the critical stable velocity, V_{cs} , defined in Eq. 4.2.32 is different from either the stable velocity or the critical velocity defined by Dumore. The difference is due to the factor, $[C + \beta(1 - C)]^2 / \beta$, which results in the smallest value of the three critical velocities. In fact, the evaluation of $\frac{d\rho_m}{dC} / \frac{d\mu_m}{dC}$ at the average concentration of the mixture may represent the mixing and dispersion process more precisely. It is suggested that this critical stable velocity may be

used to determine the initiation of fingering while the stable velocity defined by Dumore may be used to determine the tendency for fingers to grow. That is, it is assumed that, at this critical stable velocity, viscous fingers may initiate, but that they may be suppressed by diffusion. However, at the stable velocity defined by Dumore, fingers may start to grow slowly when the displacing velocity is lower than the stable velocity, and more quickly when the velocity is greater than the stable velocity.

5. EXPERIMENTAL

Laboratory fluid flow experiments have great utility in discovering and investigating fundamental displacement mechanisms and in developing mathematical techniques as tools for predicting and simulating miscible displacement processes. Experimental models are also useful in studying extremely complex processes and in evaluating the reliability of mathematical descriptions and techniques. Consequently, laboratory models provide one of the most convincing methods for verifying a particular solution, or suggesting improved assumptions to be used in the theoretical model.

In order to validate the effect of a permeable core's length on the instability of miscible displacements, a series of experiments was carried out in several rectangular core holders which varied in length, and which were packed with glass beads. For each experiment, the glass-bead pack was saturated with a white oil, Marcol 72, which was displaced downwards by a gasoline, Varsol, at several constant rates. The effluent was collected in cylinders to measure the volume of total production, and samples were taken regularly to measure their refractive index. The refractive index of the samples was used to determine the proportion of each oil in each of the samples. No attempt was made to simulate an actual reservoir. The results, therefore, reflect only some aspects of the fundamental behavior of miscible displacement processes in unconsolidated porous media.

5.1 Experimental Apparatus

A schematic diagram of the experimental apparatus used in this investigation is shown in Figure 1. There were three essential parts included in the experimental system: 1) the

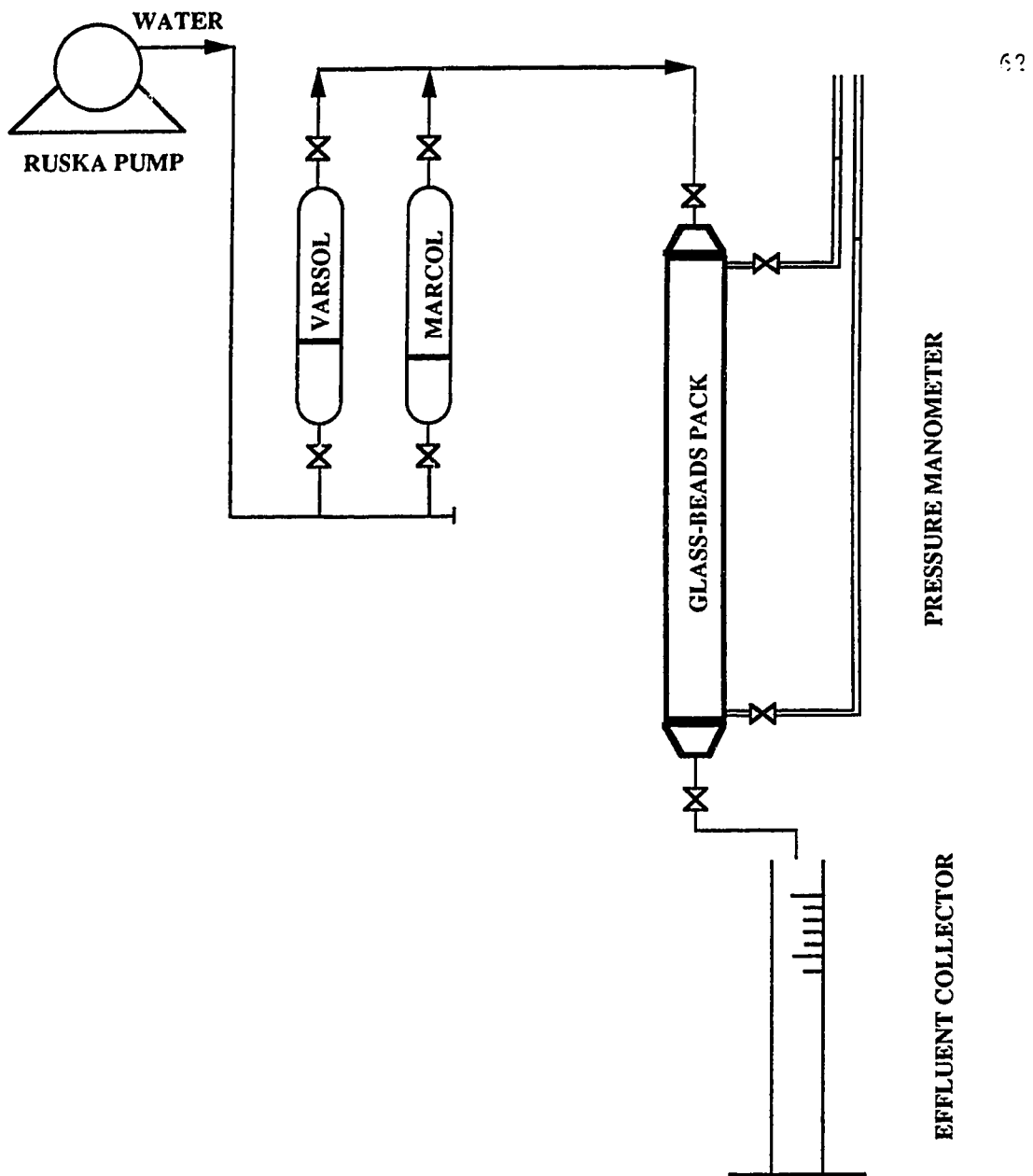


FIGURE 1: SCHEMATIC DRAWING OF EXPERIMENTAL APPRATUS

glass-bead packs used as porous media, 2) reservoirs which contained the fluids to be injected, and 3) a displacement pump to inject fluids at a constant rate.

The glass-bead packs were *15 cm* in width, *5 cm* in height and varied from *30 cm* to *150 cm* in length. Three rectangular core holders, which were *30, 60* and *90 cm* in length, were made of aluminium. The core holders were also connected together to obtain various desired lengths. The core holders were packed with glass beads, which served as the porous medium. The glass beads used were smooth and spherical and had a mean diameter of *2.643 mm (7-10 mesh)*. At the inlet and outlet ends, there were two end-pieces used to contain the glass beads in the core holder. The two end-pieces were pyramidal in shape and were filled with larger glass beads which were held in place by a glass plate made of fine fused glass beads. Such a design was considered to be capable of providing an evenly distributed entrance and discharge of fluids during displacements. Two cylinders (one containing Marcol and the other containing Varsol) were connected to the glass-bead pack to supply displacing and displaced fluids. A Ruska pump was used to inject displacing fluid at the desired constant rates for each pack length of interest. The flow rates used in the experiments were *194.6 ccl/hr, 324.8 ccl/hr* and *778.4 ccl/hr*.

5.2 Properties of the Porous Medium

The design of the laboratory experiments required high displacing rates and high permeabilities to minimize both the time required for the studies and the size of the models. Under these conditions, velocity variations between flow channels become important, and mixing (in the direction of flow) in the laboratory models between the oil and the solvent results primarily from convection. Utilizing glass beads to construct the porous media offered many advantages, especially when uniform permeability distributions having high permeabilities (>10 darcies) were desired. The properties of the porous media are shown

in Table 1. The average pore volume of the bead packs varied from *751 cc* to *3716 cc*, the average porosity was 33 per cent and the average permeabilities of each particular bead pack ranged from *2754 darcies* to *2795 darcies*. Unlike the porosities of the porous medium, which were rather consistent in value, the permeabilities increased slightly with length because of difficulties in achieving uniform bead packs.

5.3 Experimental Procedure

The experimental procedure included five steps: 1) packing, assembling and pressure-testing the bead-pack; 2) measuring pore properties of the bead-pack; 3) displacing in-situ oil (Marcol) by solvent (Varsol) at the desired constant rate and taking samples during the displacement; 4) cleaning and drying the bead-pack; and 5) measuring the refractive index of the effluent. Each step of the procedure is described in detail in the following sections.

5.3.1 Packing

The core holder used for the experiments was mounted vertically. With the outlet head attached to the bottom of the core holder, and with an extra core holder connected to the top of the core holder to allow the addition of relatively the same amount of weight on the upper layers of glass beads, *750 cc* of glass beads were poured into the core holder each time. After vibrating the pack with a vibrator for about *20* minutes, this procedure was repeated until the level of the beads rose to a height *30%* greater than the original height of the core holder.

The period of vibration time was increased with increasing pack length; that is, the core holder was vibrated for *25* minutes after each addition of the glass beads into the *120 cm* core holder, and for *30* minutes after each addition of the beads for the *150 cm* core holder. Even then, a consistent bead pack for each core holder was difficult to achieve because the

TABLE 1. THE PROPERTIES OF THE POROUS MEDIA

Pack No.	Length (cm)	Average Porosity (cc)	Average Porosity (%)	Standard Deviation	Average Permeability (darcies)	Standard Deviation
1	30	751	33.4	0.1	2755	11
2	60	1516	33.7	0.3	2766	14
3	90	2272	33.7	0.5	2778	15
4	120	2991	33.2	0.1	2787	32
5	150	3716	33.0	0.2	2796	43

vibrator was too small to vibrate adequately the longer core holders. From measurements of the permeabilities of the bead-packs, a looser packing in the longer cores was observed. In fact, some other researchers [48] also observed such a variation in both porosity and permeability along the longitudinal section of the sandpack.

5.3.2 Determination of Pore Properties

The determination of the pore properties was of importance for both experimental and theoretical reasons. The porosity and the absolute permeability of the porous media were used to evaluate instabilities of the displacements using Coskuner and Bentsen's instability criteria, and to predict the stability of the displacements using the critical stable velocity developed in the present study.

The porosities of the bead packs were determined by measuring the amount of fluid (Marcol) used to saturate the core completely. In order to achieve a better accuracy in each measurement, two approaches were taken to obtain the value. First, a vacuum was drawn on the clean bead-pack under test for a period of time, and then the displaced fluid (Marcol) was allowed to imbibe into the bead-pack. The amount of fluid imbibed was considered to be the pore volume of the bead-pack. Second, after completion of the displacement, the fluid inside the bead-pack was displaced using air. The amount of fluid collected also represented the value of the pore volume.

In comparison with the first procedure, the second one was observed to be less accurate because Varsol tended to vaporize after its arrival at the outlet end during the displacement by air, which resulted in some error in the total volume calculations. Using the first approach, the pore volume of the two end pieces was measured three times. The average pore volume of the three measurements was 322 cc. The porosity of each bead-pack was measured by taking an average value of the three measurements. The average porosity of

each bead-pack is given in Table 1. According to one of the methods for estimating standard deviation from sample range (small number of samples), the standard deviation from three samples can be determined by the formula: Mean sample range/1.693 (the constant varies according to the numbers of samples), where the mean sample range can be calculated by subtracting the minimum value from the maximum value. By using this method, the maximum and the minimum standard deviations of the mean porosity for the fifteen measurements are estimated as *0.5* and *0.1*.

After the bead-packs were saturated with oil, the absolute permeabilities of the bead-packs were determined using several flow rates with the displacing oil injected at the bottom. The pressure drop between the top and the bottom face of the core holder was measured for each flow rate. These pressure drops, together with the cross-sectional area and the length of the core holder, and the viscosity of the injected fluids, were used in conjunction with Darcy's law to estimate the absolute permeability of the bead-pack. The arithmetic average value over five measurements for each pack is given in Table 1. Similarly, by using the method mentioned above, the maximum and the minimum standard deviations of the mean permeability for the fifteen measurements are estimated as *43.3* and *10.9*.

According to the sensitivity analysis shown in the next chapter, the errors arising out of the packing procedure have negligible influence on the instability analysis of the displacements. Therefore, both the porosity and the permeability were measured only three times for each bead pack. With five groups of three points, an analysis of variance could be done. However, if one uses the power of the test for analyzing the variance, it turns out that the probability of making the second type error is about fifty percent, which means that an analysis of the variance has little utility.

5.3.3 Displacement

Displacements for each bead-pack were conducted at three different rates. These rates were selected on the basis of Dumore's criteria [46]. For solvent and oil densities of 0.841 and 0.780 gm/cc, respectively, and for solvent and oil viscosities of 1.125 and 22.001 cp, respectively, the critical rate was calculated using Eq. 2.2.12 and was multiplied by the bead-pack cross-section area. These values, for each of the different packs, are reported in Table 2. The stable rates (stable velocity multiplied by the bead-pack cross-section area), for the same values of viscosity and density, were calculated using Eq. 2.2.13, where β equals 0.529 . These results are also reported in Table 2. The critical stable rates reported in Table 2, were calculated using Eq. 4.2.32. The three displacing rates (196.4 cc/hr., 324.8 cc/hr. and 778.4 cc/hr.) were selected in such a way that the first rate was less than the estimated stable rate, the second was close to the stable rate and the third was somewhere between the stable rate and the critical rate.

In preparation for a run, the bead-pack was saturated with Marcol. Varsol, which is lighter and less viscous than Marcol, was used as the displacing fluid. The displacing fluid was injected into the top of the core holder at a constant rate. Initially, the effluent was collected in a large graduated cylinder located at the bottom of the core holder. When the arrival of the mixed zone was imminent, the large cylinder was replaced with smaller cylinders to enable more accurate measurement of the amount of fluid produced. Prior to 30 per cent of the in-situ oil being displaced, samples (5 cc) were taken for each 5 per cent of pore volume injected. After 30 per cent, the samples were taken more frequently. Each sample was assumed to be representative of the fluid passing the end of the pack during the small sampling time interval. For each run, the displacement was continued until approximately 1.5 to 2 pore volumes of displacing fluid was injected.

TABLE 2. THE STABLE AND CRITICAL RATES

Pack No.	Length (cm)	Avg. Permeability (darcies)	Stable Rate (cc/hr.)	Critical Rate (cc/hr.)	Critical Stable Rate (cc/hr.)
1	30	2754.6	354.6	2100.6	83.7
2	60	2765.7	356.0	2109.0	84.0
3	90	2778.3	357.7	2118.6	84.4
4	120	2786.5	358.7	2124.9	84.6
5	150	2795.8	359.9	2132.0	84.9

The refractive index of each sample was measured and the proportions of displacing and displaced fluid were determined from an experimental calibration curve. The oil breakthrough recoveries from each displacement were determined by noting the first refractive index which appeared to be less than *1.4610*. This breakthrough was verified by checking to see if the next sample also had a refractive index of less than *1.4610*. The oil recovery was considered to equal *100* per cent when five consecutive refractive indexes were found to equal to *1.4355*.

5.3.4 Cleaning

In order to keep consistent pore properties of each bead-pack, instead of repacking it after each run, the bead-pack was cleaned following a specific procedure. The cleaning procedure consisted of four steps: 1) displacing Varsol with air and drying the bead-pack with air, 2) circulating methanol through the bead-pack to wash away residual Varsol, 3) circulating water through the bead-pack to wash away residual methanol and 4) drying the bead pack with air and drawing a vacuum on the bead-pack.

Several experiments were repeated in order to examine the quality of the cleaning and to investigate whether the cleaning procedure had any impact on the experimental results. It was observed that the concentration profiles obtained from the different runs yielded essentially identical results. The results from two of the repeated experiments are plotted in Figure 2. As shown in the plot, good agreement was achieved between the data obtained using a new bead-pack and that obtained using a cleaned bead-pack, which suggests that the cleaning procedure was technically acceptable.

5.3.5 Measurement of Refractive Index

In order to determine the solvent (Varsol) concentration of the effluent, an experimental calibration curve had to be prepared before the displacements were undertaken. Figure 3

shows such a calibration curve. As can be seen from Figure 3, the refractive index depends linearly on the volume per cent of Varsol in the Varsol-Marcosol mixture. During each displacement, samples (5 cc) were taken from the effluent using measuring tubes, and an Abbe refractometer was used to measure the refractive index of the sample. Two to three sample readings were taken to provide a more accurate measurement, and the average value over the three readings was recorded. The difference in the readings checked was within 0.0001, which contributed to a maximum 0.78 per cent error in the solvent concentration evaluation.

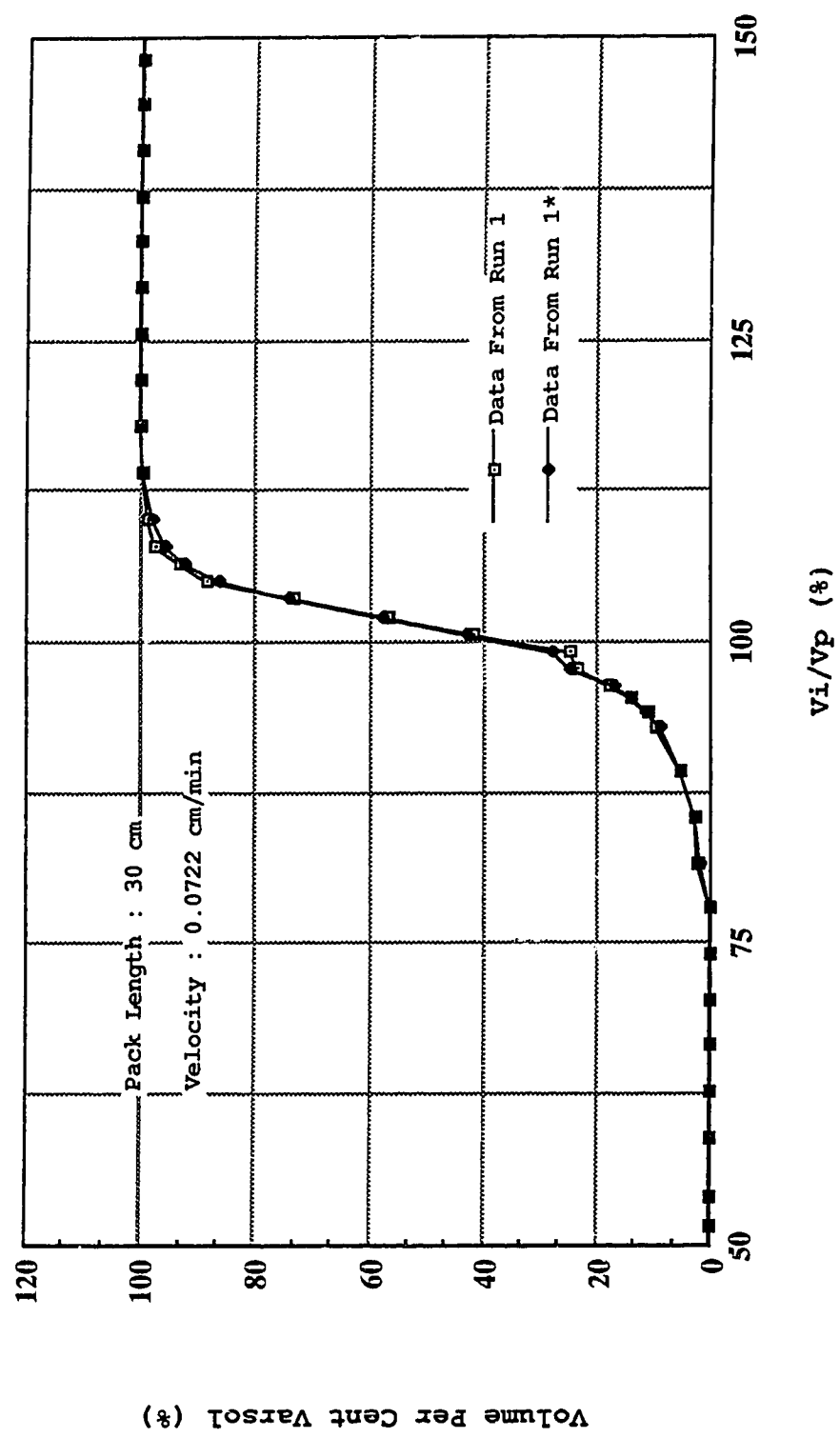


FIGURE 2: EFFLUENT CONCENTRATION PROFILE COMPARISON BETWEEN TWO RUNS AT IDENTICAL FLOW CONDITIONS

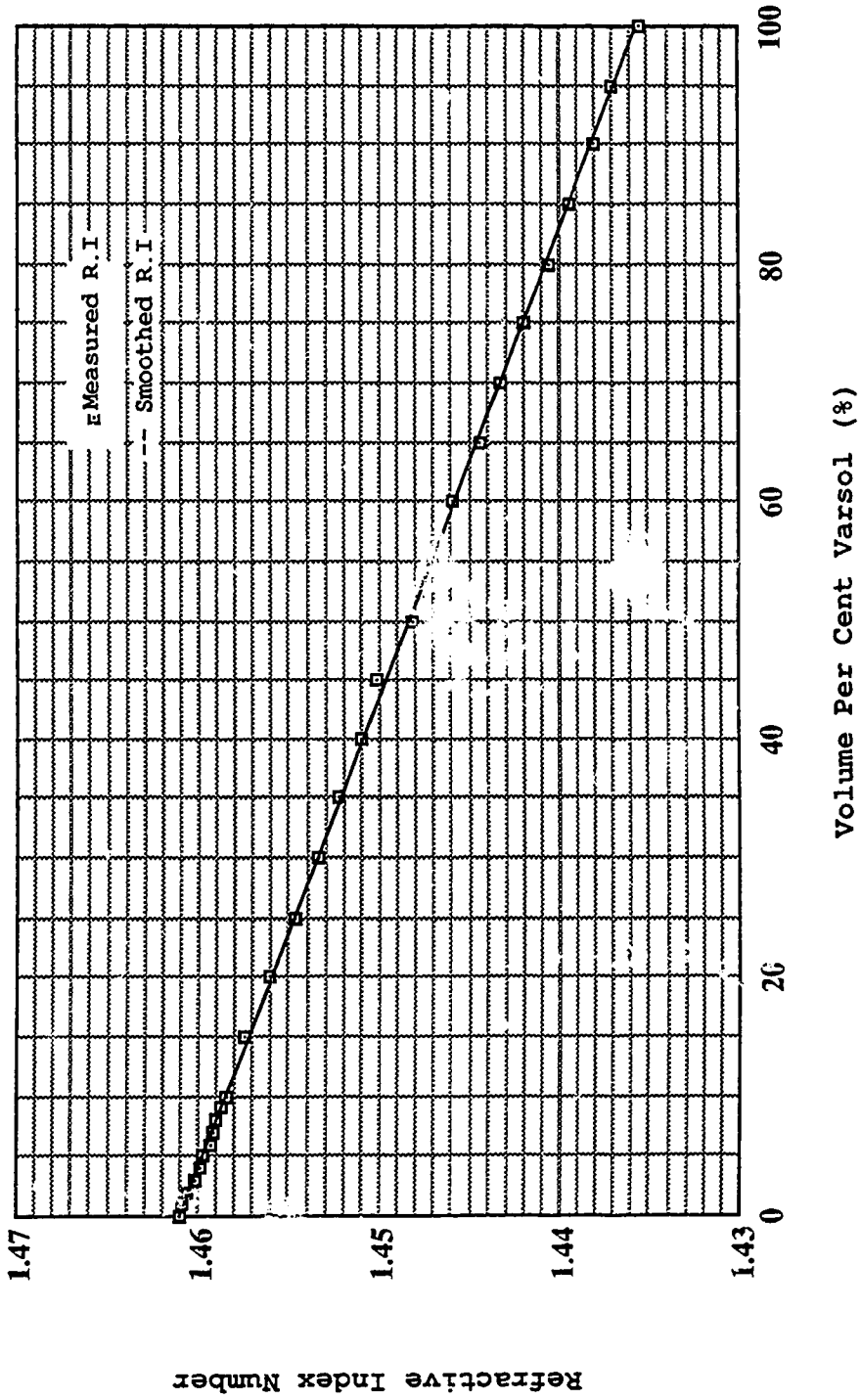


FIGURE 3: REFRACTIVE INDEX NUMBER OF VARSOL-MARCOSOL MIXTURES AS A FUNCTION OF VOLUME PER CENT VARSOL

6. RESULTS AND DISCUSSION

The goals of this experimental investigation were: 1) to conduct miscible displacements using glass-bead packs with various lengths; 2) to verify the theoretical prediction of a length effect on the instability of the displacements using the Coskuner-Bentsen marginal instability number; and 3) to verify that the instability had an effect on the breakthrough recovery of the displacements.

6.1 The Properties of Miscible Fluids

In order to calculate the instability number from experimental data using Coskuner and Bentsen's dimensionless scaling group (see Appendix B), the properties of the miscible fluids had to be determined experimentally. These properties include the viscosities and the densities of the oil (Marcol), the solvent (Varsol), and the mixture of the two as a function of solvent volumetric concentration at room temperature.

A density meter was used to determine the densities of the fluids, while a digital viscometer was used to determine the viscosities of the fluids. The properties of pure oil and pure solvent are given in Table 3. It is known that both the densities and the viscosities of miscible fluids are functions of solvent concentration. These functions are shown in Figure 4 and Figure 5, and the results of the measurement are given in Table 3.

In Figure 4 the empirical curve illustrates that the density of the mixed fluids, ρ_m , is a linear function of the solvent concentration, C ; in other words, the following expression is adequate to represent the relation between ρ_m and C :

TABLE 3. PROPERTIES OF THE MISCIBLE FLUIDS

Marcol (%)	Varsol (%)	Density (g/cc)		Viscosity (cp)	
		Measured	Calculated	Measured	Calculated
100	0	0.841	0.841	22.001	22.000
98	2	0.839	0.840	19.665	19.700
96	4	0.837	0.839	17.715	17.707
94	6	0.836	0.837	15.955	15.973
92	8	0.835	0.836	14.446	14.459
90	10	0.835	0.835	13.138	13.131
85	15	0.831	0.832	10.442	10.457
80	20	0.829	0.829	8.458	8.473
75	25	0.825	0.826	6.961	6.971
70	30	0.823	0.823	5.824	5.814
65	35	0.818	0.820	4.914	4.910
60	40	0.816	0.817	4.198	4.192
55	45	0.814	0.814	3.621	3.616
50	50	0.810	0.811	3.134	3.147
45	55	0.805	0.807	2.748	2.762
40	60	0.803	0.804	2.449	2.442
35	65	0.801	0.801	2.162	2.175
30	70	0.799	0.798	1.945	1.949
25	75	0.797	0.795	1.754	1.757
20	80	0.791	0.792	1.594	1.592
15	85	0.788	0.789	1.450	1.450
10	90	0.785	0.786	1.325	1.327
8	92	0.784	0.785	1.287	1.282
6	94	0.783	0.784	1.236	1.240
4	96	0.782	0.782	1.204	1.200
2	98	0.781	0.781	1.158	1.161
0	100	0.780	0.780	1.125	1.125

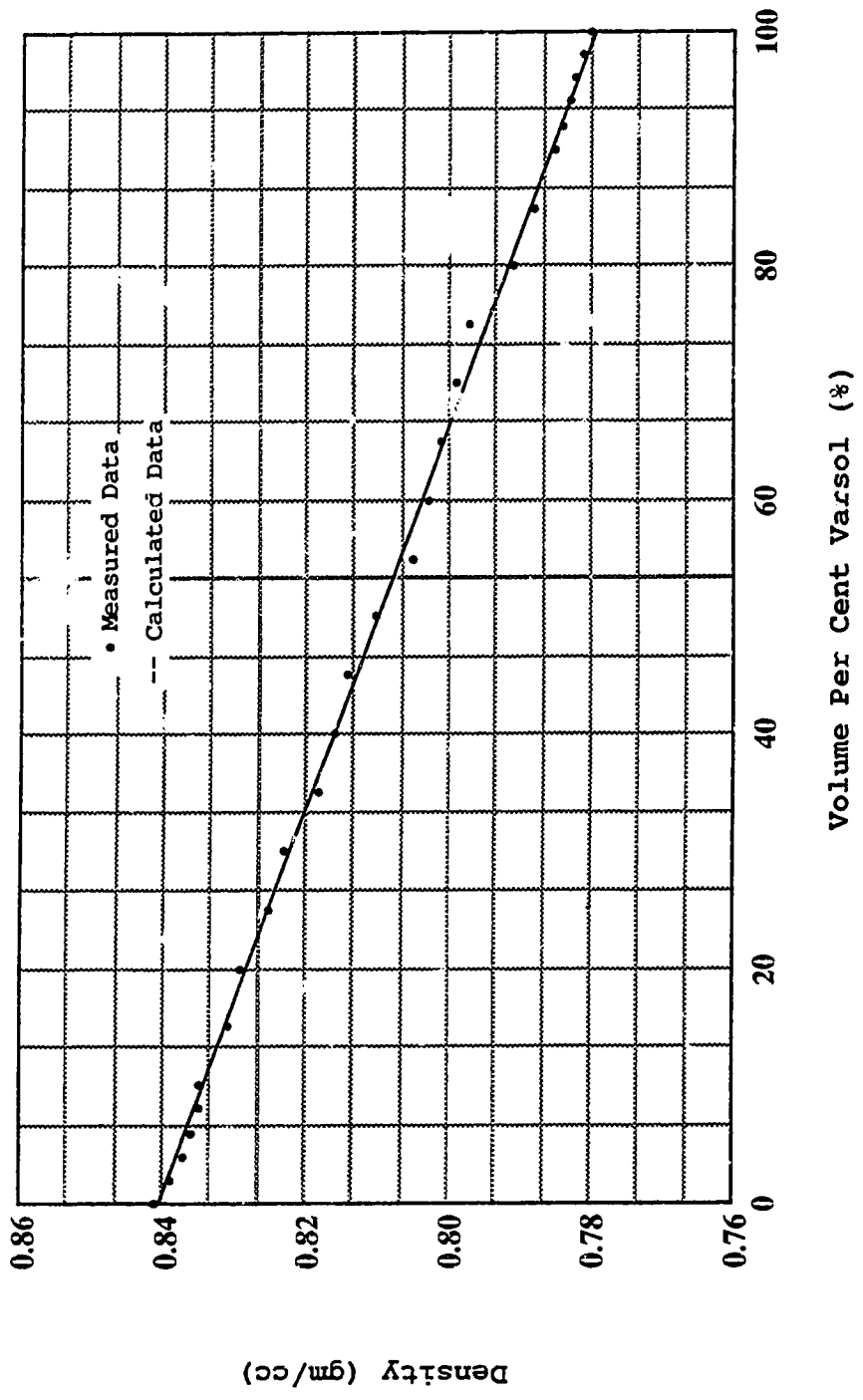


FIGURE 4: DENSITY OF VARSOL-MARCOL MIXTURES AS A FUNCTION OF VOLUME PER CENT VARSOL

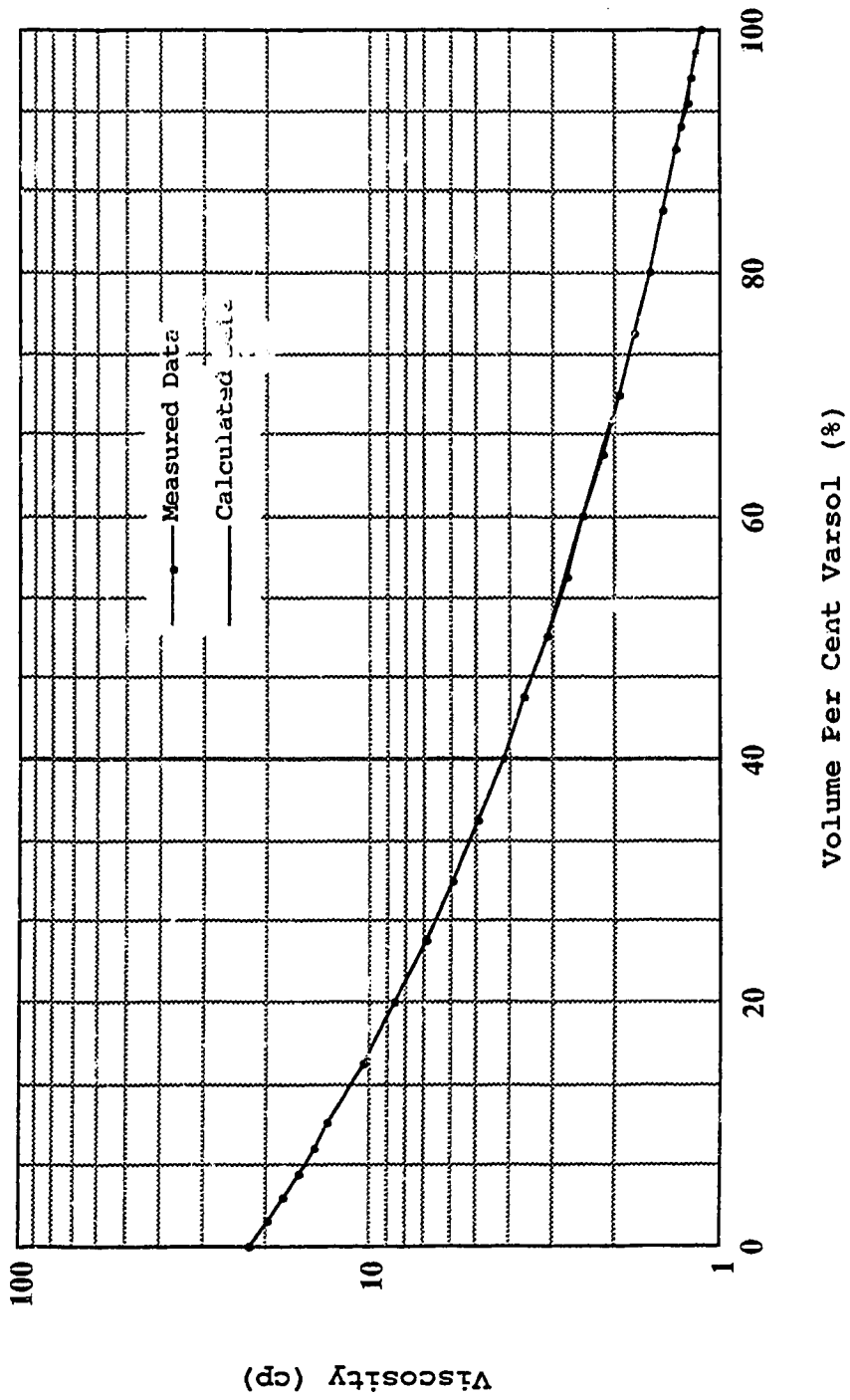


FIGURE 5: VISCOSITY OF VARSOL-MARCOL MIXTURES AS A FUNCTION OF VOLUME PER CENT VARSOL

$$\rho_m = \rho_s C + \rho_o(1 - C) \quad (6.1)$$

where C is the solvent concentration.

In Figure 5 the empirical curve shows that the viscosity of the mixed fluids, μ_m , is a non-linear function of solvent concentration. If one uses Peaceman and Rachford's correlation [43] to represent the the viscosity-concentration curve obtained in this study, the following equation is needed:

$$\ln \mu_m = X \ln \mu_s + (1-X) \ln \mu_o \quad (6.2)$$

where

$$X = \frac{C}{C + \beta(1-C)} \quad (6.3)$$

A trial-and-error approach was taken to estimate the empirical constant, β , using the viscosity-concentration curve shown in Figure 5. When $\beta = 0.529$, the correlations (Eqs. 6.2 and 6.3) give an excellent agreement with the experimental data reported in Table 3. Furthermore, the functions (Eqs. 6.1 through 6.3) are similar to those suggested previously in the literature.

If one uses Lederer's equation, which is a modified version of the classic Arrhenius expression [49], to represent the viscosity-concentration curve obtained in this study, the following equation is needed:

$$\ln \mu_m = X_A \ln \mu_o + X_B \ln \mu_s \quad (6.4)$$

where

$$X_A = \frac{\omega C}{\omega C + (1-C)}, \text{ and } X_B = 1 - X_A \quad (6.5)$$

The empirical constant, ω , is correlated to the viscosities of miscible fluids and to a function of fluid densities, or an Einsteinian constant, τ . That is,

$$\omega = \frac{\tau}{\ln(\mu_o / \mu_s)} \quad (6.6)$$

and

$$\tau = 17.04 \rho_o^{3.2745} \rho_s^{1.6316} (\rho_o - \rho_s)^{0.5237} \quad (6.7)$$

Using Eqs. 6.6 and 6.7, τ and ω are calculated to be *1.4895* and *0.5009*, respectively, for the fluids used in this study. The Lederer equation (Eqs. 6.4 through 6.7) also gave an excellent fit to the experimental data. In comparison with Peaceman and Rachford's correlation, Lederer's correlation is more desirable and easier to obtain because it requires only the input of the densities and viscosities of the oil and the solvent. Moreover, using Lederer's correlation, the two empirical coefficients, ω and τ , can be estimated empirically;

whereas the empirical constant, β , in Peaceman and Rachford's expression, has to be determined experimentally.

6.2 Evaluation of the Relevant Parameters and Variables

In order to predict the instability of the displacements, some other parameters and variables also had to be estimated [see Appendix B]. These parameters are: the viscosity gradient and the density gradient evaluated at the average unperturbed concentration, \bar{c} , which corresponds to the average viscosity, $\bar{\mu}$; the transverse dispersion and longitudinal dispersion coefficients; and the average concentration gradient evaluated at $C = 0.5$.

6.2.1 The Viscosity and Density Gradients

The arithmetic-average unperturbed viscosity of the fluids used in this study is calculated as 11.563 cp . Once $\bar{\mu}$ has been determined, the average concentration, \bar{c} , corresponding to $\bar{\mu}$, can be calculated by using Eqs. 6.2 and 6.3. That is, letting $\bar{\mu} = \mu_m$ and substituting μ_o and μ_s into Eq. 6.2, one obtains a value of X ; substituting X into Eq. 6.3, one obtains the average concentration, \bar{c} .

Having $X = 0.2164$, and $\bar{c} = 0.1275$, one may obtain the viscosity gradient, $d\mu_m / dC$, and the density gradient, dp_m / dC evaluated at $\bar{c} = 0.1275$. Differentiating Eq. 6.3 yields:

$$\left. \frac{dX}{dC} \right|_{c=\bar{c}} = \frac{0.529}{[\bar{c} + 0.529(1 - \bar{c})]^2} = 1.5246 \quad (6.8)$$

Hence, using Eq. 4.2.34, the viscosity gradient $d\mu_m / dC$ at $\bar{c} = 0.1275$ is given by

$$\left. \frac{d\mu_m}{dC} \right|_{c=\bar{c}} = \left. \frac{dX}{dC} \right|_{c=\bar{c}} \times \bar{\mu} [\ln \mu_s - \ln \mu_o] = -0.0524 \text{ Pa.s} \quad (6.9)$$

and, using Eq. 4.2.33, the density gradient $d\rho_m / dC$ at $\bar{c} = 0.1275$ is given by

$$\left. \frac{d\rho_m}{dC} \right|_{c=\bar{c}} = \rho_s - \rho_o = -61.0 \text{ Kg}\cdot\text{M}^{-3} \quad (6.10)$$

The negative values of $d\mu_m / dC$ and $d\rho_m / dC$ agree with experimental observation; that is, both viscosity and density of the mixture decrease with an increase in solvent concentration.

6.2.2 Molecular Diffusion Coefficient

The molecular diffusion coefficient of the miscible fluids is essential for estimation of the transverse dispersion coefficient using Perkins and Johnston's correlation [11]. Because no adequate experimental means were available for determining the molecular diffusion coefficient for miscible fluids with unequal density and unequal viscosity, such as the fluids used in this study, some empirical methods had to be used. In this study, a correlation [6] for estimating the molecular diffusion coefficient of fluids having equal density and equal viscosity was used. The value of the molecular diffusion coefficient was estimated to be $1.1286 \times 10^{-6} \text{ cm}^2/\text{sec}$. This value is similar in magnitude to that ($3.2 \times 10^{-6} \text{ cm}^2/\text{sec}$.) obtained experimentally by Brigham et al. [7] using two mineral oils of equal density.

6.2.3 Transverse Dispersion Coefficient

For reasons similar to those noted with respect to estimating the molecular diffusion coefficient, the transverse dispersion coefficient also had to be estimated using the available correlations for fluids having equal viscosity and equal density. In the present study, Perkins and Johnston's correlation (Eq. 2.1.7) was used to estimate the transverse dispersion coefficients. In order to use this correlation, one has to determine the formation factor of the glass beads, F , and the inhomogeneity factor, σ . Using Slawinski's [15] theoretical expression (Eq. 2.1.8), which is based on models of unconsolidated spheres in contact, the formation factor F was estimated to be 4.4784. For the unconsolidated glass beads used as a porous medium, $\sigma = 1$ [11]. Under the experimental conditions considered, the transverse dispersion coefficients varied from 9.9103×10^{-6} cm²/sec. at the lower velocity to 3.7015×10^{-5} cm²/sec. at the higher velocity.

6.2.4 Longitudinal Dispersion Coefficient

Among all the parameters to be determined, the longitudinal dispersion coefficient was found to have the greatest impact on the evaluation of the instability number. While many theoretical and empirical correlations enable an accurate estimation of the dispersion coefficient [11,13,15,17,20, 27], provided that the displacing and the displaced fluids have equal density and equal viscosity, none of the currently available correlations are capable of predicting accurately the longitudinal dispersion coefficient when the fluids have unequal densities and unequal viscosities.

In the present study, it was necessary to assume that the difference in the viscosity and density of displacing and displaced fluids was small, so that the correlation for estimating the longitudinal dispersion coefficient of equal-viscosity, equal-density fluids could be

applied approximately to unequal-viscosity and unequal-density fluids. For comparison purposes, four different approaches were chosen for estimating the longitudinal dispersion coefficient. These methods were Arya's empirical correlation (Eqs. 2.1.9 and 2.1.10), Blackwell's expression (Eq. 2.1.4), Perkins and Johnston's method and a modified method.

A comparison of the results estimated using the four methods is given in Table 4. As can be seen in Table 4, the approximations of the longitudinal dispersion coefficient vary in magnitude in accordance with the methods used. Using Arya's empirical relationship, the results show that the longitudinal dispersion coefficient increases with both velocity and core length. Using Blackwell's and Perkins and Johnston's correlations, the results show that the longitudinal dispersion coefficient varies with velocity only; that is, the higher the velocity, the greater the value of the dispersion coefficient. It is interesting to note that even if the three methods are suggested to be used for fluids having favorable viscosity and density ratios only, there is a lack of consistency in the results of the estimation using these three methods. In particular, the results obtained using Blackwell's method are approximately three order of magnitude smaller than those obtained using Perkins and Johnston's method. One possible explanation is that Blackwell's correlation represents both convective and diffusive dispersion while Perkins and Johnston's represents diffusive dispersion only.

Considering that the fluids used in this investigation had an unfavorable viscosity and density ratio, and that the difficulty encountered in choosing an adequate correlation to evaluate the longitudinal dispersion coefficient, it seems necessary to develop some other approaches for estimating the longitudinal dispersion coefficient. In the present study, a correlation for such a purpose was derived by taking into account the effects of unfavorable viscosity ratio and the core dimensions. According to Perkins and Johnston's correlation, if the fluids used have unit viscosity and density ratios, the longitudinal dispersion

**TABLE 4. COMPARISON OF EVALUATION OF
LONGITUDINAL DISPERSION COEFFICIENT**

Run No.	Length cm	Velocity cm/min.	Arya's Method sq. cm/sec.	Blackwell's Method sq. cm/sec.	Perkins and Johnston's Method sq. cm/sec.	Modified Method sq. cm/sec.	Gamma Calculated	Gamma History Matching
1	30	0.0432	0.0045	0.1695	0.0003	0.0166	973	1355
4	60	0.0432	0.0098	0.1695	0.0003	0.0259	1246	2016
7	90	0.0432	0.0155	0.1695	0.0003	0.0319	1519	555
10	120	0.0432	0.0215	0.1695	0.0003	0.0362	1792	897
13	150	0.0432	0.0276	0.1695	0.0003	0.0393	2065	915
2	30	0.0722	0.0075	0.3092	0.0005	0.0278	973	1817
5	60	0.0722	0.0164	0.3092	0.0005	0.0433	1246	1189
8	90	0.0722	0.0259	0.3092	0.0005	0.0533	1519	1355
11	120	0.0722	0.0359	0.3092	0.0005	0.0605	1792	2158
14	150	0.0722	0.0462	0.3092	0.0005	0.0657	2065	2340
3	30	0.1730	0.0179	0.8595	0.0011	0.0666	973	370
6	60	0.1730	0.0393	0.8595	0.0011	0.1038	1246	555
9	90	0.1730	0.0621	0.8595	0.0011	0.1278	1519	1355
12	120	0.1730	0.0860	0.8595	0.0011	0.1449	1792	2191
15	150	0.1730	0.1106	0.8595	0.0011	0.1575	2065	2378

coefficient is given as

$$D_L = \frac{D'}{F\phi} + 0.5U\sigma d_p \quad (6.11)$$

Let us suppose that

$$D_L^* = \frac{D_L}{f(\delta, M)} \quad (6.12)$$

where D_L^* is defined as the modified dispersion coefficient, and $f(\delta, M)$ is the correction factor for taking into account the effect of the core length and the unfavorable viscosity ratio of the fluids. Substituting Eq. 6.11 into Eq. 6.12, one obtains

$$D_L^* = \frac{D'/F\phi + 0.5U\sigma d_p}{f(\delta, M)} \quad (6.13)$$

If one knows a correlation for evaluating the correction factor, $f(\delta, M)$, the longitudinal dispersion coefficient can be determined by using Eq. 6.13. In the present study, a history matching of the experimental concentration profiles with the theoretical predictions was performed in order to obtain the correction factor. According to Brigham's observation [29], if an experimental concentration profile can be described by the error function solution, the longitudinal dispersion coefficient can be correlated to a dimensionless dispersion, γ ; that is,

$$D_L = \frac{UL}{\gamma} \quad (6.14)$$

To be consistent with the ideas developed in Section 4.1, the longitudinal dispersion coefficient, D_L' , should be used to replace D_L in Eq. 6.14. Substituting Eq. 4.1.26 into Eq. 6.14 and rearranging, one has

$$\gamma = \frac{UL}{D_L'} = \frac{UL}{D_L} \frac{\phi}{1+\phi} \quad (6.15)$$

If the fluids have unfavorable viscosity and density ratios, one may replace the longitudinal dispersion coefficient, D_L , in Eq. 6.15 by D_L^* (see Eq. 6.13). Substituting the resulting equation into Eq. 6.13 and rearranging, a new expression for dimensionless dispersion, γ , can be written as

$$\gamma = \frac{f(\delta, M)}{\left[\frac{D'}{FVL} + \frac{0.5\sigma d_p}{L} \right] \frac{1+\phi}{\phi}} = \frac{f(\delta, M)}{0.5\sigma d_p \left[1 + \frac{D'}{0.5\sigma d_p FV} \right] \frac{1+\phi}{\phi}} \quad (6.16)$$

Eq. 6.16 shows that the dimensionless dispersion, γ , is related to the correction factor, $f(\delta, M)$. Based on the values of gamma obtained by history matching, the correction factor for fluids used in this study was determined to be

$$f(\delta, M) = 4.8201\delta + 2.4719 \quad (6.17)$$

where δ is a dimensionless length defined as the ratio of the length of shorter bead packs to the length of the longest bead pack. It is to be noted that Eq. 6.17 was determined using only one value of M . Two groups of gamma are given in Table 4. The first group was obtained from history matching of the concentration profiles, and the second group was evaluated by using Eq. 6.16. As can be seen in Table 4, there is a lack of consistency in the values of gamma for the two short packs (30 cm and 60 cm), as compared with those evaluated using Eq. 6.16. One possible explanation is that when the packs were too short to meet the infinite length requirement, some model error was introduced into the theoretical predictions of the concentration profile.

The longitudinal dispersion coefficient obtained using the modified method (Eqs. 6.15, 6.16 and 6.17) is given in Table 4. The results are observed to be dependent on both the pack length and the velocity. It is also observed that, at the lowest velocity, the dispersion coefficient seems to increase slightly with core length, and at higher velocities, the increase in the magnitude of the longitudinal dispersion coefficient is more significant. In comparison with the longitudinal dispersion coefficient obtained using the three other methods, the one obtained using the modified method is comparable in magnitude with the one obtained using Arya's method.

6.2.5 The Average Concentration Gradient

In order to predict the stability of a displacement at any given displacing rate and core length using the Coskuner-Bentsen criterion, the average value of the maximum unperturbed concentration gradient, $\partial \bar{C} / \partial z$, needs to be defined and calculated. Coskuner and Bentsen [26] suggested that one should use an average concentration gradient evaluated at 50 per cent solvent concentration and averaged over the life of an experiment, which

gives the best agreement between the theoretical prediction and the experimental observation in a Hele-Shaw system. If this approach is taken, it follows that

$$\left. \frac{\partial C}{\partial z} \right|_{c=0.5} = - \sqrt{\frac{V}{\pi \phi L D_L}} \quad (6.18)$$

Because all variables in Eq. 6.18 can be obtained or determined, it is possible to calculate the average concentration gradient and to predict the stability of a displacement using other known experimental conditions.

Two other approaches were also taken for estimating the unperturbed concentration gradient. These included one that used the concentration gradient (Eq. 4.1.30) evaluated at 50 per cent solvent concentration and one that used the concentration gradient evaluated at the average concentration, $\bar{c} = 0.127$. The results obtained were different from those obtained using Eq. 6.18. Furthermore, if one evaluated the instability number by using these two concentration gradients, the stability prediction would be inconsistent with the experimental observations. As it is unclear whether or not the concentration gradient defined in Eq. 4.1.30 is equivalent to the unperturbed concentration gradient theoretically, one should be cautious about using these two methods.

6.3 Effect of Bead-Pack Length on Breakthrough Recovery

The oil recovery at solvent breakthrough was found to be relevant to the instability of the miscible displacement. In general, a stable displacement yielded a higher recovery of the displaced oil at breakthrough than that obtained in an unstable displacement. In the present study, breakthrough of the displacing solvent was identified by measuring the refractive indexes of the effluent. Furthermore, it was noticed during sampling that, when

solvent arrived at the outlet end, a visible irregular boundary between Varsol and Marcol was observed in the samples for a short period of time (5 - 10 min.). This observation was taken as evidence that the effluent contained pure solvent as well as a mixture of solvent and oil. A tabulation of the breakthrough recoveries obtained from the 15 runs conducted in this study is given in Table 5. Figure 6, which compares the data from five different pack lengths and three different velocities, shows that, at the lowest rate, breakthrough recoveries are independent of pack length. At the second rate, the breakthrough recovery decreases 2.53 per cent when the length increases from 30 to 60 cm. Because this decrease is less than maximum decrease (3.22%) in breakthrough recovery which occurred among the five lengths employed at the lowest rate, it is thought that the displacement is still stable at a length of 60 cm. When the length is increased to 90 cm, however, the magnitude of the increase in breakthrough recovery (4.53%) is greater than the variation seen at the lowest velocity. This suggests that this decrease is significant and that, as a consequence, the displacement is unstable at a length of 90 cm. Such drops in recovery become even more significant in the two longer packs (120 and 150 cm). At the highest rate, the breakthrough recoveries demonstrate a consistent decline with increasing pack length. It is noted that in Table 5 the pore volume injected at 100% recovery also increases with increasing pack length, particularly at high displacing rates.

6.4 The Stable Mixing-Zone Length

The stable mixing-zone length, as defined in Eq. 4.2.29, is the distance from the inlet face of the core at which the miscible displacement becomes unstable, or fingers start to grow at the interface. It is known that in a stable miscible displacement, there are three zones existing in a core: the solvent zone followed by the solvent-oil mixing zone and the oil zone, and that in an unstable displacement, there are possibly four zones: the solvent zone, the solvent-oil mixing zone where no distinct solvent fingers exist, the fingering zone

TABLE 5. DISPLACEMENT RESULT SUMMARY

Run No.	Length(cm)	Velocity (cm/min)	B.T Recovery(%)	P.V inj. at 100% Rec.
1	30	0.0432	82.88	1.08
4	60	0.0432	81.33	1.11
7	90	0.0432	79.82	1.14
10	120	0.0432	80.02	1.12
13	150	0.0432	79.66	1.15
2	30	0.0722	79.12	1.16
5	60	0.0722	76.59	1.20
8	90	0.0722	72.06	1.22
11	120	0.0722	68.10	1.25
14	150	0.0722	52.64	1.27
3	30	0.1730	66.35	1.21
6	60	0.1730	58.82	1.24
9	90	0.1730	50.04	1.25
12	120	0.1730	44.45	1.32
15	150	0.1730	32.92	1.39

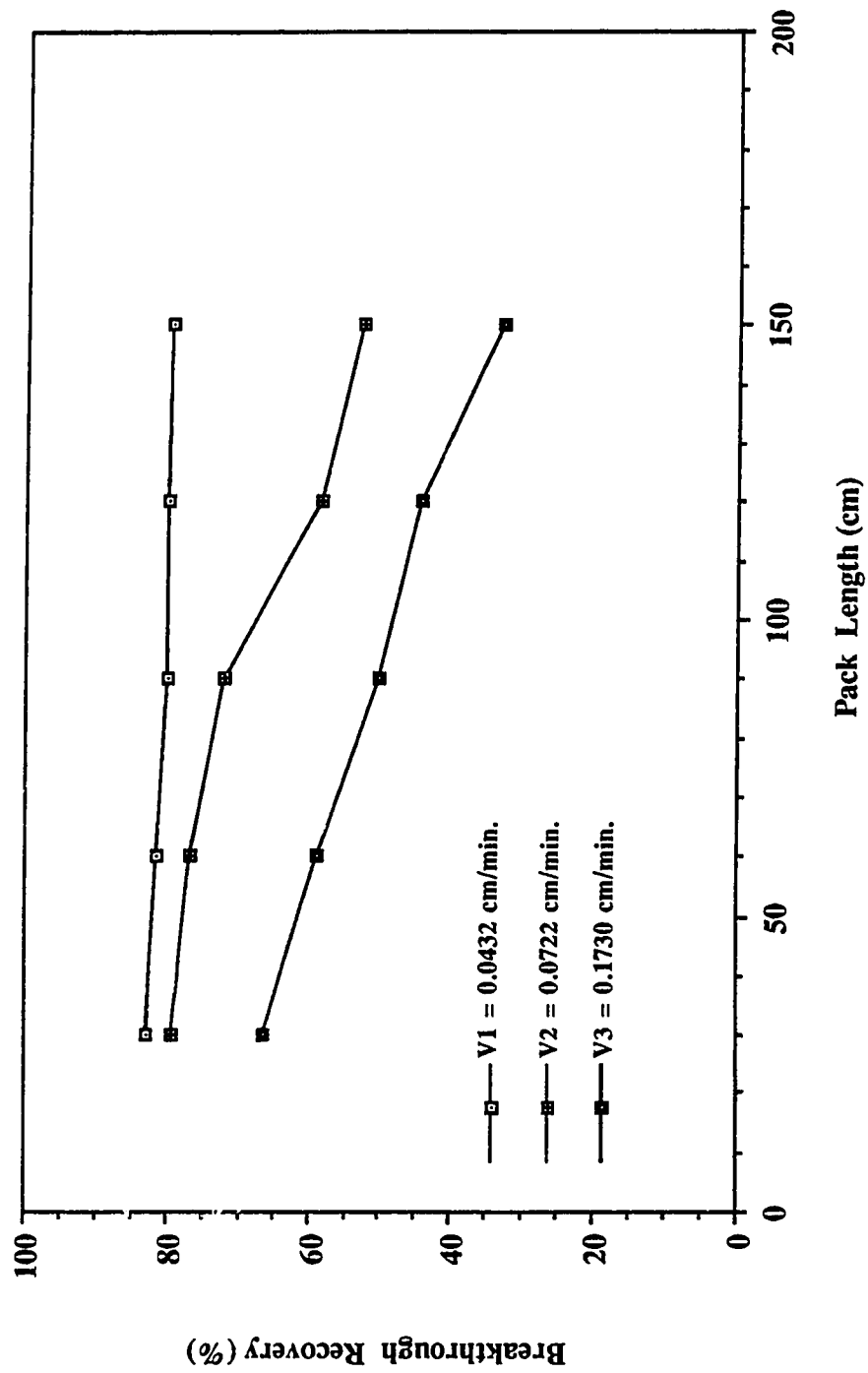


FIGURE 6: EFFECT OF BEAD-PACK LENGTH ON THE BREAKTHROUGH RECOVERIES AT DIFFERENT VELOCITIES

where distinct solvent fingers can be observed and the oil zone. During the course of the displacement, one zone is displaced by another until the time when only the pure solvent is left in the core. It is evident that the longer the stable mixing-zone length, the less severe is the fingering of solvent into the displaced oil.

In the present study, four groups of stable mixing-zone lengths were calculated by using Eq. 4.2.29, together with Eq. 4.2.30 in which $F(\bar{C})$ was evaluated at $\bar{C}=0.1277$. The results are given in Table 6 in accordance with the longitudinal dispersion coefficients recorded in Table 4. As can be seen in Table 6, the magnitude of the longitudinal dispersion coefficient affects the calculated lengths of the stable mixing-zone significantly; that is, the prediction of the stable mixing-zone length may be meaningless unless an accurate longitudinal dispersion coefficient is available.

In comparison with the experimental observations, Blackwell's dispersion coefficient gives too optimistic a prediction of the stable mixing-zone length for all the runs, whereas Perkins and Johnston's dispersion coefficient gives too pessimistic a prediction. The results obtained using Arya's and the modified dispersion coefficients are comparable, and both of the predictions show that the stable mixing-zone length is a strong function of core length, but that its dependency on velocity is less significant. While theoretically the velocity of the displacement should have an effect on the length of the stable mixing-zone length, the results of this study show that velocity has only a slight impact on the length of the stable mixing-zone length. This is because D_L has been assumed to be directly proportional to V . If, however, D_L had been assumed to be proportional to $v^{1.17}$, the impact of velocity on the stable mixing-zone length would have been more significant.

6.5 Evaluation of the Instability Number

The effect of bead-pack length on the instability of miscible displacement is of both theoretical concern and experimental interest. This is because some experimental models,

TABLE 6. COMPARISON OF THE STABLE MIXING-ZONE LENGTH

Run No.	Length (cm)	Velocity (cm/min)	Stable Mixing-Zone Length (z, cm)			
			Arya's	Blackwell's	Perkins & Johnston's	Modified Method
1	30	0.0432	4.00	154.03	0.27	14.83
4	60	0.0432	8.80	154.44	0.27	23.33
7	90	0.0432	13.92	153.84	0.27	28.70
10	120	0.0432	19.06	151.54	0.26	32.14
13	150	0.0432	24.32	150.41	0.26	34.67
2	30	0.0722	3.98	166.03	0.27	14.79
5	60	0.0722	8.80	167.02	0.27	23.25
8	90	0.0722	13.88	166.65	0.27	28.60
11	120	0.0722	18.99	164.33	0.26	32.04
14	150	0.0722	24.30	163.23	0.26	34.57
3	30	0.1730	3.96	190.27	0.24	14.74
6	60	0.1730	8.78	192.06	0.24	23.19
9	90	0.1730	13.86	191.93	0.24	28.53
12	120	0.1730	18.95	189.47	0.24	31.93
15	150	0.1730	24.22	188.32	0.24	34.50

either scaled or unscaled, may not have sufficient core length to meet the "infinitely long" requirement in modeling the displacement process, and one should know how a short core length at the same experimental conditions as those for the long core, affects the theoretical prediction of the displacement and experimental results. Moreover, it is also desirable to have a more appropriate understanding of how dispersive mixing is related to viscous fingering in miscible displacements when the effect of length is taken into account.

It is apparent from the definition of the marginal instability number, I_m , (see Appendix B, Eq. B-4) that the marginal instability number can be defined either as a function of dimensionless length, Ω , or as a constant, π^2 . In the present study, as the ratio of the transverse dispersion coefficient to the longitudinal dispersion coefficient, K_d , varies slightly with velocity, the constant ($\pi^2 = 9.87$) was chosen as the onset instability number.

In order to predict the instability of each displacement, the actual instability number, I_e , (see Appendix B) has to be evaluated according to each specific experimental condition. Coskuner and Bentsen have shown that displacements in a Hele-Shaw system were observed to be stable if the experimental instability number, I_e , fell below the marginal instability boundary, and that the displacements were observed to be unstable if I_e fell above the marginal instability boundary. Similarly, in the present study, the instability numbers for displacements in the porous medium were evaluated and compared with the onset instability number, π^2 , to determine whether or not the displacement was stable. The experimental instability numbers calculated are summarized in Table 7. Table 7 shows the instability numbers calculated using the four groups of longitudinal dispersion coefficients recorded in Table 4. It can be seen that the differences in the value and magnitude of dispersion coefficients result in significant differences in the prediction of the instability of the displacement. The experimental observation of the instability of the displacements is also given in Table 7. The displacement was considered to be stable when the

TABLE 7. COMPARISON OF THE INSTABILITY NUMBERS

Run No.	Length (cm)	Velocity (cm/min)	Ie	Experimental Observation	Ie	Experimental Observation
			Arya's		Blackwell's	
1	30	0.0432	-171.37	Stable	-0.80	Stable
4	60	0.0432	-146.97	Stable	-2.34	Stable
7	90	0.0432	-130.59	Stable	-4.33	Stable
10	120	0.0432	-117.02	Stable	-6.58	Stable
13	150	0.0432	-107.79	Stable	-9.07	Stable
2	30	0.0722	48.70	Stable	0.20	Stable
5	60	0.0722	36.19	Stable	0.51	Stable
8	90	0.0722	30.92	Unstable	0.89	Unstable
11	120	0.0722	30.84	Unstable	1.51	Unstable
14	150	0.0722	29.15	Unstable	2.15	Unstable
3	30	0.1730	242.56	Unstable	0.79	Unstable
6	60	0.1730	196.18	Unstable	2.19	Unstable
9	90	0.1730	172.49	Unstable	3.99	Unstable
12	120	0.1730	161.05	Unstable	6.32	Unstable
15	150	0.1730	149.85	Unstable	8.85	Unstable

TABLE 7. COMPARISON OF THE INSTABILITY NUMBERS (CONTINUED)

Run No.	Length (cm)	Velocity (cm/min)	Ie		Experimental Observation	Ie		Experimental Observation
			Perkins&Johnston's			Modified Method		
1	30	0.0432	-4712.75		Stable	-25.67		Stable
4	60	0.0432	-5179.42		Stable	-37.36		Stable
7	90	0.0432	-4728.33		Stable	-48.81		Stable
10	120	0.0432	-4202.01		Stable	-58.94		Stable
13	150	0.0432	-3826.26		Stable	-68.81		Stable
2	30	0.0722	1358.27		Stable	7.23		Stable
5	60	0.0722	1308.70		Stable	9.19		Stable
8	90	0.0722	1147.68		Unstable	11.53		Unstable
11	120	0.0722	1133.85		Unstable	15.48		Unstable
14	150	0.0722	1062.13		Unstable	18.60		Unstable
3	30	0.1730	7387.80		Unstable	35.78		Unstable
6	60	0.1730	7661.18		Unstable	49.68		Unstable
9	90	0.1730	6877.12		Unstable	64.16		Unstable
12	120	0.1730	6332.93		Unstable	80.68		Unstable
15	150	0.1730	5822.67		Unstable	95.29		Unstable

breakthrough recovery was high, and the displacement was considered to be unstable when the breakthrough recovery declined significantly.

As can be seen in Table 7, evaluation of the experimental instability number depends strongly on how the longitudinal dispersion coefficient is evaluated. Using Arya's dispersion coefficients, the prediction of the instability is consistent with the experimental observations except for the prediction for the two short packs (30 cm and 60 cm) at the second velocity. Using Blackwell's dispersion coefficients, the displacements are predicted to be absolutely stable for all the displacements, which is in good agreement with the experimental observations for the displacements at the lowest velocity, but is in disagreement for the displacements at higher velocities. Using Perkins and Johnston's dispersion coefficients, the prediction is similar to that of using Arya's, but the magnitude of the instability numbers are one to two orders of magnitude greater than the latter, which results from the difference in the values of the longitudinal dispersion coefficient used to calculate the instability number. As can be seen in Table 7, using the modified dispersion coefficients, the prediction of the instability is in good agreement with the experimental observation of the breakthrough recoveries for all the displacements.

A comparison of the breakthrough recoveries with the instability numbers calculated using the modified dispersion coefficients is given in Figure 7. As can be seen in Figure 7, a vertical line divides the graph into two zones: the zone on the left-hand side represents the stable zone, in which the instability numbers are less than the onset instability number, π^2 , and the zone on the right-hand side represents the unstable zone, in which the instability numbers are greater than the onset instability number. In the stable zone, a dashed line was drawn through the data points, which represents the average value of the breakthrough recoveries obtained from the displacements at the lowest velocity. As the pack lengths decrease from the shortest pack length (the data point above the average line), the breakthrough recoveries show a slight decline from the data point above the average line to

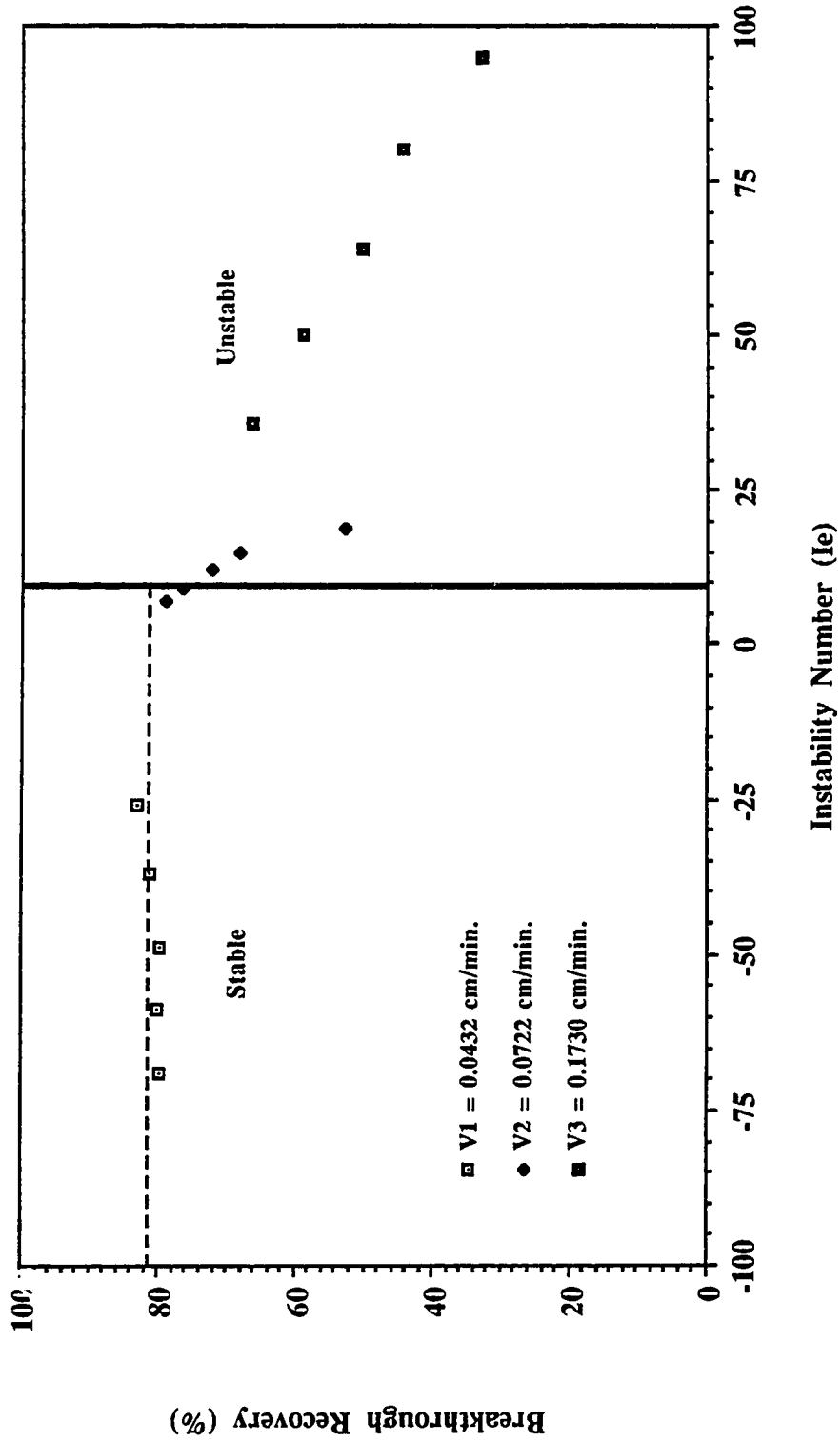


FIGURE 7: COMPARISON OF BREAKTHROUGH RECOVERY WITH INSTABILITY NUMBER

the data points below the average line. Two of the data points from the displacements at the second velocity are in the stable zone; as a result, the breakthrough recoveries from these two runs remained high. When the bead pack got longer, the displacements became unstable; as a consequence, the breakthrough recoveries decreased significantly. At the highest velocity, the data points are all in unstable zone, and the breakthrough recoveries declined consistently.

Consequently, the instability of the displacement seems to be core-length dependent when the displacement is predicted to be unstable. That is, if the displacement is unstable, under the same experimental conditions, the displacement may yield a lower breakthrough recovery in a longer porous medium. However, the instability of the displacement appears to be unaffected by core length when the displacement is stable. This observation can be explained as follows. It is thought that finger initiation processes existed for all three of the velocities used because the displacements were carried out at velocities greater than the stable critical velocity estimated using Eq. 4.2.32. In fact, this suggestion agrees with the stable mixing-zone length estimations, as the mixing-zone lengths (see Table 6) are shorter than the core lengths, except for the evaluation using Blackwell's dispersion coefficient. Therefore, fingers may start to grow at a very early stage of the displacement. However, at the lower displacing rate, the displacing time was long enough to allow transverse dispersion to eliminate finger development. In the longer packs, possibly because of the existence of inhomogeneity and permeability stratification in the bead-packs [48], the penetration of the finger into the displacing front worsened during the displacement process.

6.6 Comparison of the Concentration Curves

When one analyzes concentration curves from miscible displacements it is always desirable to have an approximate analytical model for predicting the concentration profiles

as well as for predicting the breakthrough recoveries. The solution (Eq. 4.1.31) to the generalized convection-dispersion equations (Eq. 4.1.16 and Eq. 4.1.22) enables the theoretical prediction of breakthrough recoveries, provided that certain conditions are met. These conditions are 1) the differences in viscosity and density of the displacing and displaced fluids are small; and 2) the dispersion coefficients can be determined either experimentally or empirically.

Assuming that the miscible fluids used in the experiments of this study satisfy the above conditions, the theoretical predictions of the breakthrough recovery and the concentration profiles are made using a numerical approximation of Eq. 4.1.31 [see Appendix C]. The longitudinal dispersion coefficients used for the calculation are the ones obtained using the modified Method.

Table 8 shows a comparison of the experimental breakthrough recoveries estimated for the fifteen runs with the theoretical predictions. As can be seen in Table 8, for the three longer packs (90, 120 and 150 cm), good agreement between the prediction and the breakthrough recovery was obtained for both stable and unstable displacements. For the two short packs (30 and 60 cm), the predicted breakthrough recovery, on average, was about 30 per cent less than the observed value, and therefore was not given in Table 8. One possible explanation for this inaccurate prediction in short packs is that the two short bead packs failed to meet the assumption that the porous medium was "infinitely long", which was invoked to simplify the solution.

A matching approach was taken to compare experimental concentration profiles with those obtained theoretically. Figures 8 through 10 show such plots (results from the rest of the runs are shown in Appendix D). In Figure 8, when the displacement (Run 13) was predicted to be stable, the results of the comparison showed that both the observed breakthrough recovery and the experimental concentration profile were well matched with

TABLE 8. COMPARISON OF EXPERIMENTAL BREAKTHROUGH RECOVERY WITH THEORETICAL PREDICTIONS

Run No.	Pack Length (cm)	Velocity (cm/min.)	B.T Recovery (%) (Experimental)	B.T Recovery (%) (prediction)
1	30	0.0432	82.88	-
4	60	0.0432	81.33	-
7	90	0.0432	79.82	78.9
10	120	0.0432	80.02	80.02
13	150	0.0432	79.66	79.66
2	30	0.0722	79.12	-
5	60	0.0722	76.59	-
8	90	0.0722	72.06	73.1
11	120	0.0722	58.45	58.45
14	150	0.0722	52.64	52.64
3	30	0.1730	66.35	-
6	60	0.1730	58.82	-
9	90	0.1730	50.04	48.23
12	120	0.1730	44.45	44.45
15	150	0.1730	32.92	35.46

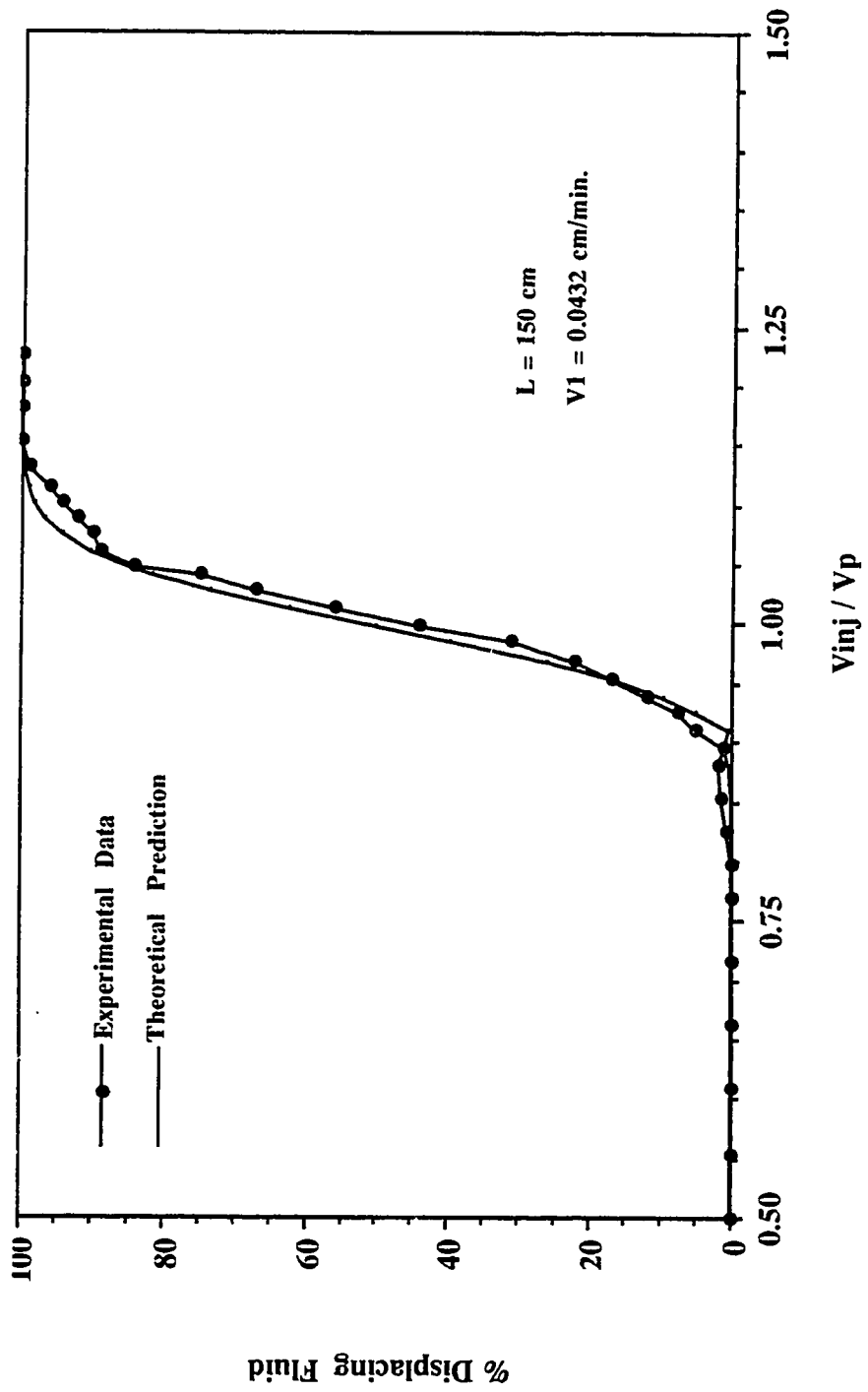


FIGURE 8: COMPARISON OF EXPERIMENTAL CONCENTRATION CURVE WITH THEORETICAL PREDICTION FOR RUN I3

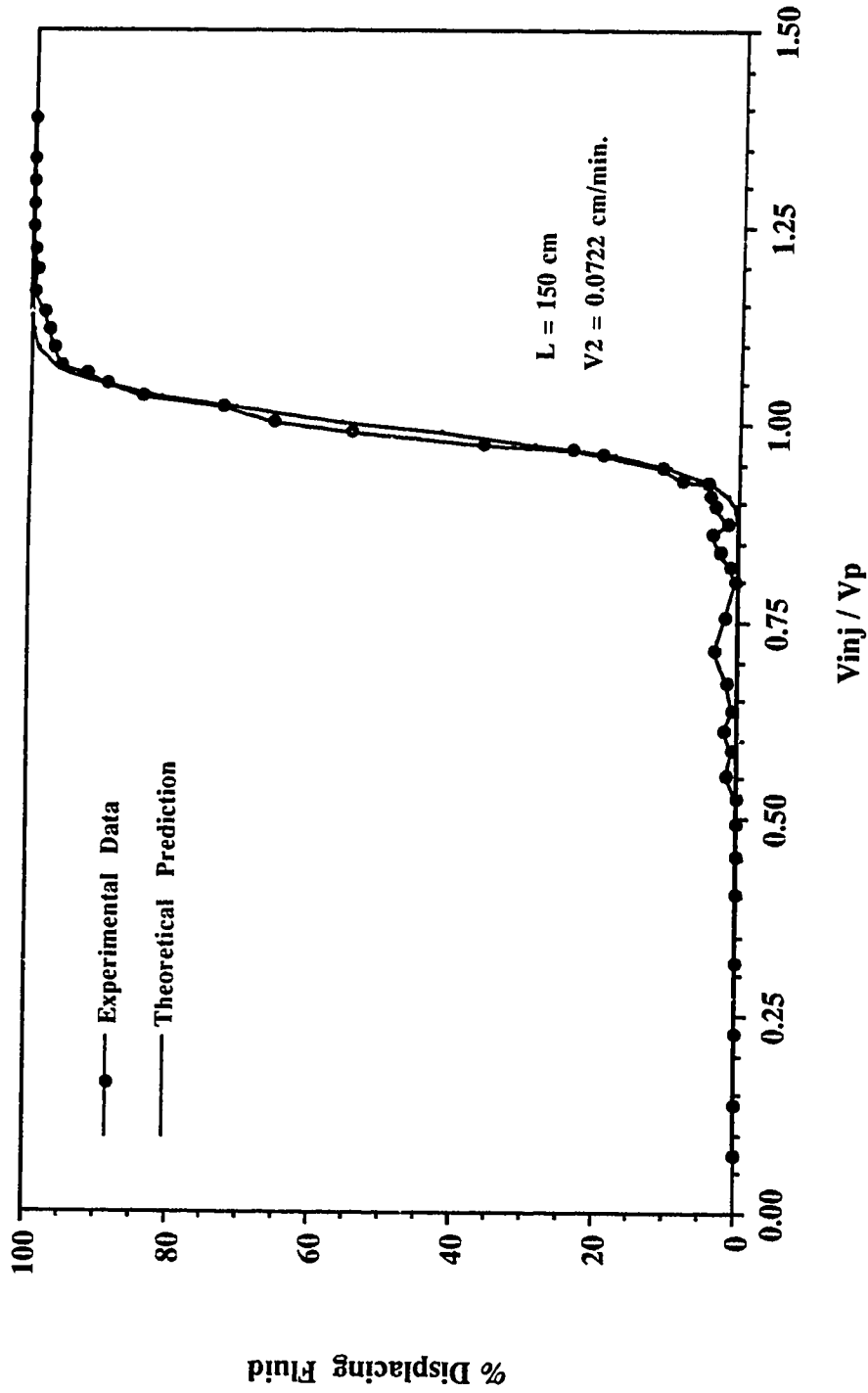


FIGURE 9: COMPARISON OF EXPERIMENTAL CONCENTRATION CURVE WITH THEORETICAL PREDICTION FOR RUN 14

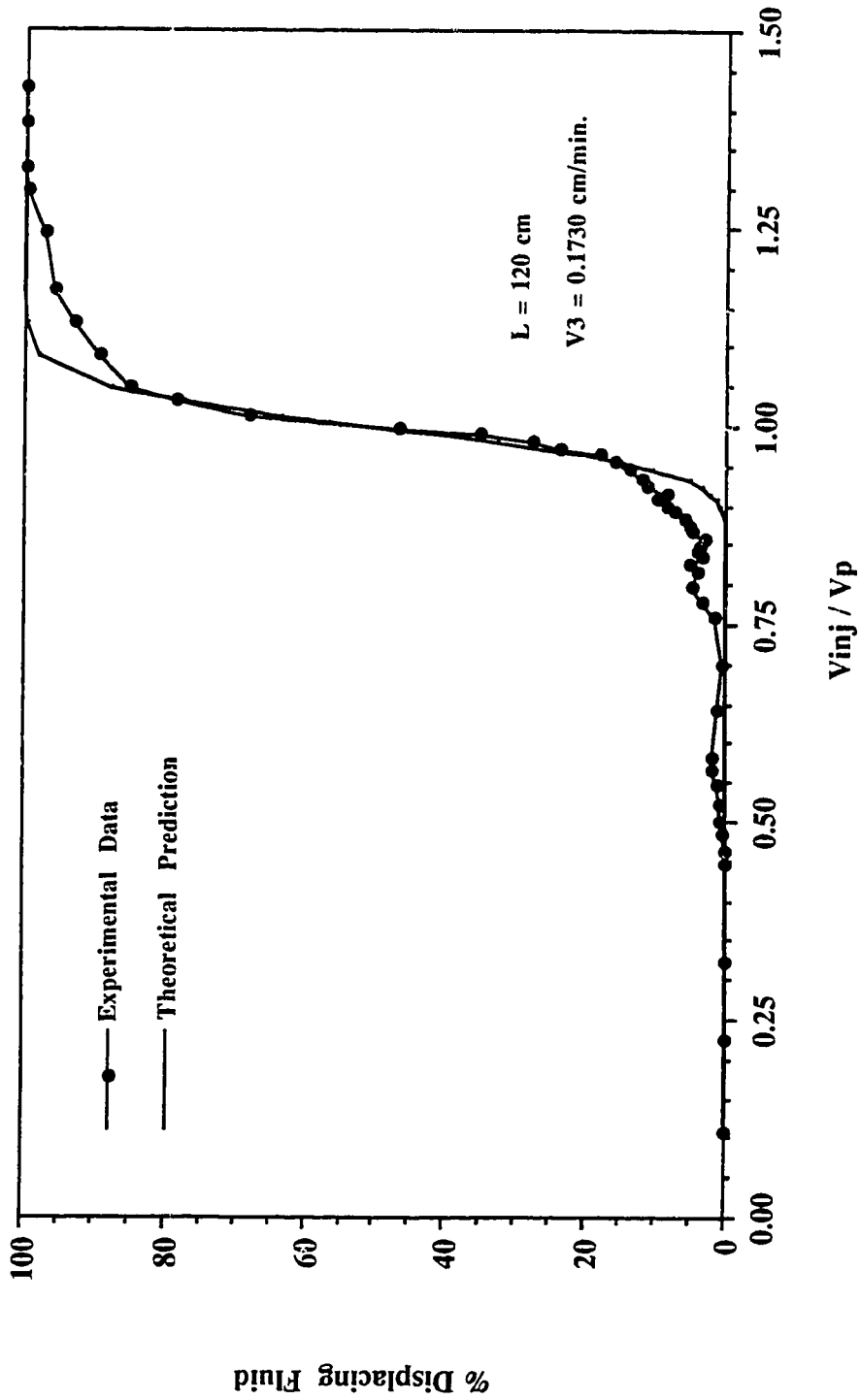


FIGURE 10: COMPARISON OF EXPERIMENTAL CONCENTRATION CURVE WITH THEORETICAL PREDICTION FOR RUN 15

the theoretical prediction. However, in Figures 9 and 10, when both of the displacements (Run 14 and Run 15) were predicted to be unstable, the calculations showed a considerable disagreement between the observed and the predicted breakthrough recoveries if the same longitudinal dispersion coefficient was used to predict both the theoretical concentration profile and the breakthrough recovery. Note that the breakthrough recoveries reported in Table 8 were estimated using a different longitudinal dispersion coefficient. In fact, the theoretical model failed to describe the concentration perturbations at early breakthrough which demonstrated the breakthrough of a long solvent finger. It is interesting to note that the observed concentration profiles match the predicted concentration profiles when the mixing-zone arrives at the outlet end, which is represented by the portion of the curves appearing as an "S" shape. It appears that, after solvent finger breakthrough at the outlet, the experimental concentration curves exhibit perturbations until mixing-zone breakthrough occurs.

Figure 11 is presented so as to be able to compare one set of Brigham's experimental data [7] with the theoretical prediction using the same approach as above. The concentration data were obtained from an unstable displacement using fluids having an unfavorable viscosity ratio. As can be seen in Figure 11, good agreement between the observed and predicted concentration profiles was also achieved. However, such a match may not prove that the theoretical model is valid for the whole displacement process; rather, the theoretical model may be valid only subsequent to the arrival of the mixing zone.

In order to obtain a good match of the experimental and the theoretical concentration profiles, a trial and error approach had to be taken to obtain the modified dimensionless dispersion coefficient, γ_m . The modified dimensionless dispersion coefficient defined in this study differs from the one defined by Brigham because an extra term involving porosity appears in the expression. That is,

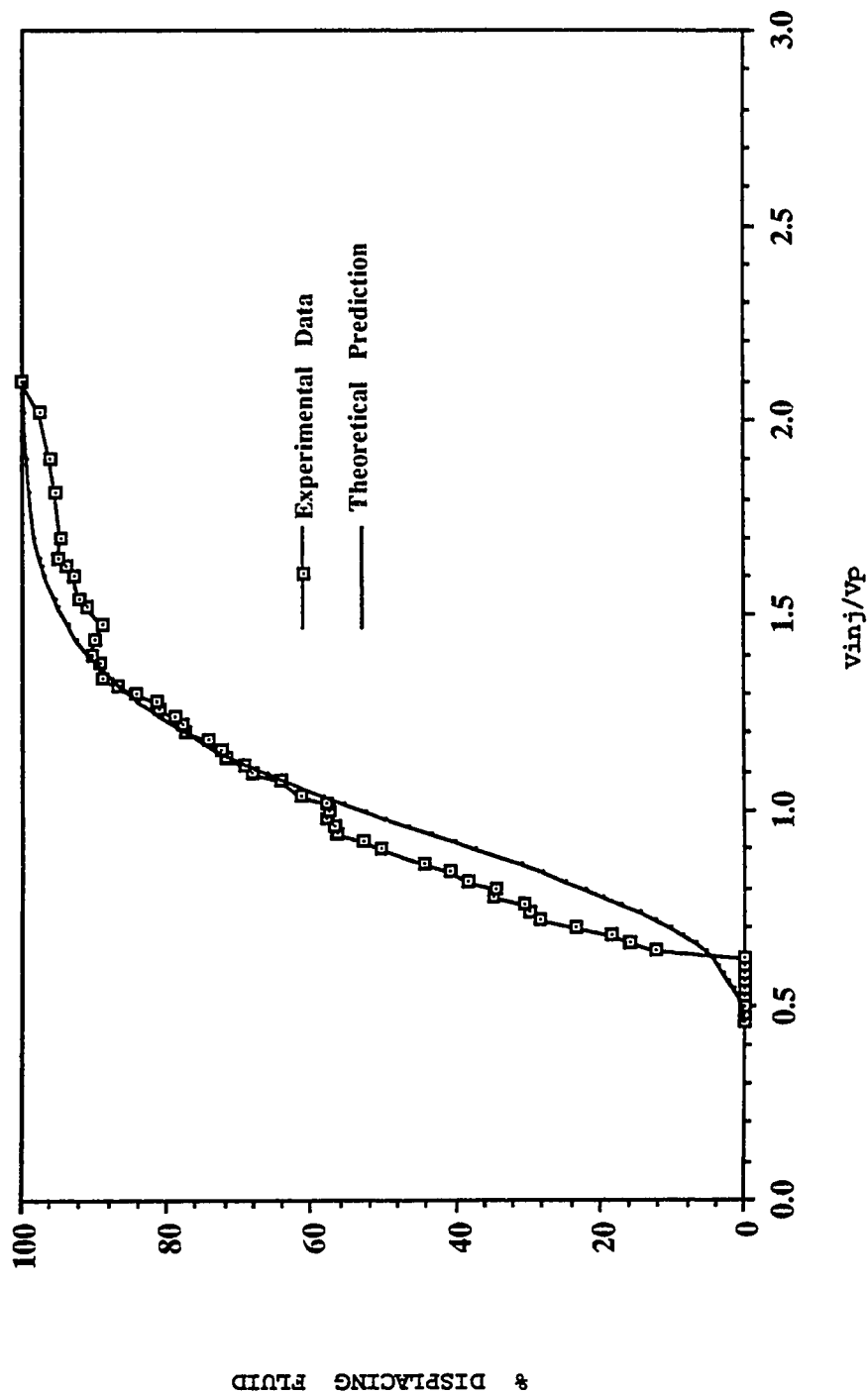


FIGURE 11: COMPARISON OF BRIGHAM'S EXPERIMENTAL DATA WITH THE MONIFIED THEORETICAL PREDICTION

(μ_o/μ_s : 5.71, Pack No. 113-3)

$$\gamma_m = \left(\frac{\phi}{\phi + 1} \right) \left(\frac{V_L}{D_p} \right) \quad (6.19)$$

where D_p is defined as a pseudo-dispersion coefficient. The pseudo-dispersion coefficient, D_p , was found to have different values from the longitudinal dispersion coefficient, D_L , obtained from the experimental concentration profile even for stable displacements, as can be seen in Table 9. One possible explanation is that the two dispersion coefficients represent different stages of the mixing process. In other words, D_L represents mainly the mixing at early breakthrough, or at solvent finger breakthrough, and D_p represents the mixing of the mixing zone which is an average effect of all the mixing processes. An attempt was made to correlate the pseudo-dispersion coefficient with the transverse dispersion coefficient, D_T , and the longitudinal dispersion coefficient, D_L , but no evident correlation was found.

Two sets of the dimensionless dispersion coefficient, γ_m , are given in Table 9. As can be seen in Table 9, when the displacement is stable, γ_m has the same value for predicting the breakthrough recovery and the concentration profiles. When the displacement is unstable, one has to use different values of γ_m for predicting the breakthrough recovery and the concentration profiles. It is interesting to note that this inconsistency appears only when the displacement is unstable. One possible explanation is that when the displacement is unstable, different values of the longitudinal dispersion coefficient should be used to define the early and late periods of the displacement. In other words, if a displacement is stable experimentally and theoretically, the same dispersion coefficient may be used for the prediction of the breakthrough recovery and the concentration profile. If a displacement gives evidence of distinct "fingers" of displacing fluid running ahead of the mixing-zone front, different values of the dispersion coefficient must be used to predict the breakthrough recovery and the concentration profile. This disagreement may demonstrate that when the

TABLE 9. THEORETICAL CONCENTRATION PROFILE CALCULATIONS

Run No	Length (cm)	Velocity (cm/min)	Experimental Observation	Dimensionless Dispersion Coefficient		Dispersion Coefficient	
				For B.T	For Profile	Dl	Dp
						(cm ² /sec.)	(cm ² /min.)
1	30	0.0432	Stable	-	1255	0.1191	0.000258
4	60	0.0432	Stable	-	2016	0.1336	0.000324
7	90	0.0432	Stable	855	855	0.2962	0.001145
10	120	0.0432	Stable	897	897	0.5785	0.001441
13	150	0.0432	Stable	915	915	1.0601	0.001758
2	30	0.0722	Stable	-	1817	0.0324	0.000298
5	60	0.0722	Stable	-	1189	0.0266	0.000918
8	90	0.0722	Unstable	255	1355	0.0142	0.001208
11	120	0.0722	Unstable	258	2038	0.0061	0.001060
14	150	0.0722	Unstable	201	2340	0.0029	0.001149
3	30	0.1730	Unstable	-	370	0.0740	0.003509
6	60	0.1730	Unstable	-	555	0.0627	0.004712
9	90	0.1730	Unstable	80	1355	0.0349	0.002894
12	120	0.1730	Unstable	121	2191	0.0158	0.002363
15	150	0.1730	Unstable	78	2378	0.0069	0.002709

displacement is unstable, neither of the simplified models (Eq. 4.1.21 and Eq. 4.1.23) is suitable for representing the miscible displacement when the fluids have unequal density and unequal viscosity.

6.6 Discussion of Errors

There were two types of errors: errors from raw data, and errors from the estimation of dispersion coefficients. Errors in the raw data were those involving porosity and permeability measurements and those involving refractive index measurements, especially the readings to identify breakthrough recovery. Errors in the dispersion coefficient determination were those resulting from the use of Perkins and Johnston's expression for calculating transverse dispersion coefficients, which was valid only for fluids having favorable viscosity ratios, and those resulting from estimating the solvent concentration at one pore volume injected from the experimental concentration curves.

The errors in porosity and permeability measurements have a negligible effect on the instability predictions and the theoretical concentration profile calculations. For example, a five per cent increase (or decrease) in porosity results in a 0.2 per cent decrease (or increase) in the values of the instability number. A seven per cent increase (or decrease) in permeability results in less than a three per cent decrease (or increase) in the values of the instability number. These changes makes no difference in identifying the instability condition of the displacements.

Errors in the refractive index measurements were kept under control by checking the first sample appearing to show a slight drift of the refractive index from that for pure displaced fluid (Marcol) against a sample reference at least three times. The same procedure was followed for identifying 100 per cent oil recovery. Unlike the refractive index measured at the beginning and the end of each displacement, the refractive index of

samples taken after the mixing zone had arrived at the outlet were easier to distinguish from one another, which reflects a greater variation in the solvent concentration.

Little was known about the errors introduced when one determines the transverse dispersion coefficients using an inadequate estimation, particularly when viscous fingers developed. The evaluation of the longitudinal dispersion coefficients presented in this study had a significant effect on the determination of the instability of the displacements, as can be seen in Table 7. Consequently, it seems that comparison of the experimental instability number with the marginal instability number could be an adequate approach for identifying whether or not a displacement is stable, provided that the longitudinal dispersion coefficient can be determined adequately. However, a more accurate way for estimating the longitudinal dispersion coefficients of miscible fluids at unfavorable viscosity ratios needs to be defined, and the method used in this study needs further investigation for application purposes.

7. SUMMARY AND CONCLUSIONS

An experimental investigation has been carried out in glass-bead packs using miscible fluids to study the effect of system length on linear miscible displacements. The porous medium was made of five different lengths, and three different displacing rates were used to perform the floods downward. The displacing and displaced fluids were chosen to have unequal viscosities and unequal densities in order to achieve a relatively greater dispersion than that of fluids with matched properties. Effluent concentration profiles developed at the outlet were obtained by taking frequent samples and measuring their refractive indices.

Based on the experimental and analytical results presented herein, the following conclusions have been drawn for displacements conducted in this investigation:

1. Theoretically, the dimensionless scaling group proposed by Coskuner and Bentsen is valid only when the fluids used have same density and viscosity. However, it is observed from the present study that, when fluids of unequal density and unequal viscosity are used, the dimensionless scaling group for the theoretical prediction of instability of the miscible displacements may be applicable for fluids having small differences in density and viscosity, provided that the dispersion coefficients can be determined adequately. A comparison of the experimental instability number with the marginal instability number may be used to predict the instability condition of the displacement.
2. The length of the porous medium is an important variable which may affect the instability of miscible displacements. That is, longer systems result in earlier breakthroughs in comparison with shorter ones under the same displacing conditions, or a displacement may change from stable in a short bead pack to

- unstable in a longer one. When the displacements are stable, however, the effect of length on breakthrough recovery seems to be insignificant.
3. It is shown from the modified method that the longitudinal dispersion coefficient appears to be a function of the bead-pack length. Moreover, at low velocities, the dispersion coefficient increases slightly with the bead-pack length, and at high velocities, the dispersion coefficient increases with the bead-pack length more significantly.
 4. If the core-length dependency of the longitudinal dispersion coefficient is theoretically conclusive, the stable mixing-zone length is also length dependent. Moreover, the greater the longitudinal dispersion coefficient, the longer the stable mixing-zone length. Because D_L has been assumed to be proportional to V , the impact of velocity on the length of stable mixing zone has been slight.
 5. Contrary to the observations of Brigham et al., at viscosity ratios above 1.0, the theoretical error function curve may still be valid when a displacement is stable, provided that one uses a properly defined longitudinal dispersion coefficient.

8. SUGGESTIONS FOR FUTURE STUDY

The following investigations are suggested in future studies of miscible displacements:

1. Numerical solution of the generalized convection-dispersion equation should be studied, and experiments using fluids having an unfavorable density ratio should be conducted to verify the theory presented in this study.
2. Experiments should be conducted to study the relationship between the stable mixing-zone length and the longitudinal dispersion coefficient using fluids of unequal density and unequal viscosity. The experimental apparatus should allow one to measure the stable mixing-zone length at different times during the displacement.
3. Experiments should be conducted using the same displacing rate and the same porous medium to investigate the effect of unfavorable viscosity ratio on the estimation of the longitudinal dispersion coefficient.
4. Experiments should be conducted to investigate how to determine the transverse dispersion coefficient for miscible fluids having unfavorable viscosity ratios. The experimental apparatus should allow one to measure the stable mixing-zone width which relate approximately to the transverse dispersion coefficient.
5. A theoretical and experimental investigation of the molecular diffusion coefficient for miscible fluids of unequal viscosities and unequal densities should be made for more practical miscible displacement studies.

REFERENCES

1. Collins, R. E. : "*Flow of Fluids through Porous Media*"; Reinhold Publishing Co., New York City (1961), 201.
2. Taylor, G. I. : "*Dispersion of Soluble Matter in Solvent Flowing Slowly through a Tube*"; Proc. Roy. Soc. (1953), Vol. 219,186.
3. Van der Poel, C. : "*Effect of Lateral Diffusivity on Miscible Displacement in Horizontal Reservoirs*"; Soc. Pet. Eng. Jour. (Dec. 1962), 317.
4. Reamer, H. H. and Sage, B. H. : "*Chemical Engineering Data*"; (1959), Vol. 4, 15.
5. Trevoy, D. J. and Drickamer, H. G. : Chem. Phys. Jour. (1949), Vol. 17, 1117.
6. Warren, J. E. and Skiba, F. F. : "*Macroscopic Dispersion*"; (Sept. 1964), Trans. AIME, 231, 215-30.
7. Brigham, W. E., Read, P. W. and Dew, J. N. : "*Experiments on Mixing During Miscible Displacements in Porous Media*"; Soc. Pet. Eng. Jour. (March 1961). Trans. AIME, 225, 1-8.
8. Crane, F. E. and Gardner, G. H. F. : "*Measurements of Transverse Dispersion in Granular Media*"; Jour. Chem. Eng. Data (1961), Vol. 6, 283.
9. Morse, R. A. : "*Discussion*"; Trans. AIME (1954), Vol. 201, 315-316.
10. Kyle, C. R. and Perrine, R. L. : "*Experimental Studies of Miscible Displacement Instability*"; Soc. Pet. Eng. Jour. (Sept. 1965), Trans. AIME, 234, 189-95.

11. Perkins, T. K. and Johnston, O. C. : "*A Review of Diffusion and Dispersion in Porous Media*"; Soc. Pet. Eng. Jour. (March 1963), 70-79.
12. Slobod, R. L. and Thomas, R. A. : "*Effect of Transverse Diffusion on Fingering in Miscible-Phase Displacement*"; Soc. Pet. Eng. Jour. (March 1963), 9-40.
13. Blackwell, R. A. : "*Laboratory Studies of Microscopic Dispersion Phenomena*"; SPE Reprint Series No. 8, Miscible Processes, 69-76.
14. Aris, R. and Amundson, N. R. : "*Some Remarks on Longitudinal Mixing or Diffusion in Fixed Beds*"; AIChE Jour. (1957), 3, 280.
15. Slawinski, A. : "*Conductivity of an Electrolyte Containing Dielectric Bodies*"; Chem. Phys. Jour. (1962).
16. Arya, A. , Hewett, T. A. , Carson, R. G. and Lake, L. W. : "*Dispersion and Reservoir Heterogeneity*"; SPE Reservoir Engineering (March 1988), 139-148.
17. Pickens, J. F. and Grisak, G. E. : "*Scale - Dependent Dispersion in a Stratified Granular Aquifer*"; Water Resources Research, 17 (1981), 1191-1121.
18. Udey, N. and Spanos, T. J. T. : "*A New Approach to Predicting Miscible Flood Performance* "; Paper No. 91-5, presented at the 1991 CIM/AOSTRA Technical Conference in Banff, April 21-24, 1991.
19. Pozzi, A. L. and Blackwell, R. J. : "*Design of Laboratory Models for Study of Miscible Displacement*"; SPE Reprint Series No. 8, Miscible Processes, 183-195.
20. Lacey, J. W., Draper, A. L., Binder, G.G, Jr. : "*Miscible Fluid Displacement in Porous Media*" ; Trans. AIME (1958), Vol. 213, 76-81.

21. Blackwell, R. J., Rayne, W. M. and Terry, W. M. :"*Factors Influencing the Efficiency of Miscible Displacement*", Trans. AIME (1959), Vol. 216, 1-8.
22. Keulemans, A. I. M. :"*Gas Chromatography*", Reinhold Press. N. Y. (1957).
23. Aronofsky, J. S. and Heller, J. P. :"*Diffusion Model to Explain Mixing of Flowing Miscible Fluids in Porous Media*", Trans. AIME (1957), Vol. 210, 345.
24. Offeringa, J. and Van der Poel, C. :"*Displacement of Oil from Porous Media by Miscible Liquids*", Trans. AIME (1954), Vol. 201, 310.
25. Coskuner, G., :"*A New Approach to the Onset of Instability for Miscible Displacement*", PhD. Dissertation, University of Alberta, Dec. 1986.
26. Coskuner, G. and Bentsen, R. G.:"*Effect of Length on Unstable Miscible Displacements*", JCPT (Jul.-Aug. 1989), Vol. 28, No. 4, 34-44.
27. Scheidegger, A. E.:"*Statistical Hydrodynamics in Porous Media*", Jour. Appl. Phys. (1954), Vol. 25, No. 8, 994.
28. Frankel, Stanley:"*Mixing of Fluid Flowing in a Porous Medium*", Conference on Theory of Fluid Flow in Porous Media, U. of Oklahoma, March 23-24, 1959.
29. Brigham, W. E., :"*Mixing Equations in Short Laboratory Cores*", Soc. Pet. Eng. Jour. (Feb. 1974), 91-99.
30. Correa, A. C., Pande, K. K., Ramey, H. J. and Brigham, W. E., :"*Computation and Interpretation of Miscible Displacement Performance in Heterogeneous Porous Media*", SPE Reservoir Engineering (Feb. 1990), 69-78.

31. Deans, H. A. : "*A Mathematical Model for Dispersion in the Direction of Flow in Porous Media*", Trans. AIME (1963), Vol. 228, 49.
32. Coats, K. H. and Smith, B. D. : "*Dead-End Pore Volume and Dispersion in Porous Media*", Soc. Pet. Eng. Jour. (March 1964), 78-84; Trans. AIME, Vol. 231.
33. Bretz, R. E. and Orr F. M., Jr. : "*Interpretation of Miscible Displacements in Laboratory Cores*", Soc. Pet. Eng. Jour. (Nov. 1987), 492-500.
34. Grisak, G. E. and Pickens, J. F. : "*An Analytical Solution for Solute Transport through Fractured Media with Matrix Diffusion*", Jour. Hydrol. (1981), Vol. 52, 47-57.
35. Warren, J. E. and Skiba, F. F. : "*Macroscopic Dispersion*", Soc. Pet. Eng. Jour. (Sept. 1964), 215-30; Trans. AIME, Vol. 231.
36. Habermann, B. : "*The Efficiencies of Miscible Displacement as a Function of Mobility Ratio*", Trans. AIME, Vol. 219, 264; Miscible Processes Printing Series, SPE, Dallas (Aug. 1965), 205-214.
37. Perkins, T. K. and Johnston, O. C. : "*A Study of Immiscible Fingering in Linear Models*", Soc. Pet. Eng. Jour. (March 1969), 39-48.
38. Dougherty, E. L. : "*Mathematical Model of an Unstable Miscible Displacement*", Soc. Pet. Eng. Jour. (June 1963), 155-165.
39. Perrine, R. L. : "*The Development of Stability Theory for Miscible Liquid-Liquid Displacement*", Soc. Pet. Eng. Jour. (March 1961), 17-25.

40. Koval, E. J. :"*A Method for Predicting the Performance of Unstable Miscible Displacement in Heterogeneous Media*", Soc. Pet. Eng. Jour. (June 1963), 145-54; Trans. AIME, Vol. 228.
41. Jankovic, M. S. :"*Analytical Miscible Relative Permeability Curves and their Usage with Compositional and Pseudo-Miscible Simulators*", JCPT (July-August 1986), 55-56.
42. Gardner, J. W. and Ypma, J. G. J. :"*An Investigation of Phase Behavior - Macroscopic Bypassing Interaction in CO₂ Flooding*", SPE/DOE Paper No.10686, presented at the 3rd Joint Symp. on EOR of the SPE, Tulsa, OK, April 4-7, 1982.
43. Peaceman, D. W. and Rachford, H. H. Jr.: "*Numerical Calculation of Multidimensional Miscible Displacement*", Soc. Pet. Eng. Jour. (Dec. 1962), 327-329; Trans. AIME, Vol. 225.
44. Vossoughi, Shapour, Smith, J. E., Green, D. W. and Willhite, P.: "*A New Method to Simulate the Effects of Viscous Fingering on Miscible Displacement Process in Porous Media*", Soc. Pet. Eng. Jour. (Feb. 1984), 56-64.
45. Price, H. S., Cavendish, J. C. and Varga, R. S.: "*Numerical Method of Higher - Order Accuracy for Diffusion - Convection Equations*", Soc. Pet. Eng. Jour. (Sept. 1968), 293-303; Trans. AIME, Vol. 243.
46. Dumore, J. M., : "*Stability Considerations in Downward Miscible Displacements*", Soc. Pet. Eng. Jour. (Dec. 1964), Trans. AIME, Vol. 231, 356.
47. Coskuner, G. and Bentsen, R. G., : "*Effect of Length on Unstable Miscible Displacements*", JCPT (July-August 1989), Vol. 28, No. 4, 34-44.

48. Peters, E. J and Afzal, N.: "*Characterization of Heterogeneities in Permeable Media with Computed Tomography Imaging*", Journal of Petroleum Science and Engineering, Vol. 7 (1992), 283-296.
49. Shu, W. R.: "*A Viscosity Correlation for Mixture of Heavy Oil, Bitumen, and Petroleum Fractions*", Soc. Pet. Eng. Jour. (June 1984), 277-282.
50. Bentsen, R. G.: "*A Study of Plane Radial Miscible Displacement in a Consolidated Porous Medium*"; Msc. Dissertation, The Pennsylvania State University, June 1964.

BIBLIOGRAPHY

1. Stalkup, F. I., Jr. : "*Miscible Displacement*"; Henry L. Doherty Series, AIME, Monograph Vol. 8.
2. SPE Reprint Series : "*Miscible Processes*"; No. 8.
3. SPE Reprint Series : "*Miscible Processes II*"; No. 18.
4. Crank, J.: "*The Mathematics of Diffusion*"; Second Edition, Oxford University Press, New York City (1975).
5. Collins, R. E.: "*Flow of Fluids through Porous Media*"; Reinhold Publishing Co., New York City (1961).
6. Hassinger, R. C. and von Rosenberg, D. V.: "*A Mathematical and Experimental Examination of Transverse Dispersion Coefficients*"; Soc. Pet. Eng. Jour. (June 1968), 195-204; Trans. AIME, Vol. 243.
7. "*Tables of the Error Function and Its Derivative*"; Ntal. Bureau of Standards, Applied Mathematics Series No. 41 (Oct. 1954).
8. Crane, F. E., Kendall, H. A. and Gardner, G. H. F.: "*Some Experiments of the Flow of Miscible Fluids of Unequal Density through Porous Media*"; Soc. Pet. Eng. Jour. (Dec. 1963), 277-80; Trans. AIME, Vol. 228.
9. Craig, F. F. Jr. et al. : "*A Laboratory Study of Gravity Segregation in Frontal Drives*"; Trans. AIME (1957), Vol. 210, 275-82.

10. Habermann, B. :"*The Efficiencies of Miscible Displacement as a Function of Mobility Ratio*"; Trans. AIME (1960), Vol. **219**, 264.
11. Benham, A. L. and Olson, R. W. :"*A Model Study of Viscous Fingering*"; Soc. Pet. Eng. Jour. (June 1963), 138-44; Trans. AIME, Vol. **228**.
12. Perkins, T. K., Johnston, O. C. and Hoffman, R. N.: "*Mechanics of Viscous Fingering in Miscible Systems*"; Soc. Pet. Eng. Jour. (Dec. 1965), 301-17; Trans. AIME, Vol. **234**.
13. Perrine, R. L.: "*A Unified Theory for Stable and Unstable Miscible Displacement*"; Soc. Pet. Eng. Jour. (Sept. 1963), 205-13; Trans. AIME, Vol. **228**.
14. Bentsen, R. G. and Nielsen, R. F.: "*A Study of Plane Radial Miscible Displacement in a Consolidated Porous Medium*"; Soc. Pet. Eng. Jour. (March 1965), 1-5; Trans. AIME, Vol. **234**.
15. Claridge, E. L.: "*Prediction of Recovery in Unstable Miscible Flooding*"; Soc. Pet. Eng. Jour. (April 1972), 143-55.
16. Chuoke, R. L., van Meurs, P. and van der Poel, C.: "*The Instability of Slow, Immiscible Viscous Liquid-Liquid Displacements in Permeable Media*"; Trans. AIME (1959), Vol. **216**, 188-94.
17. Outmans, H. D.: "*Nonlinear Theory for Frontal Stability and Viscous Fingering in Porous Media*"; Soc. Pet. Eng. Jour. (June 1962), 165-76.
18. Dyes, A. B., Caudle, B. H. and Erikson, R. A.: "*Oil Production after Breakthrough - As Influenced by Mobility Ratio*"; Trans. AIME (1954), Vol. **201**, 81-86.

19. Hall, H. N. and Geffen, T. M.: "*A Laboratory Study of Solvent Flooding*"; Trans. AIME (1957), Vol. 210, 48-57.
20. Coskuner, G. and Bentsen, R. G.: "*A New Stability Theory for Designing Graded Viscosity Banks*"; JCPT (Nov-Dec 1987), Vol. 26, No. 6, 26-30.
21. Coskuner G. and Bentsen, R. G.: "*A Scaling Criterion for Miscible Displacements*"; JCPT (Jan.-Feb. 1990), Vol. 29, No. 1, 86-88.
22. Fayers, F. J.: "*An Approximate Model with Physically Interpretable Parameters for Representing Miscible Viscous Fingering*"; SPE Reservoir Engineering (May 1988), 551-558.
23. Fayers, F. J. and Newley, T. M. J.: "*Detailed Validation of an Empirical Model for Viscous Fingering with Gravity Effects*"; SPE Reservoir Engineering (May 1988), 542-550.
24. Cristie, M. A. and Bond, D. J.: "*Detailed Simulation of Unstable Process in Miscible Flooding*"; SPE Reservoir Engineering (November 1987), 514-522.

APPENDIX A

A Generalized Convection-Dispersion Equation

Assuming that the flow system is comprised of two miscible fluids: fluid 1 and fluid 2, Udey and Spanos [18] derived a generalized convection-dispersion equation which took into account the differences in fluid properties. It is written as

$$\frac{\partial C_{f2}}{\partial t} + \bar{V} \cdot \bar{\nabla} C_{f2} = \frac{1}{\rho} \bar{\nabla} \cdot (\rho \bar{D}_m \cdot \bar{\nabla} C_{f2}) \quad (\text{A.1})$$

where C_{f2} is defined as the solvent flowing concentration which is related to the solvent mass concentration C_2 by $C_{f2} = C_2 / \rho$, and D_m is defined as the apparent dispersion which varies from point to point in the flow system. Other variables are defined as follows:

$$\rho = \rho_2 + (\rho_1 - \rho_2)S_1 \quad (\text{A.2})$$

and

$$\bar{V} = \frac{C_1 \bar{V}_1 + C_2 \bar{V}_2}{\rho} \quad (\text{A.3})$$

where

$$\bar{V}_i = \frac{1}{S_i A} \frac{q_i}{\phi} \quad (i=1, 2) \quad (\text{A.4})$$

$$q_i = \frac{K K_{r_i} A \Delta P}{L \mu_i} \quad (i = 1, 2) \quad (\text{A.5})$$

and

$$S_i = \frac{C_i}{\rho_i} \quad (i = 1, 2) \quad (\text{A.6})$$

Assuming a one-dimensional flow system and that the apparent dispersion, D_m , may be replaced by the longitudinal dispersion coefficient, D_L , substituting Eqs. A.2 through A.6 into Eq. A.1 and rearranging the equation, one obtains

$$D_L \frac{\partial^2 C_2}{\partial X^2} + D_L \frac{1}{\rho} \frac{\partial \rho}{\partial X} \frac{\partial C_2}{\partial X} - \frac{1}{\rho} \left(\frac{\rho_1 K_{r1}}{\mu_1} + \frac{\rho_2 K_{r2}}{\mu_2} \right) \frac{K \Delta P}{\phi L} \frac{\partial C_2}{\partial X} = \frac{\partial C_2}{\partial t} \quad (\text{A.7})$$

Differentiating Eq. A.2 with respect to X and noting that $S_1 = 1 - S_2$ yields

$$\frac{\partial \rho}{\partial X} = \frac{\rho_2 - \rho_1}{\rho_1} \frac{\partial C_2}{\partial X} \quad (\text{A.8})$$

Substituting Eq. A.8 into Eq. A.7 shows that

$$D_L \frac{\partial^2 C_2}{\partial X^2} - \frac{1}{\rho} \left(\frac{\rho_1 K_{r1}}{\mu_1} + \frac{\rho_2 K_{r2}}{\mu_2} \right) \frac{K \Delta P}{\phi L} \frac{\partial C_2}{\partial X} + D_L \frac{\rho_2 - \rho_1}{\rho \rho_1} \left(\frac{\partial C_2}{\partial X} \right)^2 = \frac{\partial C_2}{\partial t} \quad (\text{A.9})$$

It should be noted that it may be difficult to obtain values of relative permeability for each miscible fluid, which may limit the utility of Eq. A.9. When the fluids have equal densities and equal viscosities, $K_{r1} = K_{r2} = 1/2$, and Eq. A.9 becomes

$$D_L \frac{\partial^2 C_2}{\partial X^2} - U \frac{\partial C_2}{\partial X} = \frac{\partial C_2}{\partial t} \quad (\text{A.10})$$

That is, Eq. A.10 becomes the well-known convection-dispersion equation.

APPENDIX B

Marginal Instability and Instability Number of Experiments

The marginal instability number of a displacement in a three-dimensional porous system, which is the stability criterion used to determine the condition for marginal instability, was initially defined by Coskuner and Bentsen. The condition of marginal instability divides perturbations which are damped periodically from those which grow periodically, provided that the principle of exchange of stabilities holds true. Dictated by the smallest non-zero eigenvalue, the approximation to the condition for the onset of instability is given as

$$\frac{K \left(\frac{U d\mu}{K dC} - \frac{d\rho}{dC} g \right) \frac{\partial \bar{C}}{\partial z} \frac{L_x^2 L_y^2}{L_x^2 + L_y^2}}{\mu \phi D_L} = \pi^2 \left(\frac{1}{\Omega} + 1 \right) \left(\frac{1}{\Omega} + K_d \right) \quad (\text{B.1})$$

where K_d is the ratio of the transverse dispersion, D_T , to the longitudinal dispersion coefficient, D_L . The gradients $d\mu/dC$ and $d\rho/dC$ are evaluated at the average concentration value defined at the average viscosity of the two fluids, and Ω is a dimensionless length defined by

$$\Omega = \frac{L^2 (L_x^2 + L_y^2)}{L_x^2 L_y^2} \quad (\text{B.2})$$

Previous studies [20, 23] have indicated that longitudinal and transverse dispersion coefficients vary with displacing rate and core length. Hence, it seems prudent to assume that K_d is also dependent on displacing rate and core length. For the flow conditions used in this study, the maximum variation in the values of $(1/\Omega + K_d)$ based on the three velocities and the five core lengths used is about 0.5%. In order to eliminate the velocity dependence of the group of parameters on the right-hand side of Eq. B.1, it seems preferable to bring $(1/\Omega + K_d) (1/\Omega + 1)$ to the left-hand side of Eq. B.1. Rearranging Eq. B.1 in such a way leads to

$$\frac{K\left(\frac{U}{K} \frac{d\mu}{dC} - \frac{d\rho}{dC} g\right)}{\bar{\mu}\phi D_L \left(\frac{1}{\Omega} + 1\right) \left(\frac{1}{\Omega} + K_d\right)} \frac{\partial \bar{C}}{\partial z} \frac{L_x^2 L_y^2}{L_x^2 + L_y^2} = \pi^2 \quad (\text{B.3})$$

If one defines the right-hand side of Eq. B.3 as the marginal instability number, I_m , it follows that

$$I_m = \pi^2 \quad (\text{B.4})$$

Moreover, if one defines the left-hand side of Eq. B.4 as the experimental instability number, I_e , it follows that

$$I_e = \frac{K\left(\frac{U}{K} \frac{d\mu}{dC} - \frac{d\rho}{dC} g\right)}{\bar{\mu}\phi D_L \left(\frac{1}{\Omega} + 1\right) \left(\frac{1}{\Omega} + K_d\right)} \frac{\partial \bar{C}}{\partial z} \frac{L_x^2 L_y^2}{L_x^2 + L_y^2} \quad (\text{B.5})$$

According to the Coskuner-Bentsen stability theory, which has been validated experimentally only for a Hele-Shaw system, when I_e , for a particular core length, is less than I_m , the displacement should be stable. In other words, no viscous fingers will appear to distort the isoconcentration line at the displacing front. However, when I_e is greater than I_m , viscous fingers will develop and cause early breakthrough recovery.

The instability numbers I_m and I_e in Eqs. B.4 and B.5 were calculated in the following manner. Given that

$$L = 0.6 \text{ m}$$

$$L_x = 0.05 \text{ m}$$

$$L_y = 0.15 \text{ m}$$

it may be shown that

$$\Omega = \frac{L^2(L_x^2 + L_y^2)}{L_x^2 L_y^2} = 160 \quad (\text{B.6})$$

and

$$I_m = \pi^2 = 9.8696 \quad (\text{B.7})$$

For the following experimental conditions applied in this study one has

$$\begin{aligned}
 V &= 1.2033 \times 10^{-5} \text{ m/s} \\
 K &= 2.7657 \times 10^{-9} \text{ m}^2 \\
 \phi &= 0.3368 \\
 \bar{\mu} &= 0.01156 \text{ Pa}\cdot\text{s}
 \end{aligned}$$

and the other parameters were calculated as those presented in Chapter 6; that is,

$$\left. \frac{d\mu_m}{dC} \right|_{c=\bar{c}} = -0.0524 \text{ Pa}\cdot\text{s}$$

$$\left. \frac{d\rho_m}{dC} \right|_{c=\bar{c}} = \rho_s - \rho_o = -61.0 \text{ Kg}\cdot\text{M}^{-3}$$

Following the modified Method, one may estimate the longitudinal dispersion coefficient, D_L . For Run 5, the longitudinal dispersion coefficient was estimated to be 0.0433 sq. cm/sec.

The values of longitudinal dispersion coefficients are given in Table 4. The maximum unperturbed concentration gradient is

$$\left. \frac{\partial C}{\partial z} \right|_{c=0.5} = -\sqrt{\frac{U}{\pi L D_L}} = -2.1137 \text{ m}^{-1} \quad (\text{B.8})$$

Using Eq. 2.1.7 to calculate the transverse dispersion coefficient, and then the ratio of the transverse to longitudinal dispersion coefficient, K_d , one may evaluate the instability number of the displacement from Run 5. If one has

$$D_T = 1.5574 \times 10^{-9} \text{ m}^2 / \text{s}$$

and $K_d = 3.5968 \times 10^{-4} \text{ m}^2 / \text{s}$

then

$$I_e = \frac{K \left(\frac{U d\mu}{K dC} - \frac{d\rho}{dC} g \right)}{\bar{\mu} \phi D_L \left(\frac{1}{\Omega} + K_d \right) \left(\frac{1}{\Omega} + 1 \right)} \frac{\partial \bar{C}}{\partial z} \frac{L_x^2 L_y^2}{L_x^2 + L_y^2} = 9.19 \quad (\text{B.9})$$

The values of the instability number for other runs are given in Table 7.

APPENDIX C

Numerical Evaluation of Concentration Curves

Typically, concentration and pore-volumes-injected data from miscible displacements are reported in the form of concentration curves. After breakthrough of the displacing fluid, such curves should show an "S" shape, if fluids with a favorable viscosity have been used. When such is the case, the convection-dispersion equation (Eq. 2.1.1) can be applied to describe the concentration curve. Brigham et al. [7] observed that the instability effects of an even slightly unfavorable viscosity ratio (1.002) would cause disproportionately more elongated concentration curves as compared to those pertaining to a favorable viscosity-ratio (0.998) displacement, and that with a higher viscosity ratio (i.e., 5.71), the concentration curve failed to keep an "S" profile. As a result, the convection-dispersion equation (Eq. 2.1.1) was no longer valid.

The concentration curves obtained in this study, which used fluids with an unfavorable viscosity (19.55), do have "S" shapes after the arrival of the mixing zone. The "S" shape concentration curves obtained from the experimental data of this study suggested that the simplified form of the convection-dispersion equation (Eq. 4.1.18) might be used to describe and interpret the data theoretically. The solution of Eq. 4.1.18 is the well-known error function given in Eq. 4.1.31. The error function, $erfc(X)$, can be evaluated numerically, which returns the complementary calculation of the error function with a fractional error everywhere less than 1.2×10^{-7} . The numerical procedure is shown as follows. If one defines:

$$Z = \text{ABS}(X) \quad (\text{C.1})$$

and

$$T = \frac{1}{1 + Z/2} \quad (\text{C.2})$$

one has

$$\begin{aligned} \text{erfc}(X) = & T \times \text{EXP}(-Z^2 - 1.26551223 + T \times (1.00002368 + T \times (0.37409196 + T \times (0.09678418 \\ & + T \times (-0.18628806 + T \times (0.27886807 + T \times (-1.13520398 + T \times (1.48851587 + T \times \\ & (-0.82215223 + T \times 0.17087277)))))))))) \end{aligned} \quad (\text{C.3})$$

If $X < 0$, one has

$$\begin{aligned} \text{erfc}(X) = & 2 - T \times \text{EXP}(-Z^2 - 1.26551223 + T \times (1.00002368 + T \times (0.37409196 + T \times (0.09678418 \\ & + T \times (-0.18628806 + T \times (0.27886807 + T \times (-1.13520398 + T \times (1.48851587 + T \times \\ & (-0.82215223 + T \times 0.17087277)))))))))) \end{aligned} \quad (\text{C.4})$$

APPENDIX D

Concentration Profiles

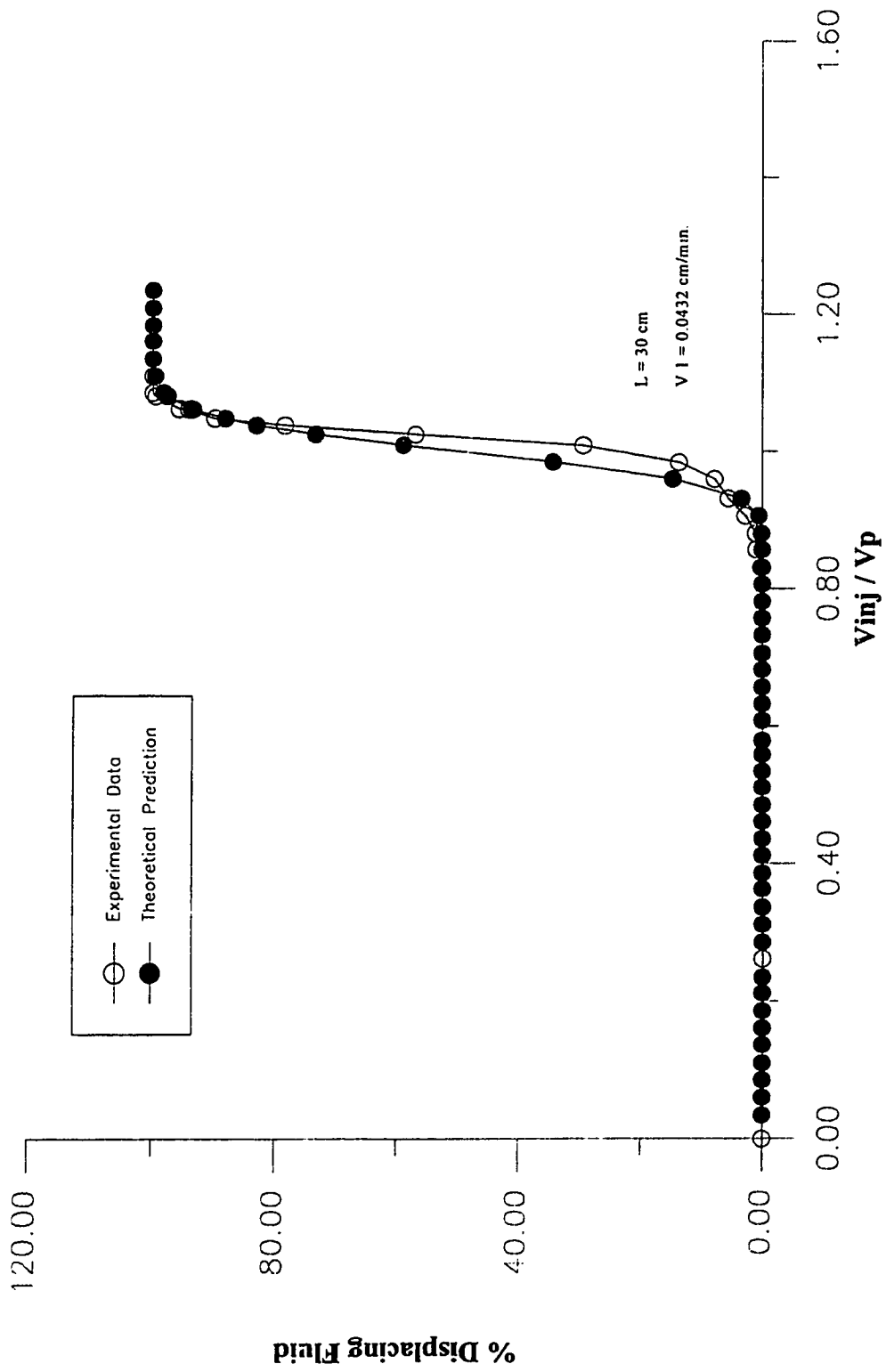


FIGURE 11: COMPARISON OF EXPERIMENTAL CONCENTRATION CURVE WITH THEORETICAL PREDICTION FOR RUN 1

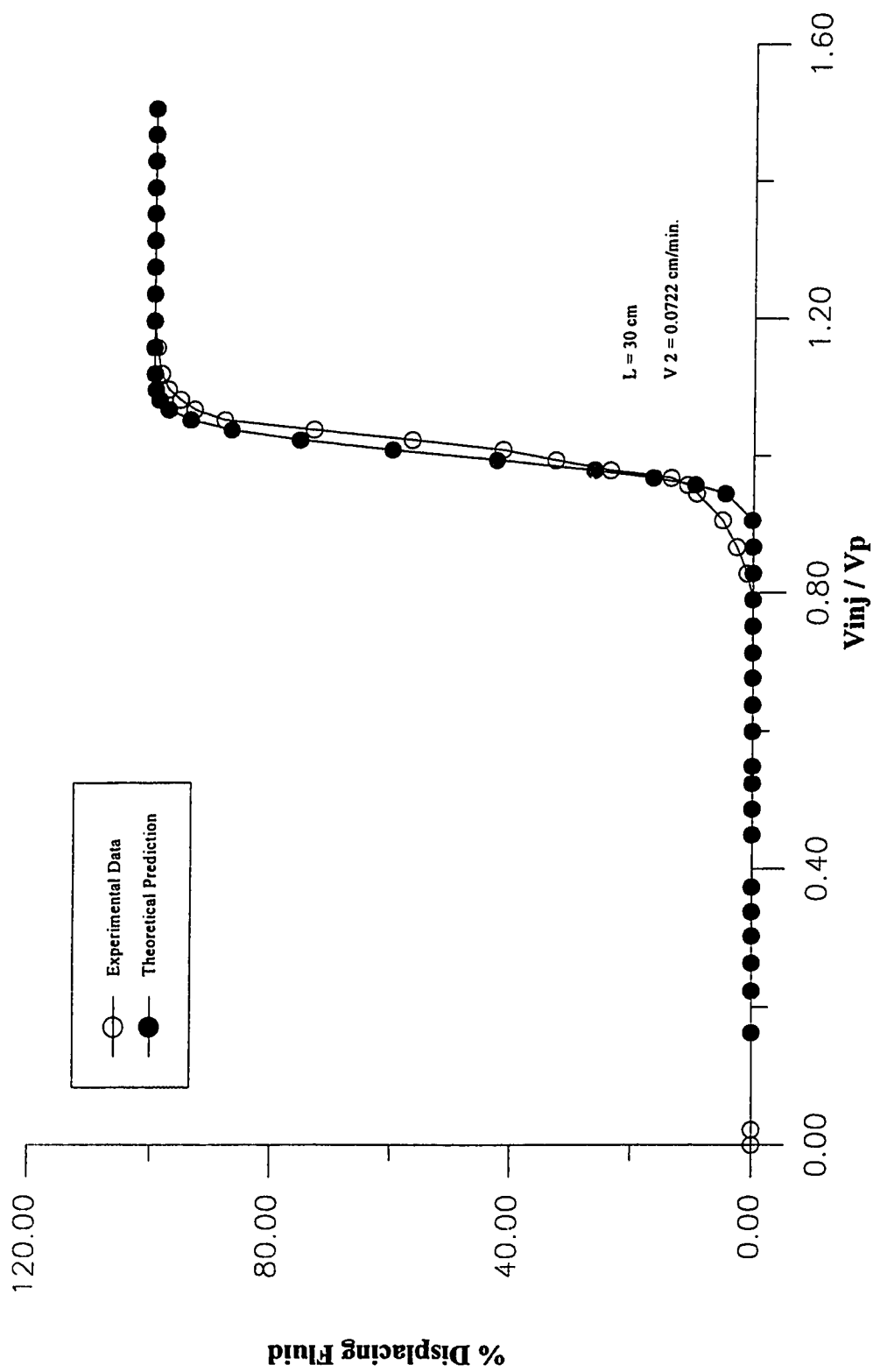


FIGURE 12: COMPARISON OF EXPERIMENTAL CONCENTRATION CURVE WITH THEORETICAL PREDICTION FOR RUN 2

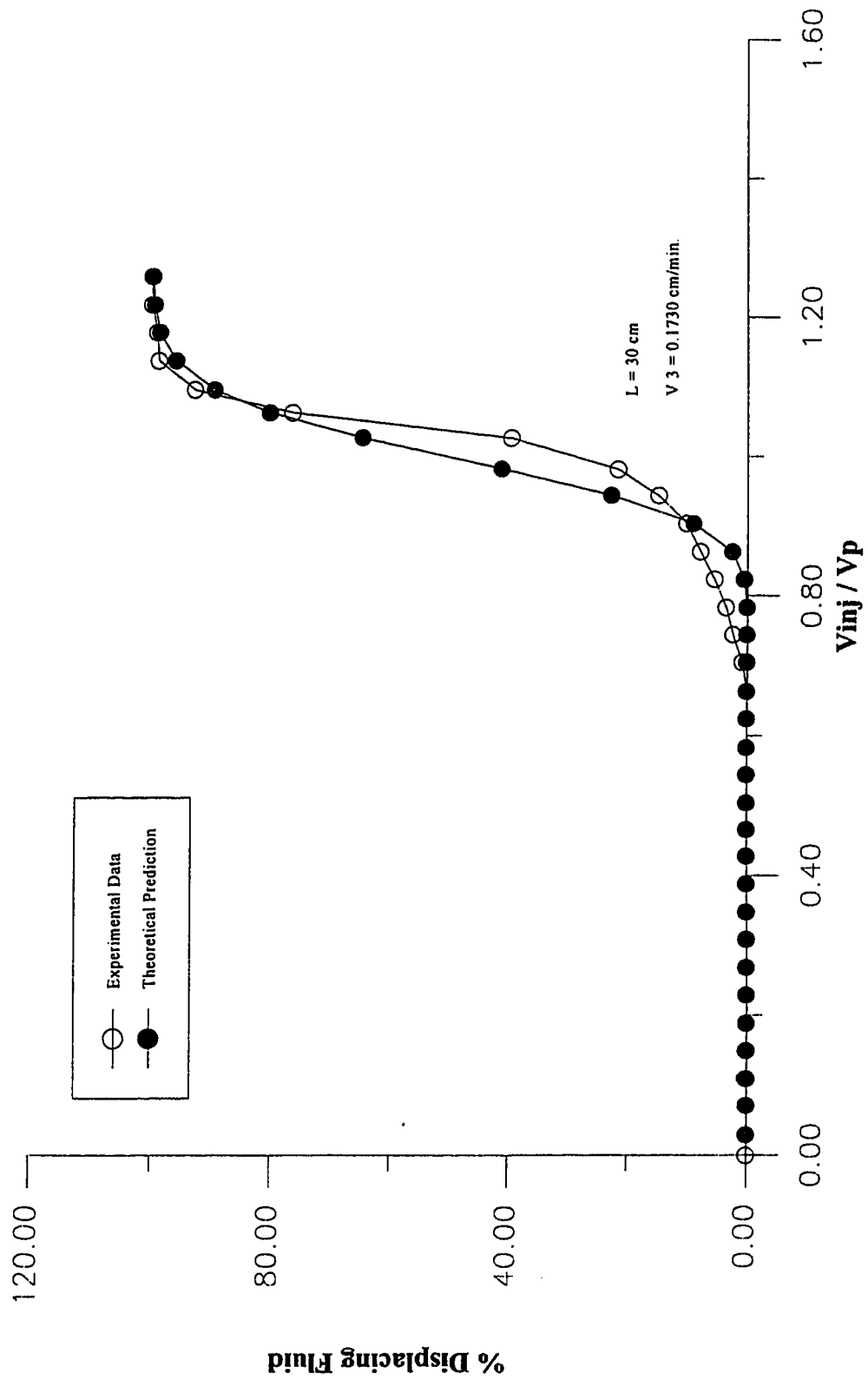


FIGURE 13: COMPARISON OF EXPERIMENTAL CONCENTRATION CURVE WITH THEORETICAL PREDICTION FOR RUN 3

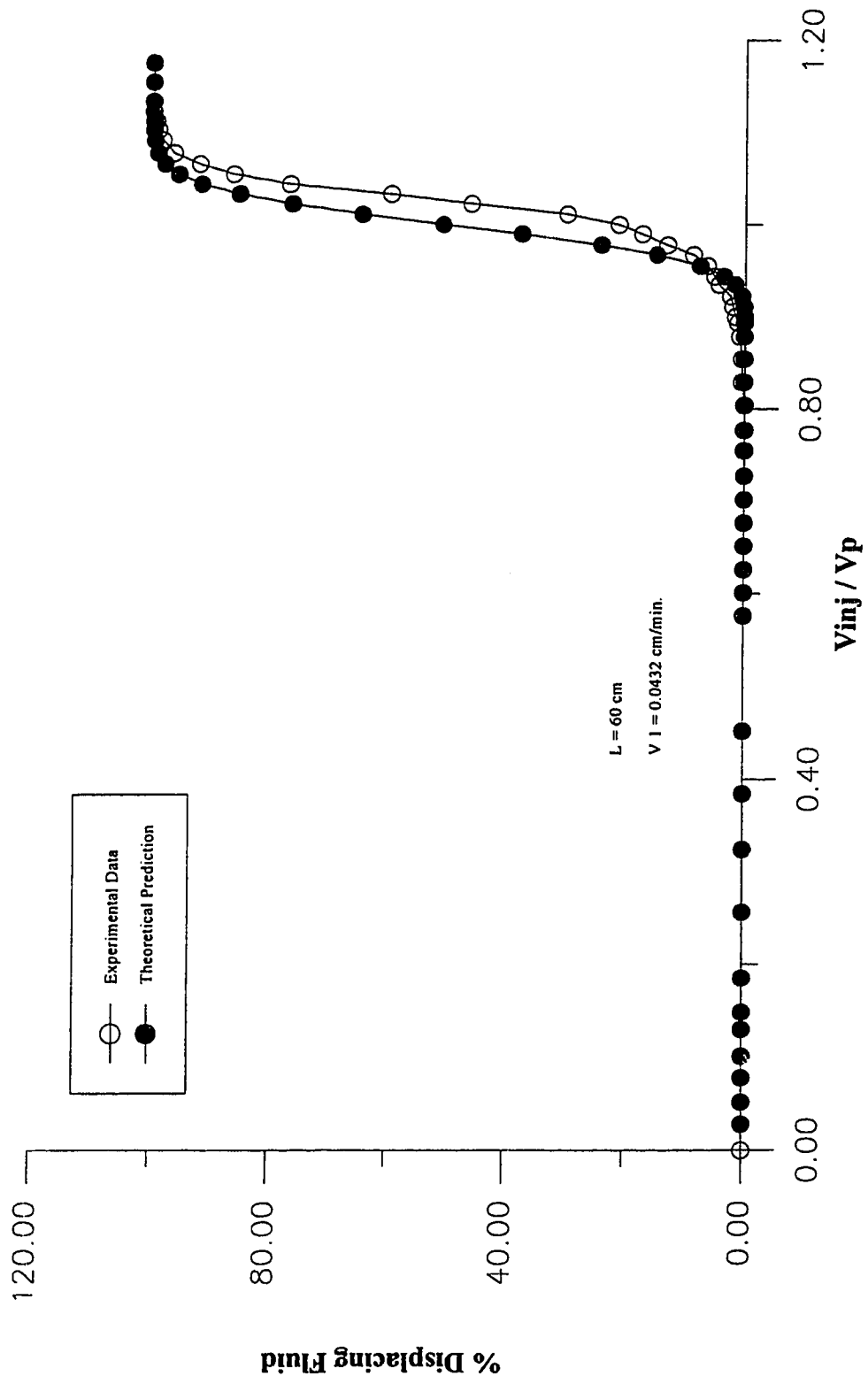
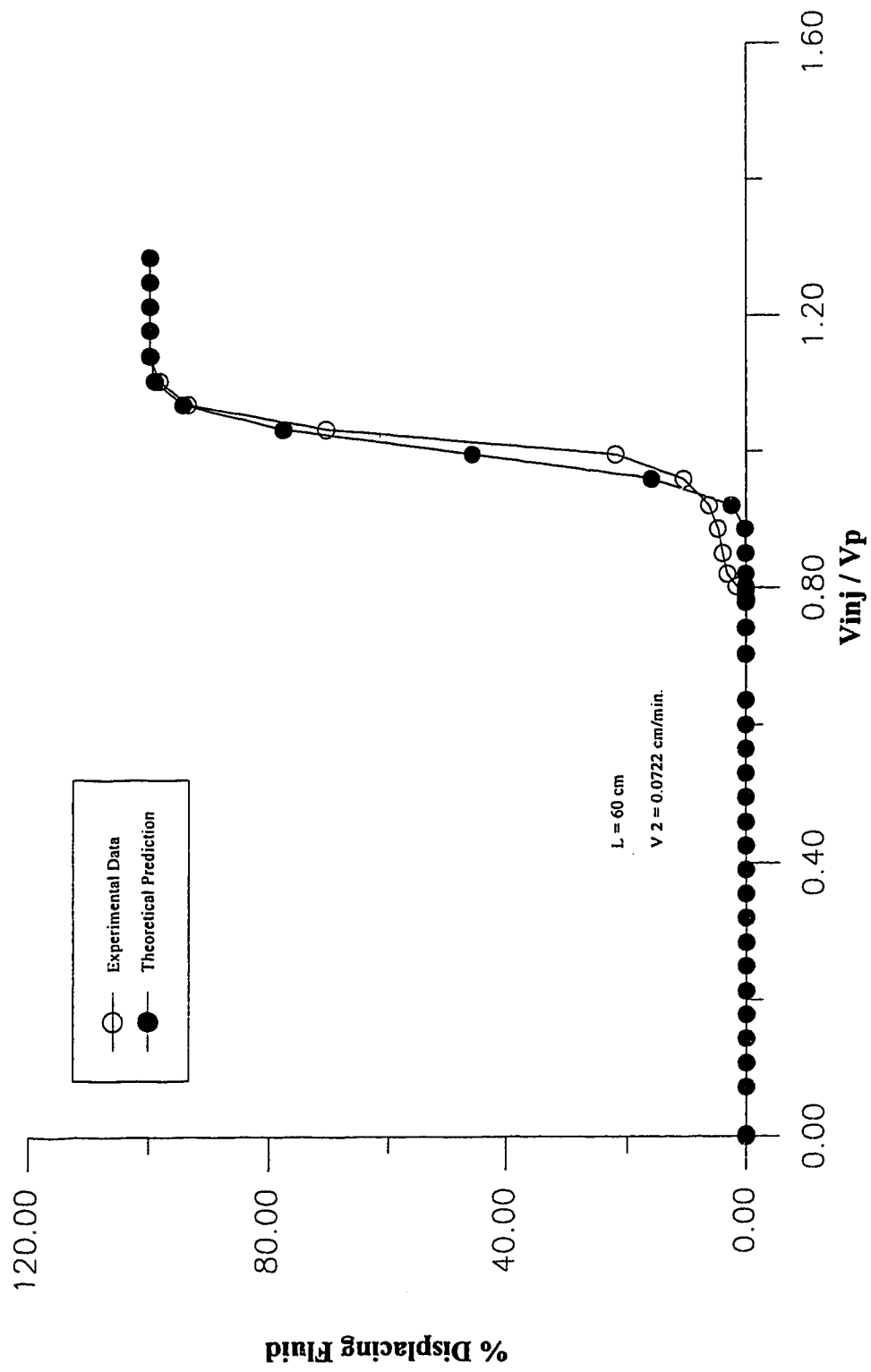


FIGURE 14: COMPARISON OF EXPERIMENTAL CONCENTRATION CURVE WITH THEORETICAL PREDICTION FOR RUN 4



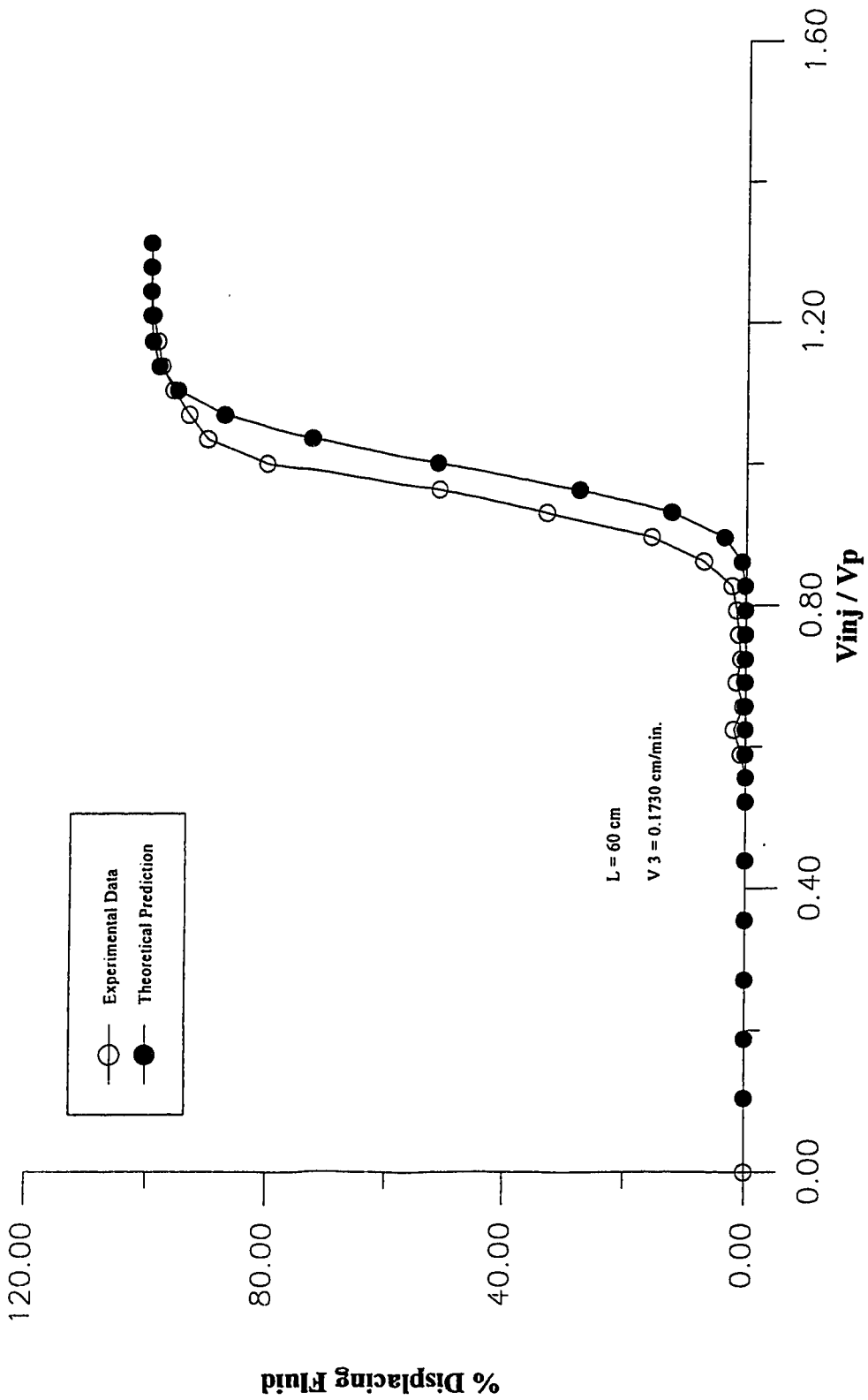


FIGURE 16: COMPARISON OF EXPERIMENTAL CONCENTRATION CURVE WITH THEORETICAL PREDICTION FOR RUN 6

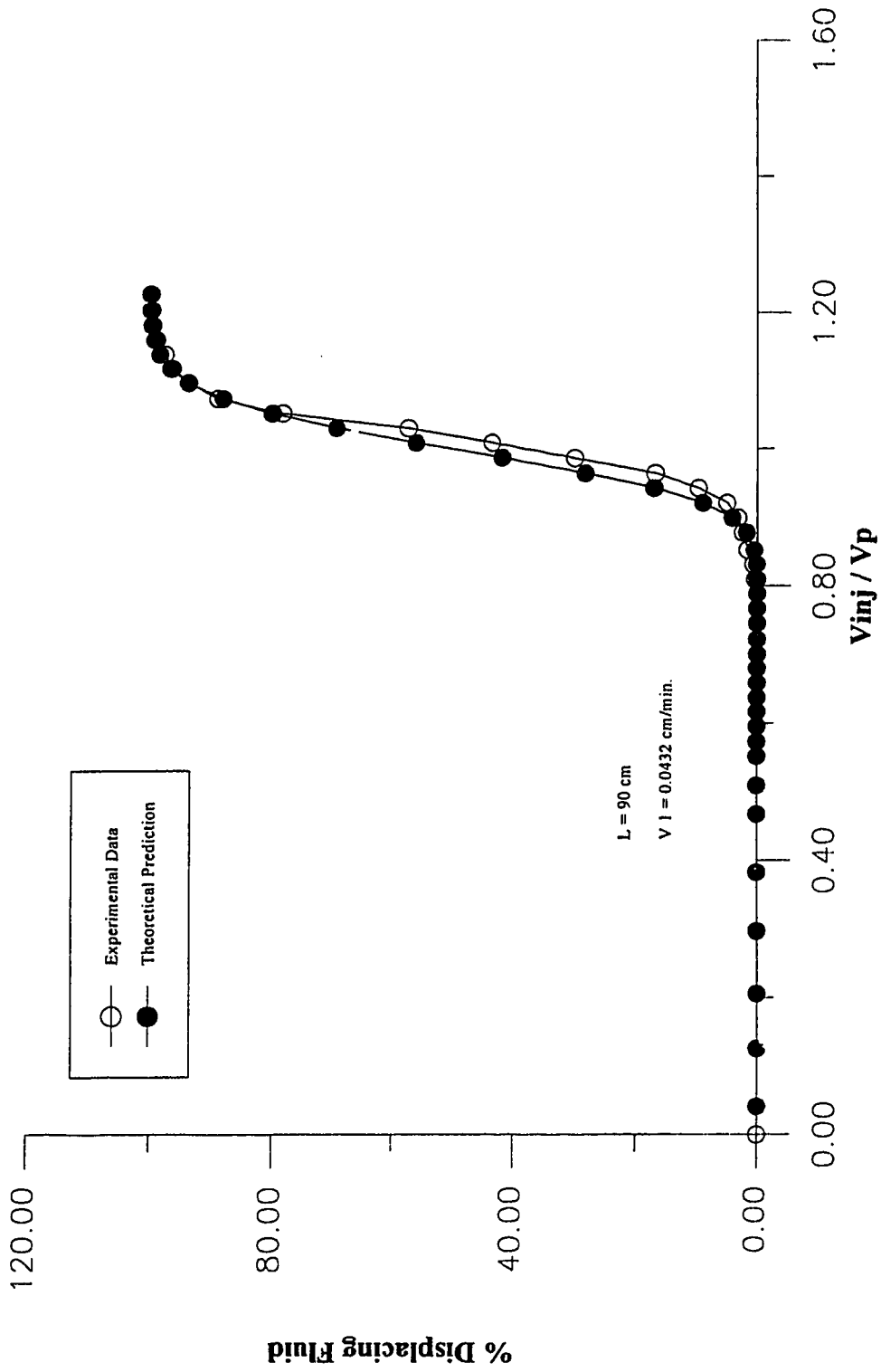


FIGURE 17: COMPARISON OF EXPERIMENTAL CONCENTRATION CURVE WITH THEORETICAL PREDICTION FOR RUN 7

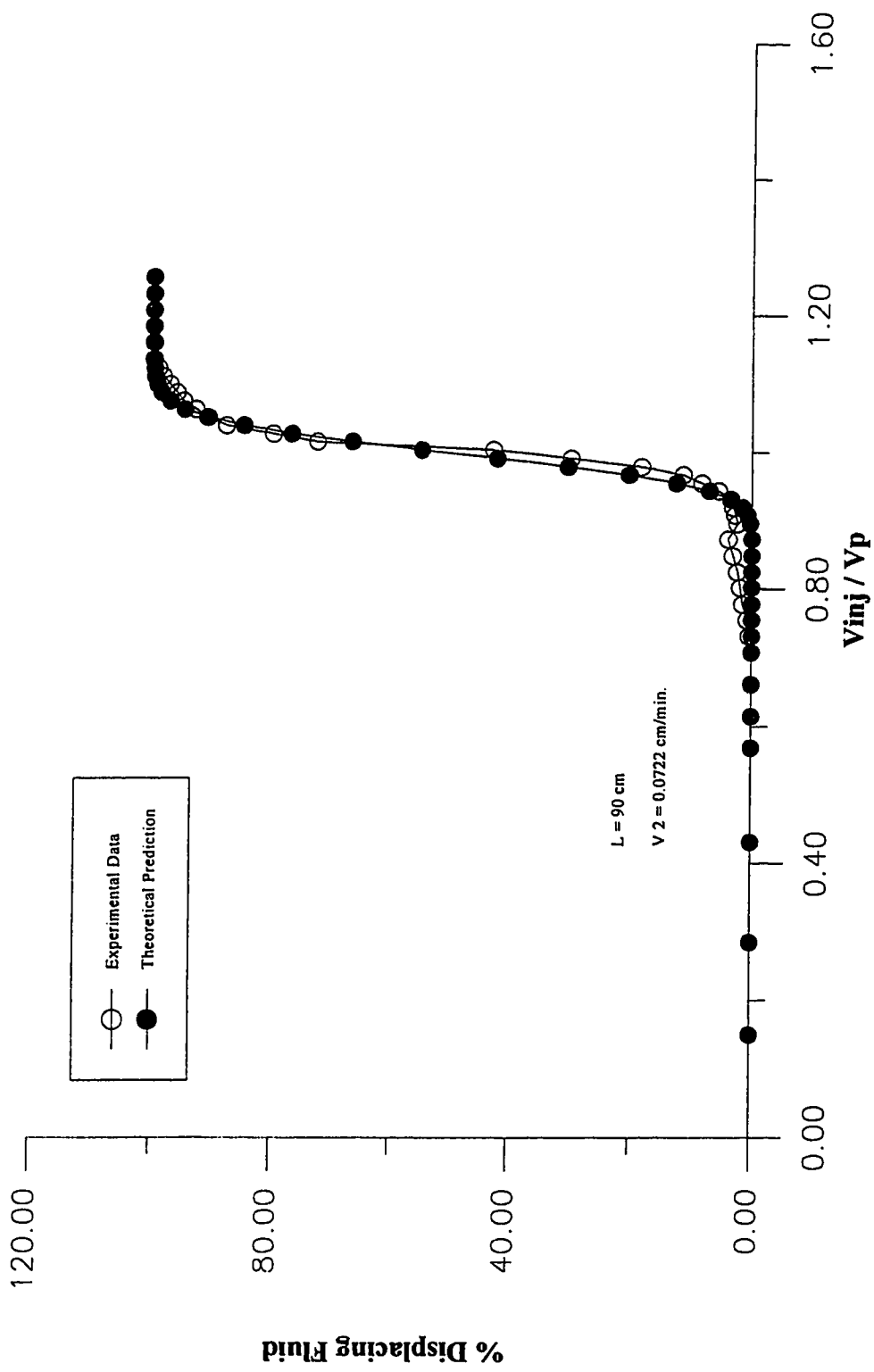


FIGURE 18: COMPARISON OF EXPERIMENTAL CONCENTRATION CURVE WITH THEORETICAL PREDICTION FOR RUN 8

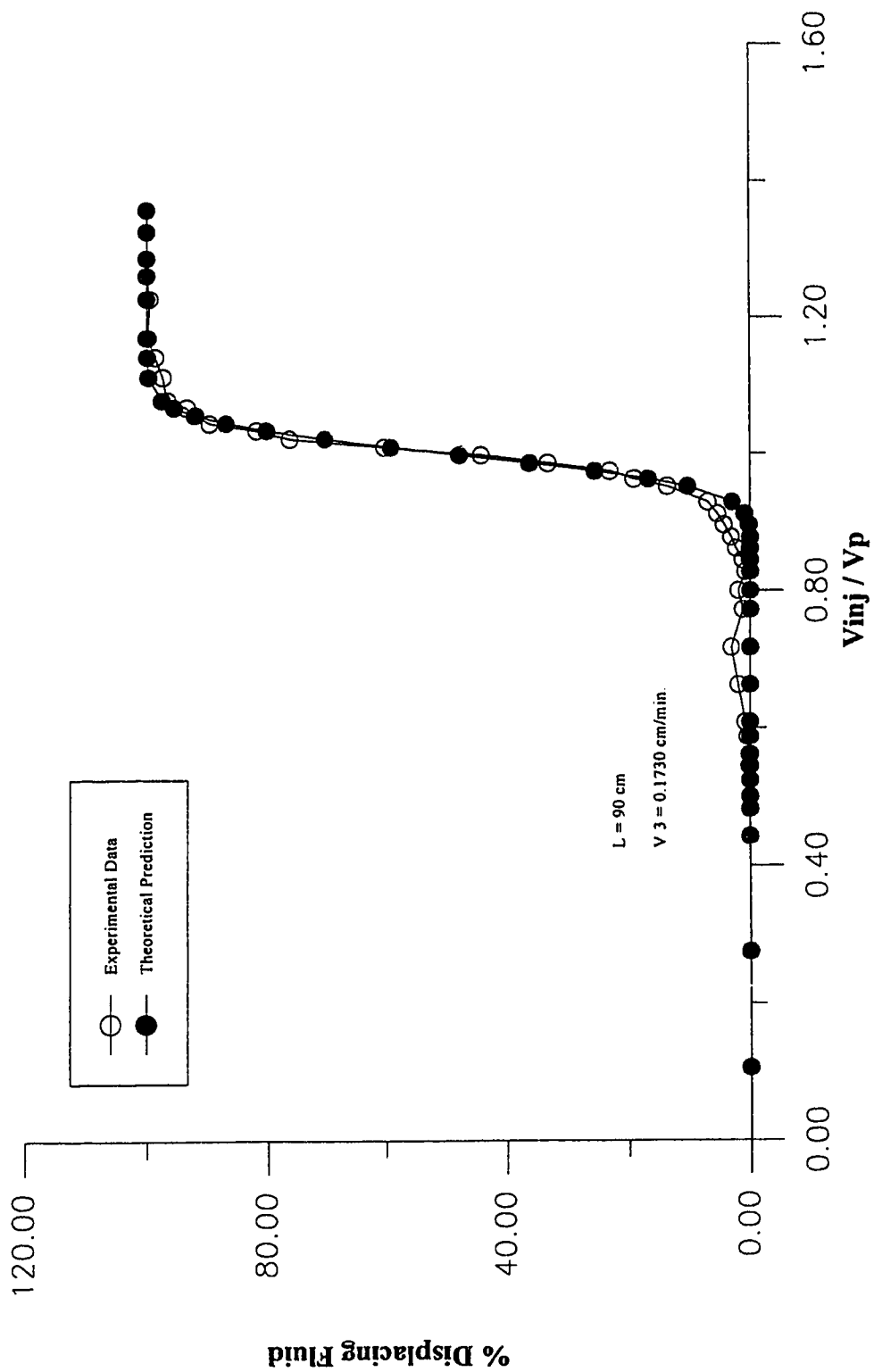


FIGURE 19: COMPARISON OF EXPERIMENTAL CONCENTRATION CURVE WITH THEORETICAL PREDICTION FOR RUN 9

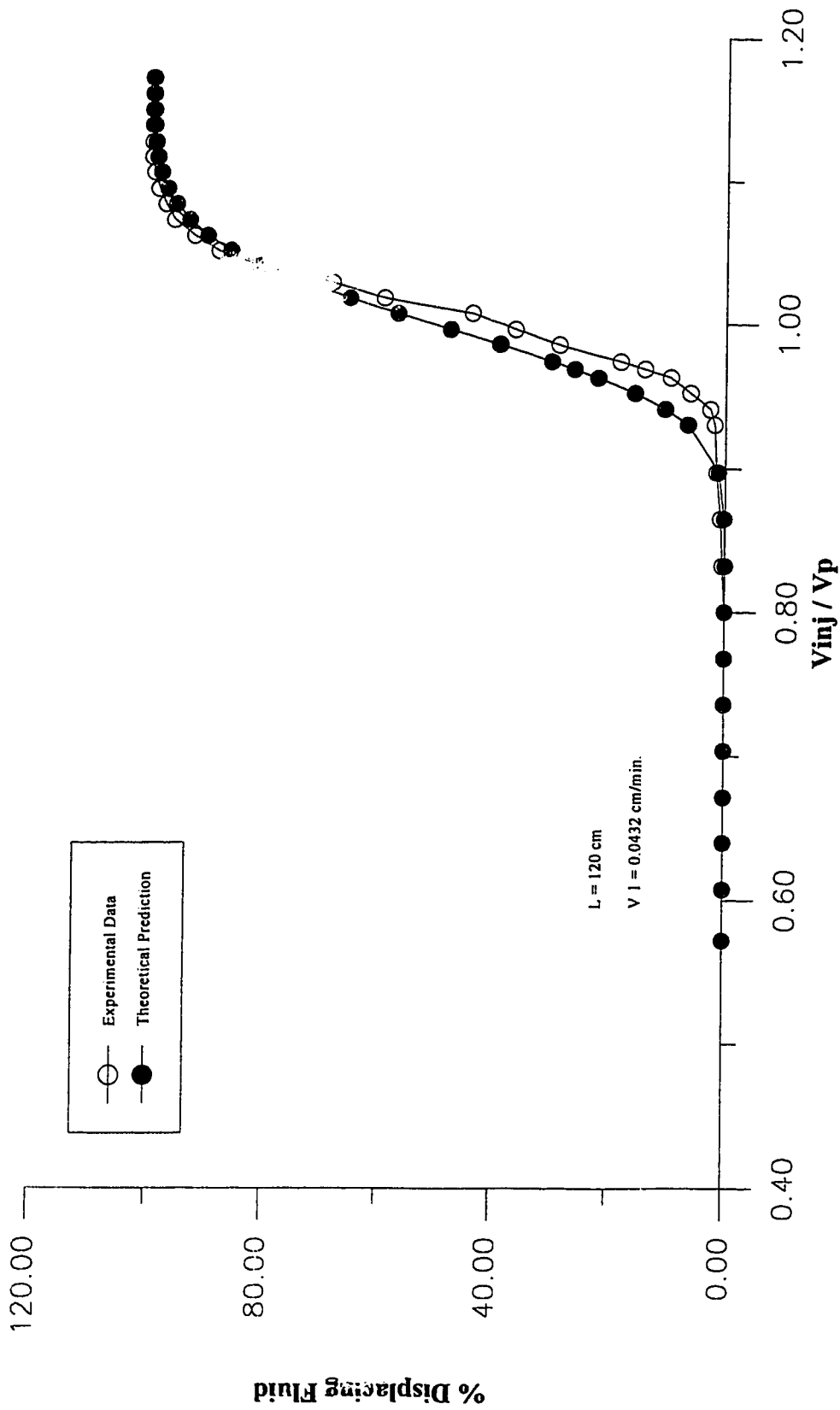


FIGURE 20: COMPARISON OF EXPERIMENTAL CONCENTRATION CURVE WITH THEORETICAL PREDICTION FOR RUN 10

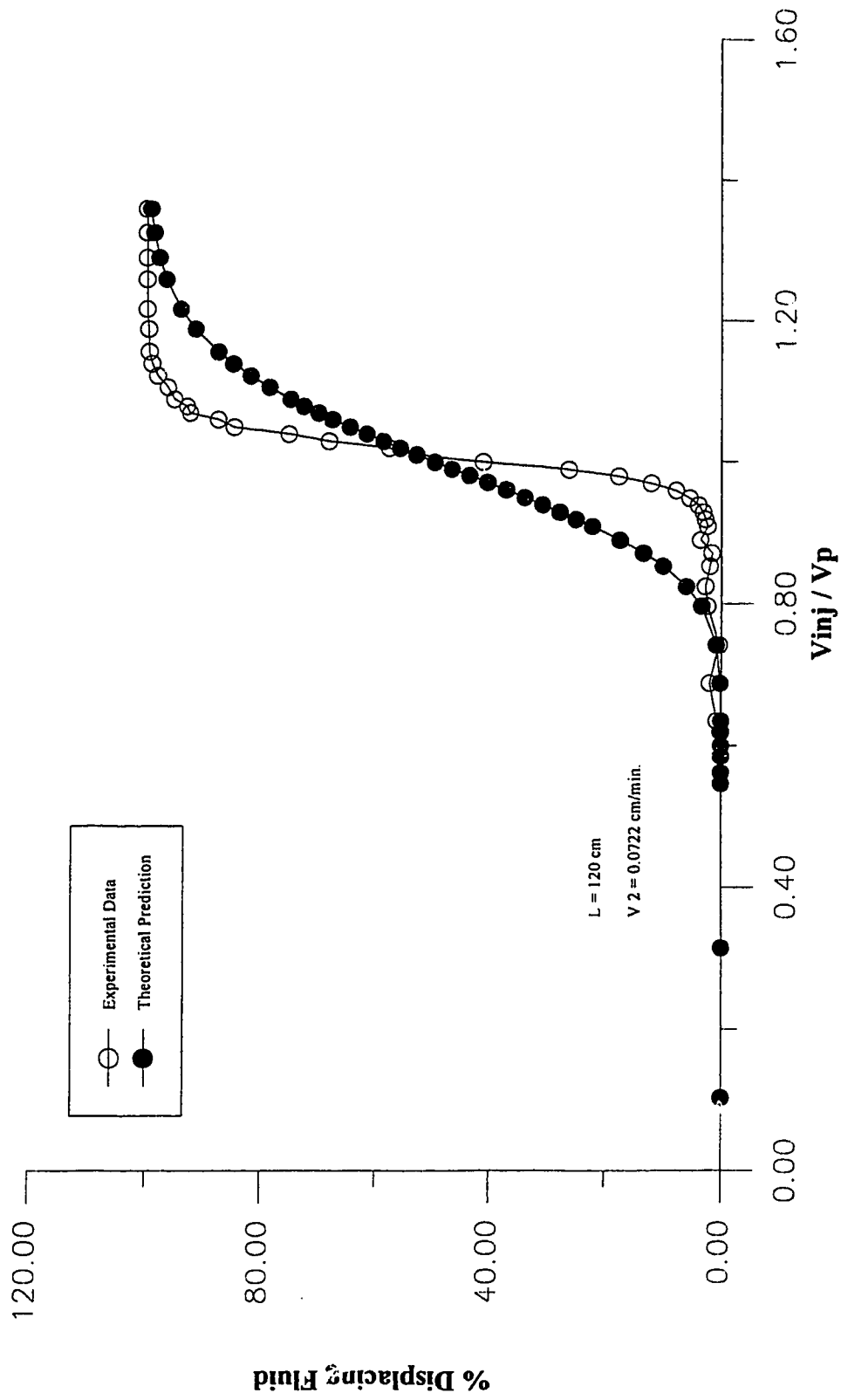


FIGURE 21: COMPARISON OF EXPERIMENTAL CONCENTRATION CURVE WITH THEORETICAL PREDICTION FOR RUN 11

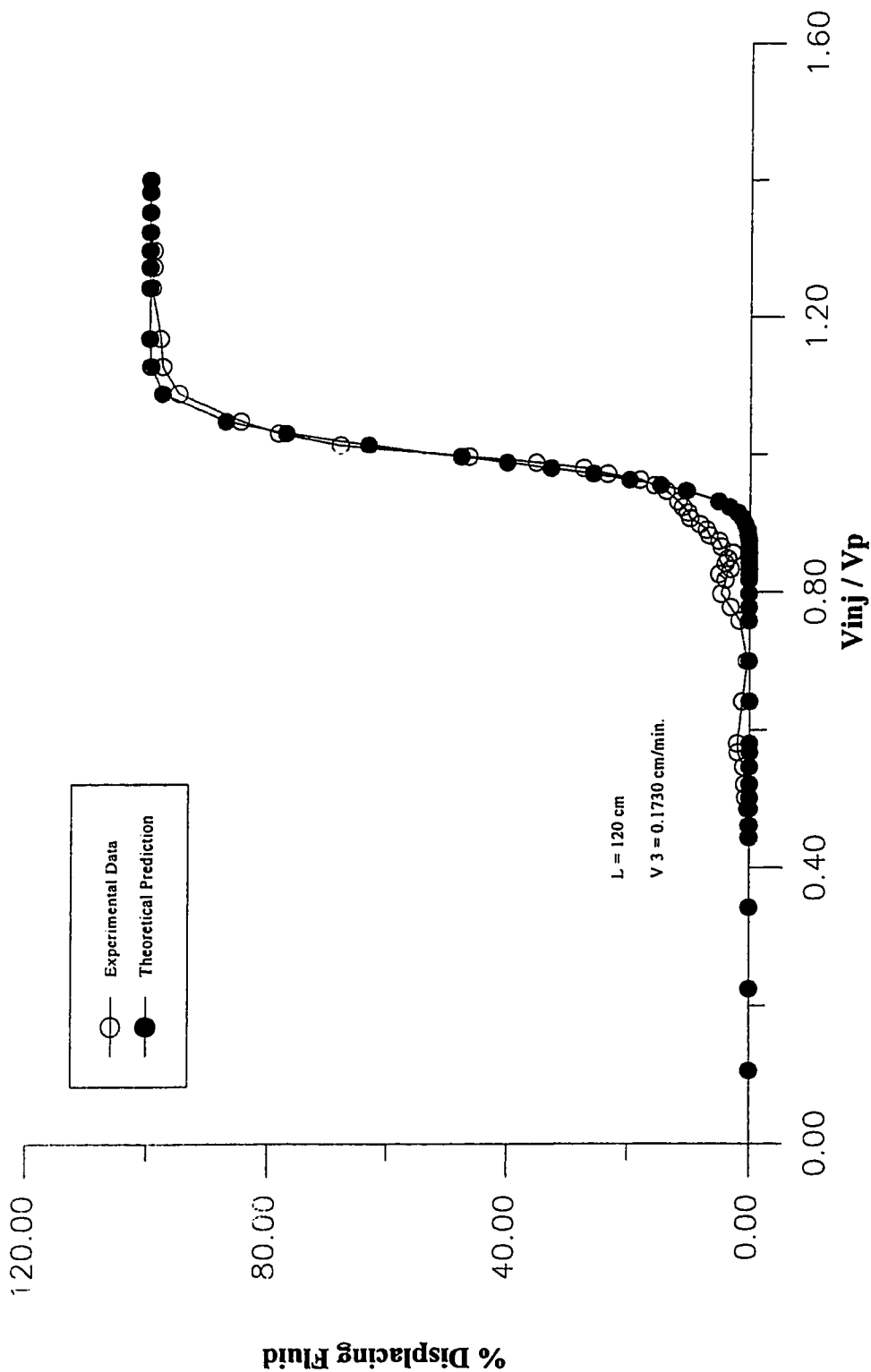


FIGURE 22: COMPARISON OF EXPERIMENTAL CONCENTRATION CURVE WITH THEORETICAL PREDICTION FOR RUN 12